

# Hydrograph Separation Method (HSM) for the Design of Storm Drain Inlets

By:

Ihan-Jarek Tzuriel Acevedo González

A thesis submitted in partial fulfillment of the requirements for the degree of:

MASTER OF SCIENCE

IN

CIVIL ENGINEERING

ENVIRONMENTAL ENGINEERING

UNIVERSITY OF PUERTO RICO

MAYAGÜEZ CAMPUS

2022

Approved by:

---

Walter Silva Araya, Ph.D.

President, Graduate Committee

---

Date

---

Daniel Rodríguez Román, Ph.D.

Member, Graduate Committee

---

Date

---

Ismael Pagán Trinidad, MSCE.

Member, Graduate Committee

Chairperson, Department of Civil Engineering and Surveying

---

Date

---

Nancy Méndez, MEIE.

Graduate Studies Representative

---

Date

## **ABSTRACT**

Urban stormwater drainage systems are part of the urban drainage infrastructure. They encompass the transportation system, structural surroundings, and the topography of the adjacent environment. Adequate stormwater drainage design prevents flooding hazards and protects life and properties. This research proposes a methodology to improve stormwater drainage design named the Hydrograph Separation Method (HSM).

The Hydraulic Engineering Circular No. 22 drainage manual (FHWA, 2013) defines storm drain inlet efficiency through a series of semi-theoretical equations. Efficiency is the effectiveness of an inlet to collect the discharge along a street gutter as compared with the total discharge flowing on the street. This project used those relations and developed an algorithm that takes the street runoff hydrograph and separates it into intercepted flow by the inlet, and carryover flow bypassing the inlet and continuing along the roadway. The software is written in MS Excel Visual Basic for Applications (VBA). It facilitates the design process of street drainage systems and allows the analysis of different alternatives and how they impact the system's performance. A sensitivity analysis provided additional information regarding individual parameter impact on overall inlet efficiency and flood levels, concluding that longitudinal slopes and cross slopes have the least and most effect, respectively, on horizontal flow spread and inlet efficiency. It also showed that grate width has a greater impact on grate interception efficiency than grate length, suggesting a correct orientation when installing them.

Stormwater levels on the streets will be estimated with higher precision and, the minor system design will be improved by having better estimates of inlet discharges. Results from the HSM are incorporated in stormwater simulation programs, such as EPA SWMM, for better design of the minor and major drainage systems. Design of low-impact development (LID) measures will benefit from the HSM by having better estimates of flows into areas with vegetation or infiltration sites.

## RESUMEN

Sistemas urbanos de drenaje pluvial son parte de la infraestructura de drenaje urbana. Incluyen los sistemas de transportación, los alrededores de las estructuras y la topografía del ambiente adyacente. Un diseño adecuado de los sistemas de drenaje pluvial previene inundaciones y protege vidas y propiedades. Esta investigación propone una metodología para mejorar el diseño de drenajes pluviales, nombrado el Método de Separación de Hidrogramas (HSM, por sus siglas en inglés).

El manual de drenaje urbano Hydraulic Engineering Circular No. 22 (por sus siglas en inglés) (FHWA, 2013) define la eficiencia de entradas pluviales a través de ecuaciones semi-teóricas. Eficiencia es la efectividad de un poceto para recolectar la descarga de agua en una cuneta, comparada con la descarga total que fluye por la carretera. En este proyecto se utilizaron esas relaciones y se desarrolló un algoritmo que, dado un hidrograma de escorrentía, lo separa en el flujo interceptado por el poceto y el flujo que continua a lo largo de la carretera. El programa de computadora está escrito en MS Excel Visual Basic for Applications (VBA). Él facilita el proceso de diseño de sistemas de drenaje pluvial, permite el análisis de distintas alternativas y cómo estas afectan el rendimiento del sistema. Un análisis de sensibilidad proveyó información adicional sobre el impacto individual de los parámetros de diseño en la eficiencia del drenaje y los niveles de inundación, concluyendo que pendientes longitudinales y transversales tienen el menor y mayor efecto respectivamente en el alcance horizontal del flujo y la eficiencia de las entradas. También mostró que el ancho de un poceto tiene mayor impacto en su eficiencia que su largo, sugiriendo una orientación correcta al instalarse.

Con esta herramienta los niveles de escorrentía sobre las carreteras se estimarán con mayor precisión y el diseño del sistema menor mejorará al tener mejores estimados de descargas interceptadas. Resultados del HSM serán incorporados en programas de simulación de escorrentía, tal como EPA SWMM, para mejorar el diseño de sistemas mayores y menores de drenaje. El diseño de medidas de desarrollo de bajo impacto (LID, por sus siglas en inglés) se beneficiará del HSM al tener mejores estimados de flujo hacia áreas vegetativas o de infiltración.

## **ACKNOWLEDGMENTS**

This research was funded by the Puerto Rico Water Resources and Research Institute (PRWRERI) under program 104b USGS Water Resources Research Institutes. The research assistantship and support provided by the PRWRERI are greatly appreciated. The support from family and friends helped push through the most difficult aspects of working on this thesis, providing energy during the ups and downs. The shared knowledge from the advisor and the rest of the committee gave perspective to my work, which will prove to be of value inside and outside of academic circle. I would like to acknowledge them as mentors throughout my life. Without all of them, this document would not exist at this time.

## Table of Contents

<b>Abstract .....</b>	<b>ii</b>
Resumen .....	iii
Acknowledgments .....	iv
Table of Contents .....	v
List of Figures .....	vi
<b>1. Introduction.....</b>	<b>1</b>
1.1. Background and Motivation .....	1
1.2. Literature Review .....	2
1.2.1. Determination of Inlet Efficiency .....	2
1.2.2. EPA SWMM Software and Inlet Modeling.....	6
1.3. Goals and Objectives .....	7
<b>2. Runoff Interception Analysis .....</b>	<b>8</b>
2.1. Gutter Flow.....	8
2.1.1. Triangular Gutter Section .....	8
2.1.2. Composite Gutter Section.....	9
2.2. Inlet Efficiency .....	11
2.2.1. Curb-Opening Inlets.....	11
2.2.2. Grate Inlets.....	13
2.2.3. Combination Inlets .....	16
2.2.4. Clogging Effect.....	17
<b>3. HSM Methodology.....</b>	<b>20</b>
3.1. HSM Description .....	20
3.2. Description of VBA Program Interphase and Visualization of Results .....	23
<b>4. Model Applications.....</b>	<b>28</b>
4.1. HSM Application Example 1 .....	28
4.1.1. Part 1: Initial Evaluation.....	28
4.1.2. Part 2: Reevaluation by Improving Existing Inlets .....	33
4.1.3. Part 3: Reevaluation by Adding Inlet Locations .....	35
4.2. HSM Application Example 2 .....	37
4.2.1. Part 1: Initial Evaluation.....	37
4.2.2. Part 2: Evaluation by Varying Inlet Types .....	39
<b>5. Sensitivity Analysis and Design Curves .....</b>	<b>40</b>

5.1. Relative Sensitivity of Flow Spread in Gutter Flow .....	40
5.2. Relative Sensitivity of Curb-Opening Efficiency .....	42
5.3. Relative Sensitivity of Grate Inlet Efficiency.....	44
<b>6. Summary of Results.....</b>	<b>48</b>
6.1. Capabilities of the Hydrograph Separation Method (HSM).....	48
6.2. Results of the Relative Sensitivity Analysis.....	49
<b>7. Conclusions and Recommendations.....</b>	<b>51</b>
7.1. Conclusions .....	51
7.2. Recommendations.....	52
<b>References.....</b>	<b>54</b>
<b>Appendix A.....</b>	<b>56</b>
<b>Appendix B.....</b>	<b>68</b>

---

## List of Figures

Figure 1. Schematic of intercepted versus carryover flows (Uyumaz, 1992). .....	2
Figure 2. Two typical gutter cross-sections. (a) Uniform or Triangular section. (b) Composite section. Adapted from FHWA, 2013.....	3
Figure 3. Comparison of inlet interception capacity and longitudinal slope (FHWA, 2013). .....	4
Figure 4. Relation of inlet interception capacity and flow rate variable (FHWA, 2013).....	4
Figure 5. Multiple grate designs. Top: P-50 x 100 (P-50 when removing the 10mm [3/8"] transverse rods), Bottom: P-30 (FHWA, 2013).....	5
Figure 6. Curb-opening inlet.....	12
Figure 7. Grate inlet.....	13
Figure 8. Top view schematic of frontal and side flows.....	13
Figure 9. Composite gutter section with installed grate inlet. (a) Grate width ( $W_g$ ) equal to depression width ( $W$ ). (b) Grate width lesser than depression width. ....	15
Figure 10. Combination inlets. (a) With curb-opening beside grate. (b) Without curb-opening beside grate.....	16
Figure 11. Inlet equivalent lengths from clogging factor. (a) Multi-unit grate inlet. (b) Single-unit grate inlet. (c) Multi-unit curb-opening inlet. (d) Single-unit curb-opening inlet.....	19
Figure 12. Hydrograph from first drainage zone.....	20
Figure 13. Efficiency versus Total Flow, derived from Figure 12 Efficiency at storm peak = 75.9%.....	21
Figure 14. Separated hydrographs derived from Figure 12 and Figure 13. ....	21

Figure 15. SWMM schematic for simulating a minor (bottom) and major system (top) of the same stormwater system.....	22
Figure 16. SWMM schematic for half a street-gutter cross section. ....	23
Figure 17. VBA interphase runoff hydrograph input table. (Left) Time/Value format. (Right) Date/Time/Value format.....	24
Figure 18. VBA interphase parameter input tables and interactive buttons.....	24
Figure 19. Gutter geometry (Left) and Unit selection (Right) windows. ....	25
Figure 20. Runoff hydrograph input table with spread (T) results after algorithm run. Maximum spread highlighted. ....	25
Figure 21. Parameter input tables after algorithm run. Peak spread (T) and depth (H) highlighted. ....	26
Figure 22. Separated hydrograph tables for inlet alternatives. Efficiency during storm peak highlighted. ....	26
Figure 23. Export results window. ....	27
Figure 24. Storm event hyetograph. ....	28
Figure 25. SWMM simulation without using HSM. ....	29
Figure 26. Screens from SWMM for the input of inlet and street hydrographs.....	30
Figure 27. Major system (top) and minor system (bottom) after HSM in J1/J5 and J3/J7. ....	31
Figure 28. Systems after HSM in J2/J6. ....	32
Figure 29. Efficiency vs Total Flow, derived from Figure 16. Efficiency at peak = 65.7%.....	33
Figure 30. Resultant flows in the last portion of the systems (C4 roadway and C8 pipe). ....	33
Figure 31. [Case 2] Separated hydrographs at upstream node, J1 .....	34
Figure 32. [Case 2] Separated hydrographs at end of system (C4 roadway and C8 pipe).....	34
Figure 33. Redrawn system with an extra inlet location, J4/J9. ....	34
Figure 34. [Case 3] Separated hydrographs at end of system (C4 roadway and C8 pipe).....	34
Figure 35. [Case 3] Separated hydrographs at upstream node, J1 .....	34
Figure 36. System with a 4-way intersection. ....	34
Figure 37. [Case 4] Separated hydrographs at upstream nodes; J1, J2, J4 and J5.....	34
Figure 38. [Case 4] Separated hydrographs at the end of the system (C6 roadway and C12 pipe).....	34
Figure 39. [Case 5] Separated hydrographs at end of system (C6 roadway and C12 pipe) using curb-opening inlets. ....	34

# **1. INTRODUCTION**

## **1.1. Background and Motivation**

Adequate storm drainage design within an urban environment is the direct line of defense between safe day-to-day activities and floods that cause property damages and life-threatening hazards that could easily add up to millions of dollars in losses. Urban environments are interconnected by streets and highways, which is why these are used as the major drainage system to control the flow of storm runoff. These are designed together with the minor drainage system; the storm sewer lines underneath. It is common practice, when designing these systems, to assume that all the runoff within a particular drainage zone on the road goes through the corresponding drainage inlet into the storm sewer system directly below and, therefore, it is considered that no water overpasses the gutter into the next drainage zone downstream.

Although some design manuals (City of San Diego, 2017) or design methods assume that the system is 100% efficient by intercepting the surface runoff in its entirety, it is unlikely that this is the case, because a drainage inlet's efficiency is affected by factor, e.g., inlet type, clogging, splash-over velocity, that limit the amount of flow captured at the inlet. As more and more miles of roadways are constructed, surface runoff that does not get intercepted is carried over into the next drainage zone as shown in Figure 1, eventually adding up enough runoff volume to overcome the design specifications downstream of the drainage system and causing flooding where calculations would estimate otherwise. It is assumed that 100% efficiency can result in overdesigning or overspending in the upstream portion of the storm sewer system. Those misused funds could be relocated to further improve the downstream portions that would be affected by the resulting flood.



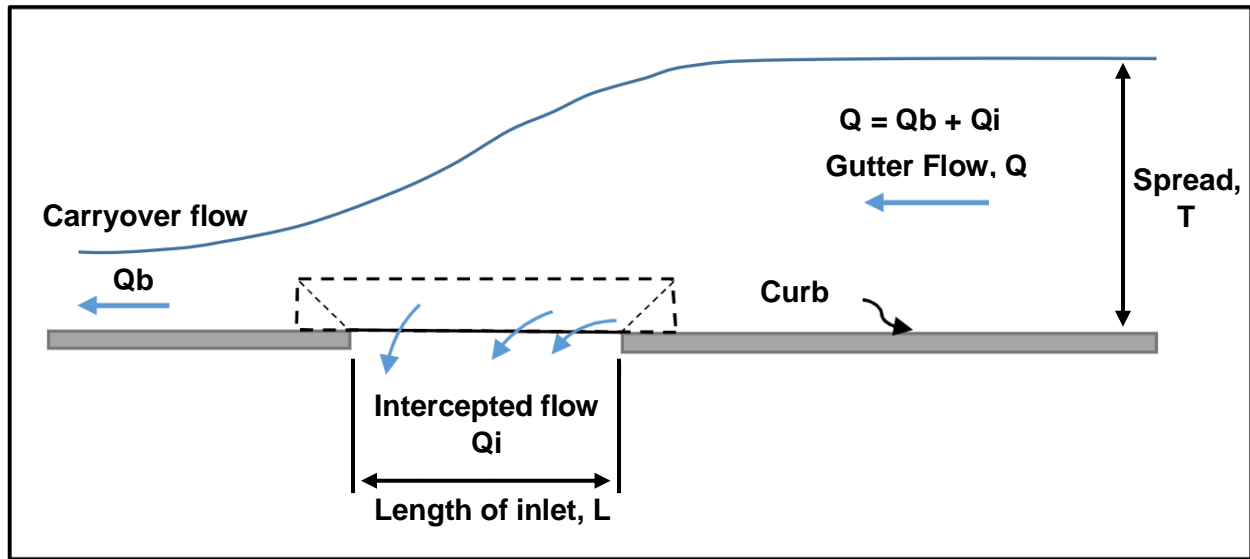


Figure 1. Schematic of intercepted versus carryover flows (Uyumaz, 1992).

Precision in runoff discharge estimates is even more critical in the context of green infrastructure (GI) and low impact development (LID) practices. Bioretention filters and other GI/LID techniques that accompany an urban road network require accurate discharge estimates to operate in their designed efficiency. The catch basin hydrographs used for designing urban drainage systems can be divided into more accurate individual hydrographs corresponding to the flow through the surface gutter and flow through the storm sewer pipes. The process of dividing a runoff hydrograph into an intercepted flow hydrograph and a carryover flow hydrograph will be referred to as the Hydrograph Separation Method or HSM. These targeted hydrographs can be used simultaneously when designing both the surface/major and the sewer/minor systems to precisely allocate construction funds where they are required.

## 1.2.Literature Review

### 1.2.1. Determination of Inlet Efficiency

The Hydrograph Separation Method (HSM) determines an inlet's efficiency and develops individual hydrographs that correspond to intercepted and bypassing flows, which can be added to and follow adjacent downstream portions of the drainage system. Comparative studies between different methodologies used to determine inlet efficiency demonstrate similarities in results when testing grate inlet types and road

geometries that are both included in the range of the methods tested (Gómez and Russo, 2005), allowing a choice of methodologies that will not skew the results. This proposal focuses on the methods presented in the Urban Drainage Design Manual, Hydraulic Engineering Circular No. 22. (FHWA, 2013) by the Federal Highway Administration. Many design regulations are based on them and most research on the topic of urban drainage uses these methods as the baseline for comparison.

The HEC-22 manual adapts semi-theoretical equations based on open-channel hydrodynamics (i.e., Manning's equation) to define runoff flow along with common gutter geometries. Figure 2 shows two typical gutter cross-sections. Grate inlets are commonly installed in a sump or on-grade within the gutter section. Grates in a sump operate either by weir or orifice flow, depending on whether the grate surface area is submerged or not. Determining on-grade grate inlet efficiency requires knowing how much flow approaches the inlet through the front and how much flow approaches through the side. Calculating the ratio between frontal flow and side flow naturally depends on the section geometry being used, which decides what equations and order of operations are required during the analysis.

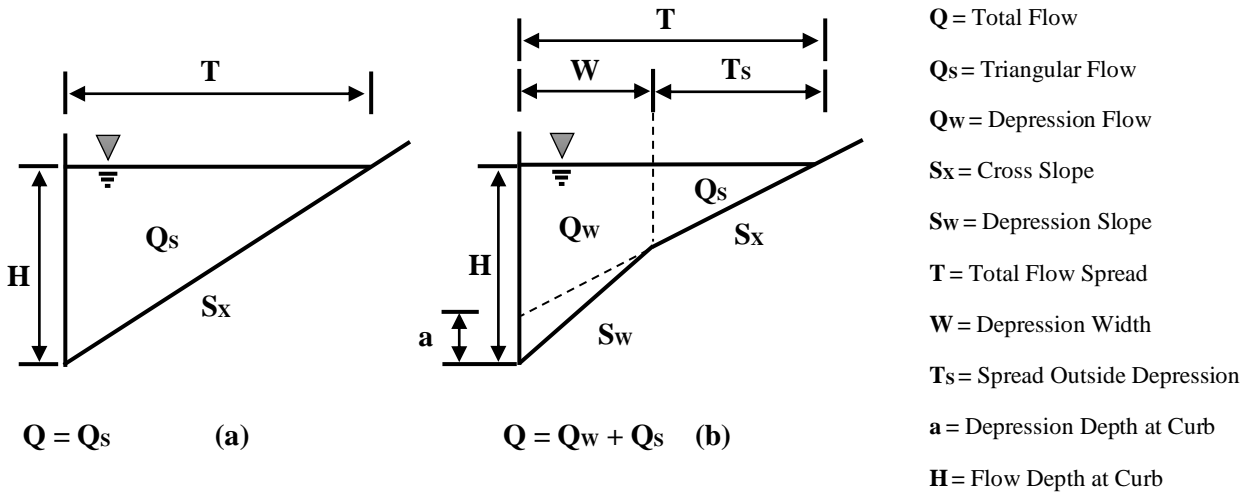


Figure 2. Two typical gutter cross-sections. (a) Uniform or Triangular section. (b) Composite section. Adapted from FHWA, 2013.

The interception capacity of an inlet is determined through its efficiency, expressed as  $E = Q_i/Q$ , where  $Q_i$  is the intercepted flow and  $Q$  is the total gutter flow. The efficiency of a grate inlet varies with multiple geometric and hydrodynamic elements that influence the flow velocity in the gutter, such as longitudinal

slope, cross slope, surface roughness, and total gutter flow. Figure 3 and Figure 4 show graphical depictions of the relations between inlet capacity and geometric characteristics of culvert inlets. Figure 5 presents two grate inlet types included in HEC-22 (FHWA, 2013).

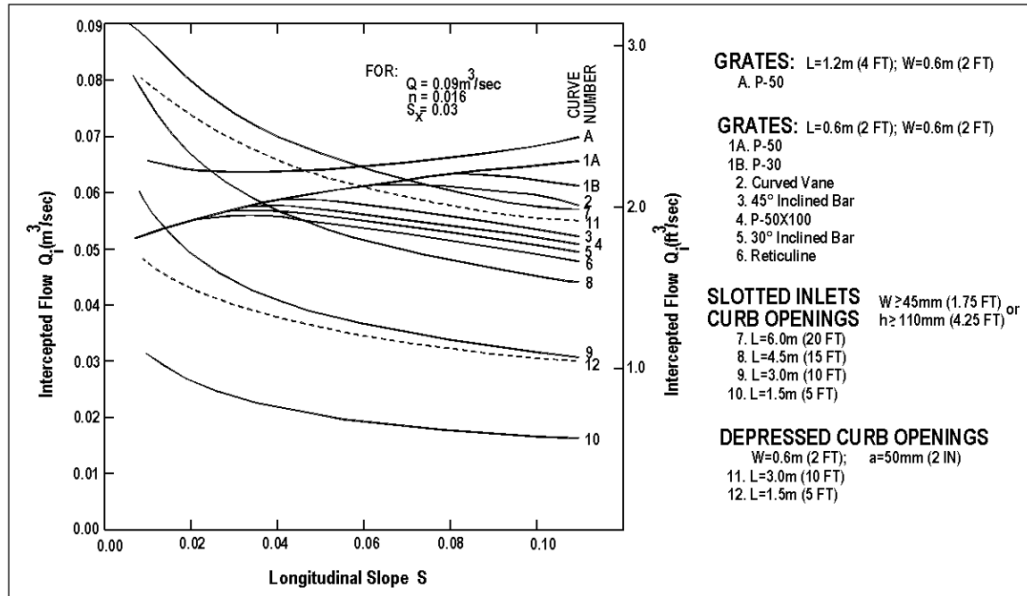


Figure 3. Comparison of inlet interception capacity and longitudinal slope (FHWA, 2013).

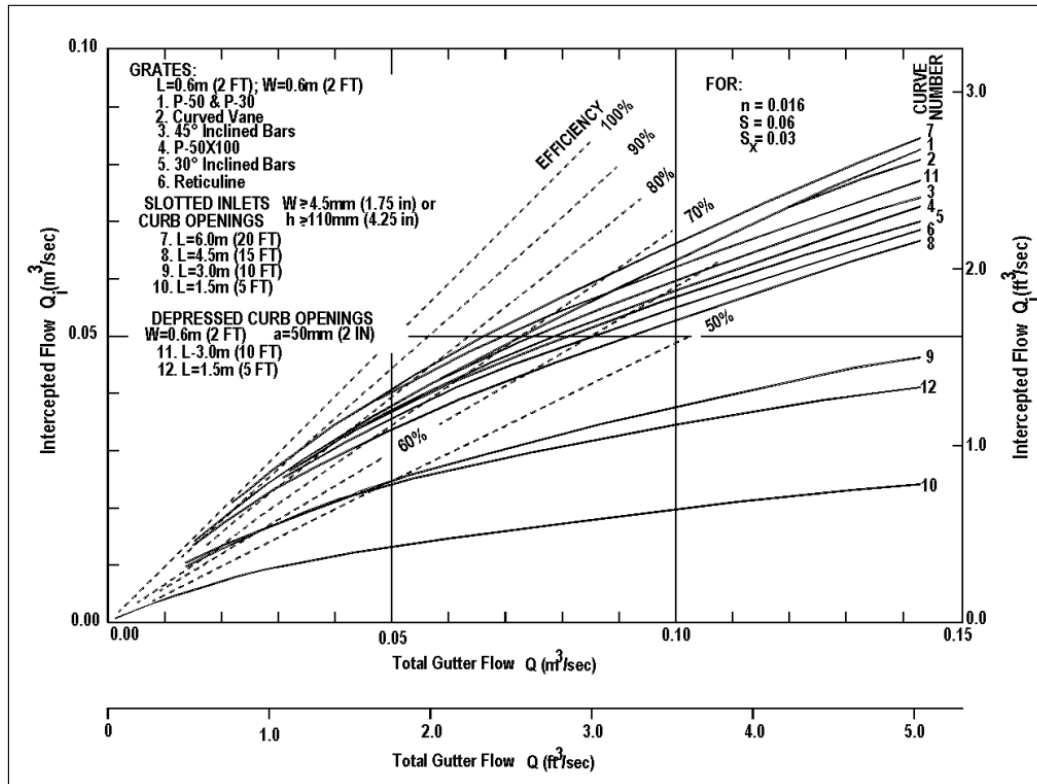


Figure 4. Relation of inlet interception capacity and flow rate variable (FHWA, 2013).

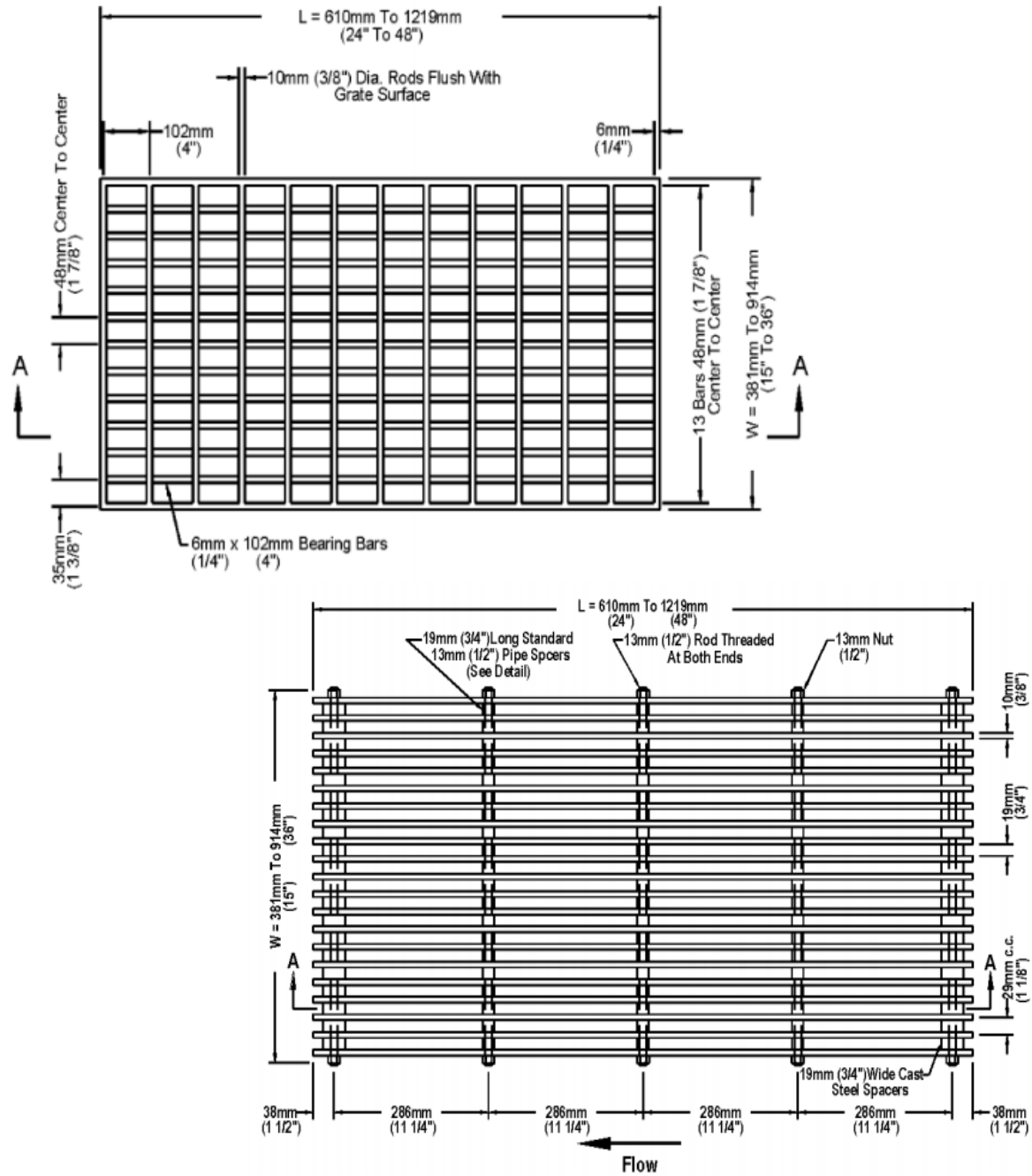


Figure 5. Multiple grate designs. Top: P-50 x 100 (P-50 when removing the 10mm [3/8"] transverse rods), Bottom: P-30 (FHWA, 2013).

Detailed observations of flow behavior at grate inlets revealed that besides collecting flow approaching in front of the grate, grates also capture a fraction of side flow, whose interception efficiency can be determined through the expected flow velocity and cross-section slopes (Gómez and Russo, 2005). In addition, high approach velocities can produce a water splash over the grate bars. Experimental results concluded that the splash-over velocity parameter ( $V_0$ ), the velocity at which water begins to jump or splash over the grate into the next drainage zone, varies with different grate designs, especially with grate length.

Grates clogging up is also a common occurrence as leaves and other debris accumulate on or around the inlet. This situation has been taken into consideration (Guo, 2006; Guo and MacKenzie, 2012) through empirically determining equivalent lengths ( $L_e$ ) for varying grate types, as shorter lengths capture less side flow.

Detailed numerical simulations have been used to obtain detailed flow fields in inlets. Improved equations for curb-inlets have been proposed as an update to those available in HEC-22 (Li et al., 2019).

### **1.2.2. EPA SWMM Software and Inlet Modeling**

The U.S. Environmental Protection Agency (EPA) developed a tool for hydrological modeling known as Storm Water Management Model (SWMM), which is available to the public for free (Rossman, 2010). SWMM offers the capability of running steady and unsteady flow simulations of rainfall-runoff processes within natural or man-made catch basins, open channels, and pipe networks, making it an adequate tool for HSM application. The model also includes pollutant transport and water quality estimates. SWMM has seen extensive use worldwide in “planning, analysis, and design related to stormwater runoff” (USA Environmental Protection Agency, 2015), even as the foundation code for other modeling software. LID modeling capabilities were implemented since the SWMM 5 update (Mogenfelt, 2017) and the climate change effects on precipitation with the SWMM Climate Adjustment Tool (SWMM-CAT) (Rossman, 2014). HSM will be an additional tool for modeling minor and major stormwater systems.

A recent study (Senior et al., 2018) presented a few methods for modeling storm drain inlets within SWMM. The simplest method forces the inlet to intercept all the inflow, resulting in an overestimated discharge into the storm sewer while underestimating carryover flow. The study also explored an alternative that visualized the inlet connecting the major and minor drainage systems as various orifice-style entries. This resulted in a comprehensive, yet computationally expensive and time-consuming methodology given its complexity. A third method fell in between by limiting inlet capacity to a design discharge, allowing excess flow to continue along with the major system, but requiring inlet specifications to correctly estimate the inlet flow. This alternative follows a similar train of thought as HSM, but no approach is revealed to be the most reliable method for accurate stormwater inlet modeling.

### **1.3. Goals and Objectives**

The goal of this project is to develop a methodology for designing urban stormwater drainage inlets that facilitates the separation of a catch basin hydrograph into the individual hydrographs that correspond to the inflow intercepted by a storm drain inlet and the carryover flow that continues within the street gutter. The effort aims to improve the design process of the major/minor drainage systems simultaneously by acquiring more accurate discharge estimates on individual parts of the system. This goal will be reached by completing the following objectives:

- A. Develop an algorithm that takes the user's inputs and separates total runoff into intercepted and carryover flows, considering varying inlet efficiencies.
- B. Create a user-friendly interface that allows the input of the urban drainage system's design parameters (e.g., runoff time-series, gutter section geometry, inlet parameters) into the algorithm.
- C. Allow the visualization of the HSM results for easy interpretation and their exportation to be implemented as SWMM input files.
- D. Perform a relative sensitivity analysis on inlet design parameters to quantify the impact of individual parameters, improving overall understanding of inlet performance.

## 2. RUNOFF INTERCEPTION ANALYSIS

This section covers the technical details of gutter flow and inlet efficiency analyses that form the main components of the Hydrograph Separation Method (HSM). The analyses are explained in the way they were implemented into the HSM algorithm and the interface tool.

### 2.1. Gutter Flow

In an urban environment, the drainage network analysis begins by determining the total runoff in each area. Sections of a roadway divided by drainage inlets can be considered individual catchments modeled as open channels that receive and direct runoff. EPA SWMM and other modeling software use a selection of equations and catch basin parameters to solve for runoff discharges within the system. The main task of the HSM add-on is to use the known runoff to determine inlet efficiency, separating incoming discharges into intercepted and bypassing flows. Once quantified and directed towards roadside gutters, HEC-22 equations are applied to determine horizontal spread (T) and flow velocity (V), as well as other aspects of interest to the designer.

#### 2.1.1 Triangular Gutter Section

When analyzing a triangular or uniform gutter section, shown in Figure 2.a., the horizontal spread can be determined through equation (2.1). This equation approximates Manning's equation derived by Izzard (1949). The runoff is used as the gutter flow (Q) and the geometrical parameters are known through the gutter design. Afterward, equation (2.2) is applied to determine flow velocity. Both values (T and V) are required to determine on-grade grate inlet efficiency, along with the ratio of flow ( $E_o$ ) over the grate width ( $W_g$ ) acquired using equation (2.3).

$$T = [(Qn)/(K_u S_x^{1.67} S_L^{0.5})]^{0.375} \quad (2.1)$$

$$Q = (K_u/n) S_x^{1.67} S_L^{0.5} T^{2.67}$$

where:

$$K_u = 0.376 \text{ (0.56 in English units),}$$

$n$	=	Manning's coefficient,
$Q$	=	Total gutter flow, $m^3/s$ ( $ft^3/s$ ),
$T$	=	Width of flow (spread), $m$ ( $ft$ ),
$S_x$	=	Cross slope, $\frac{m}{m} \left( \frac{ft}{ft} \right)$ , and
$S_L$	=	Longitudinal slope, $\frac{m}{m} \left( \frac{ft}{ft} \right)$ .

$$V = (K_u/n) S_x^{0.67} S_L^{0.5} T^{0.67} \quad (2.2)$$

where:

$K_u$	=	0.752 (1.11 in English units), and
$V$	=	Flow velocity in the triangular section, $\frac{m}{s} \left( \frac{ft}{s} \right)$ .

$$E_o = 1 - [1 - (W_g/T)]^{2.67} \quad (2.3)$$

where:

$E_o$	=	Ratio of flow over width $W_g$ and
$W_g$	=	Width of the grate inlet, $m$ ( $ft$ ).

### 2.1.2 Composite Gutter Section

The more complex geometry of a composite gutter section, shown in Figure 2.b., requires an iterative approach to determine horizontal spread ( $T$ ). The total gutter flow is  $Q$  and the flow outside of the depressed section is denoted as  $Q_s$ . A first estimate is done by assuming a flooded roadway where  $Q_s$  is significant. Equation (2.4) is then used to determine both the frontal or depression flow ( $Q_w$ ) and the frontal flow ratio ( $E_o$ ).

$$Q_w = Q - Q_s = E_o Q \quad (2.4)$$

where:

$E_o$	=	Ratio of flow over length $W$ to total gutter flow,
$Q_w$	=	Frontal flow, $\frac{m^3}{s} \left( \frac{ft^3}{s} \right)$ , and
$Q_s$	=	Side flow, $\frac{m^3}{s} \left( \frac{ft^3}{s} \right)$ .



Referring to Figure 2.b the total horizontal spread (T) is obtained through equation (2.5), followed by the spread outside of the depressed section ( $T_s$ ) with equation (2.6). This side spread can be inserted into the triangular flow equation (2.1) to calculate a side flow ( $Q_s$ ). Both the calculated and the assumed side flows are compared to determine if the assumption was correct. If not, a slightly lower  $Q_s$  is assumed and the process is repeated until both values are similar to each other. The assumption of a flooded roadway gives a large positive difference between the calculated  $Q_s$  and the assumed  $Q_s$ , and each consecutive assumption yields a smaller positive difference. The first assumed  $Q_s$  value to return a negative difference is saved as the correct flow distribution and used to determine flow spread (T), depth (H), and velocity (V).

$$E_o = 1 / \left\{ 1 + \frac{S_w/S_x}{\left[ 1 + \frac{S_w/S_x}{W^{-1}} \right]^{2.67} - 1} \right\} \quad (2.5)$$

$$T = W \left\{ 1 + \frac{S_w/S_x}{\left[ 1 + \frac{(S_w/S_x) E_o}{1 - E_o} \right]^{0.375} - 1} \right\}$$

where:

$$\begin{aligned} S_w &= \text{Depression slope, } S_w + a / W, \frac{m}{m} \left( \frac{ft}{ft} \right), \\ W &= \text{Width of depressed gutter, } m \text{ (ft), and} \\ a &= \text{Gutter depression, } mm \text{ (in).} \end{aligned}$$

$$T_s = T - W \quad (2.6)$$

where:

$$T_s = \text{Horizontal spread outside of the depressed section, } m \text{ (ft).}$$

Unlike for the triangular section, the HEC-22 does not use a flow velocity equation (2.2) for composite sections, derived from a flow rate equation (2.1). The HEC-22 procedure uses average velocity  $V=Q/A$  when handling composite gutter sections. The flow area is calculated as  $A = 0.5T^2S_x + 0.5aW$ . Once both the spread (T) and flow velocity (V) are known, the inlet efficiency is computed.

## 2.2. Inlet Efficiency

The complex nature of inlet inflow has eluded the development of purely theoretical solutions; however, experimental runs provided the previously presented relations and computational power provided the capability to obtain complete hydrographs. The most common types of inlets within urban environments are grate inlets, curb-opening inlets, and combination inlets (grates and curb-opening together). Other types of drainage inlets and drainage methods exist, such as slotted pipes and pervious pavements, where their effective application requires various evaluations and considerations. Curb-opening inlets require knowing the gutter section geometry to determine its discharge capacity. Grate inlets installed on-grade need known gutter geometry as well as flow spread (T) and velocity (V). Combination inlets use a modified approach based on grate and curb inlet equations. The inlet efficiency is used in equations (2.7) and (2.8) to separate incoming runoff into intercepted and carryover flows as follows:

$$Q_i = EQ \quad (2.7)$$

where:

$$\begin{aligned} E &= \text{Inlet Efficiency, and} \\ Q_i &= \text{Intercepted flow, } m^3/s \text{ (} ft^3/s \text{).} \end{aligned}$$

$$Q_b = Q - Q_i \quad (2.8)$$

where:

$$Q_b = \text{Bypass flow, } m^3/s \text{ (} ft^3/s \text{).}$$

### 2.2.1. Curb-Opening Inlets

Curb-opening inlets like the one depicted in Figure 6 intercept incoming runoff through an opening on the curb sidewall. The procedure to determine curb-opening efficiency relies on equation (2.9), which calculates the inlet length ( $L_T$ ) required to intercept 100% of the gutter flow (Q). The equation is derived from the perspective of a triangular gutter section, but equation (2.10) is used to transform the depression slope ( $S_w$ ) to get an equivalent triangular cross slope ( $S_e$ ) if one were to use a composite section. Afterward,

if the actual length ( $L$ ) of the curb-opening is lower than  $L_T$ , equation (2.11) estimates the efficiency ( $E$ ) of the actual inlet. Total flow ( $Q$ ) can now be divided into the intercepted flow ( $Q_i$ ) and carryover flow ( $Q_b$ ).

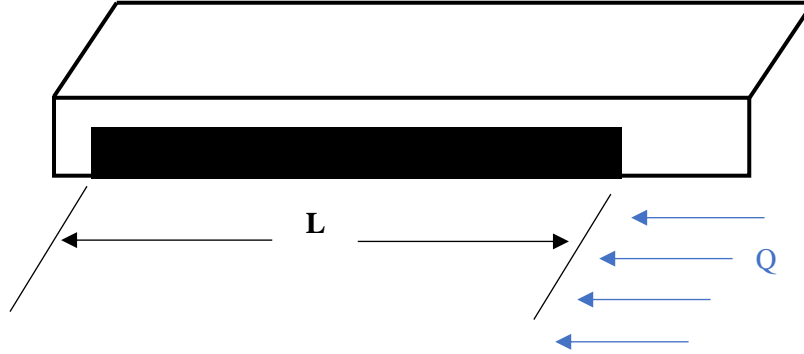


Figure 6. Curb-opening inlet.

$$L_T = K_u Q^{0.42} S_L^{0.3} [1/nS_x]^{0.6} \quad (\text{For triangular gutter section}) \quad (2.9)$$

$$L_T = K_u Q^{0.42} S_L^{0.3} [1/nS_e]^{0.6} \quad (\text{For composite gutter section})$$

where:

- $K_u$  = 0.817 (0.6 in English units),
- $L_T$  = Curb opening length required to intercept 100% of the gutter flow,  $m$  (ft), and
- $S_e$  = Equivalent cross slope  $m/m$  (ft/ft).

$$S_e = S_x + S'_w E_o \quad (\text{For composite gutter section}) \quad (2.10)$$

where:

- $S'_w$  =  $(S_w - S_x)$  or  $(a / W)$ : where both values must have the same units to acquire  $m/m$  (ft/ft),
- $a$  = Gutter depression,  $m$  (ft), and
- $E_o$  = Ratio of flow in the depressed section to total gutter flow, upstream of the inlet.

$$E = 1 - [1 - (L/L_T)]^{1.8} \quad (2.11)$$

where:

- $E$  = Efficiency of curb opening inlets shorter than  $L_T$ , and
- $L$  = Curb-opening length,  $m$  (ft).

Li et al. (2019) did extensive numerical simulations and develop an alternate set of equations for  $L_T$  and  $E$  is given by:

$$L_T = K_u Q^{0.372} S_L^{0.1} \left( \frac{1}{n S_e} \right)^{0.564} \quad (2.12)$$

$$E = 1 - \left[ 1 - \left( L/L_T \right) \right]^{2.42} \quad (2.13)$$

All the variables in these equations were defined previously. The unit constant  $K_u$  is equal to 0.387 for  $L$  in meters and  $Q$  in  $m^3/s$  and 0.337 for  $L$  in feet and  $Q$  in  $ft^3/s$ . These equations were included in the HSM tool as an upgrade to HEC-22.

### 2.2.2. Grate Inlets

Figure 7 shows an on-grade grate inlet, which intercepts incoming runoff from both the front ( $W_g$ ) and the side ( $L$ ), conceptualized in Figure 8. They can be installed as a single unit, or by placing more than one connected in series. Front flow and side flow are subjected to individual efficiency evaluations, leading to the use of equations (2.14) and (2.15) to divide the total flow into frontal and side flows.

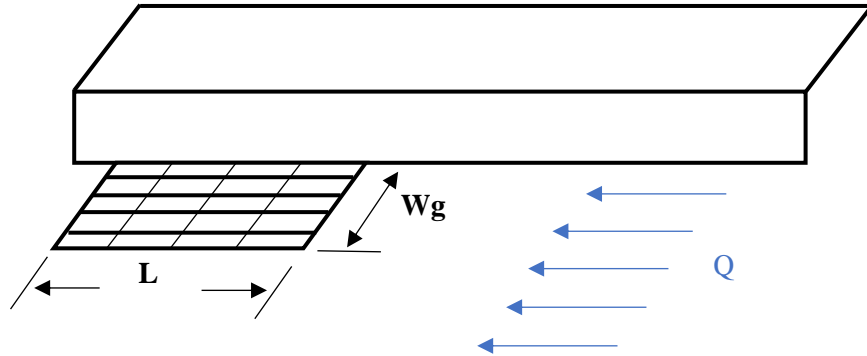


Figure 7. Grate inlet.

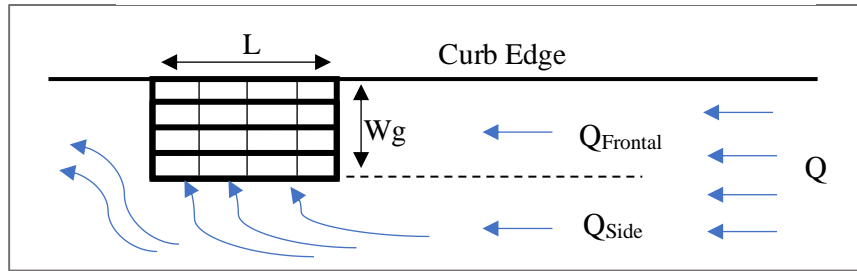


Figure 8. Top view schematic of frontal and side flows.

$$E_o = Q_w/Q \quad (2.14)$$

where:

- $E_o$  = Ratio of frontal flow to total gutter flow, and
- $Q_w$  = Frontal flow,  $m^3/s$  ( $ft^3/s$ ).

$$Q_s = Q - Q_w \quad (2.15)$$

where:

$$Q_s = \text{Side flow, } m^3/s \text{ (} ft^3/s \text{)}.$$

Frontal flow interception efficiency is affected by the ability of fast-moving runoff to jump over or splash over the grate in front of it. Experimental research (FHWA, 2013) on grate splash-over velocity ( $V_o$ ) has led to the development of equation (2.16). The various coefficients depend on the specific grate model being used, listed in Table 1. Equation (2.17) compares the splash-over velocity to the previously calculated flow velocity ( $V$ ) to determine frontal efficiency or the ratio of frontal flow intercepted ( $R_f$ ).

$$V_o = \alpha + \beta L - \gamma L^2 + \eta L^3 \quad (2.16)$$

where:

$$\begin{aligned} V_o &= \text{Grate splash-over velocity, } m/s \text{ (} ft/s \text{)}, \\ L &= \text{Grate inlet length, } m \text{ (} ft \text{)}, \text{ and} \\ \alpha, \beta, \gamma, \eta &= \text{Grate specific coefficients.} \end{aligned}$$

Table 1. Grate splash-over velocity coefficients.

GRATE TYPE	$\alpha$	$\beta$	$\gamma$	$\eta$
<b>P-50</b>	2.22	4.03	0.65	0.06
<b>P-50X100</b>	0.74	2.44	0.27	0.02
<b>P-30</b>	1.76	3.12	0.45	0.03

$$R_f = 1 - K_u(V - V_o) \quad (2.17)$$

where:

$$\begin{aligned} K_u &= 0.295 \text{ (0.09 in English units), and} \\ R_f &= \text{Ratio of frontal flow intercepted to total frontal flow (cannot be greater than 1.0).} \end{aligned}$$

Side flow interception efficiency depends on the curb-opening efficiency. Equation (2.18) takes these parameters to estimate side flow efficiency or ratio of side flow interception ( $R_s$ ). With both frontal and

side efficiencies obtained, equation (2.19) estimates overall interception efficiency ( $E$ ). If the grate is installed within the depressed section of a composite gutter, but the grate width ( $W_g$ ) is lower than the depression width ( $W$ ) like in Figure 9.b, equation (2.20) must first be applied to adjust the correct flow ratio ( $E_o'$ ). Total flow ( $Q$ ) can now be divided into the intercepted flow ( $Q_i$ ) and bypassing flow ( $Q_b$ ).

$$R_s = 1 / \left( 1 + \frac{K_u V^{1.8}}{S_x L^{2.3}} \right) \quad (2.18)$$

where:

$$\begin{aligned} K_u &= 0.0828 \text{ (0.15 in English units), and} \\ R_s &= \text{Ratio of side flow intercepted to total side flow.} \end{aligned}$$

$$E = R_f E_o + R_s (1 - E_o) \quad (2.19)$$

where:

$E$  = Efficiency of grate inlet.

$$E_o' = E_o (A_w' / A_w) \quad (2.20)$$

where:

$$\begin{aligned} E_o' &= \text{Adjusted frontal flow area for grates in composite cross-sections,} \\ A_w' &= \text{Gutter flow area in a width equal to the grate width, } m^2 \text{ (} ft^2 \text{), and} \\ A_w &= \text{Flow area in depressed gutter width, } m^2 \text{ (} ft^2 \text{).} \end{aligned}$$

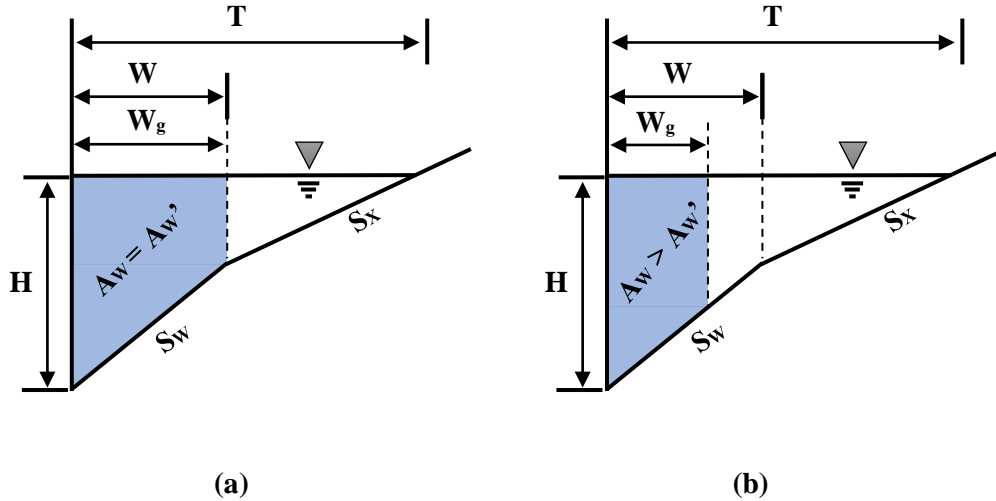


Figure 9. Composite gutter section with installed grate inlet. (a) Grate width ( $W_g$ ) equal to depression width ( $W$ ).  
(b) Grate width lesser than depression width.

### 2.2.3. Combination Inlets

Combination inlets are comprised of both a curb-opening and one or multiple grates. Existing installations vary with where the grate inlets are located. The HEC-22 evaluation requires a “sweeper” configuration, where the grate be located at the end of the curb opening, or just after it, like the ones in Figure 10. In both cases, the analysis is the same because the curb opening beside the grate has a negligible interception capacity.

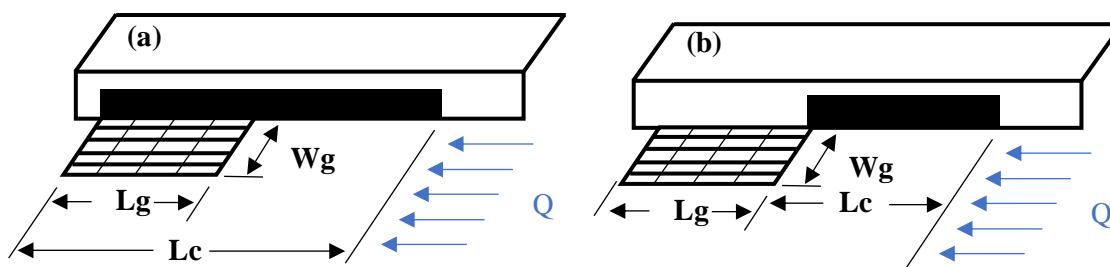


Figure 10. Combination inlets. (a) With curb-opening beside grate. (b) Without curb-opening beside grate.

Incoming runoff flow meets the curb-opening inlet first. Its efficiency must be determined before continuing with the grate inlet. The previously covered equations (2.9) through (2.13) apply when estimating the interception efficiency of the curb-opening. There is a negligible flow interception behind the grate because this part of the curb-opening does not function if the grate is not clogged or submerged. This suggests the opening length ( $L$ ) used in equation (2.11) or (2.13) is ( $L = L_c - L_g$ ) in Figure 10.a, while Figure 10.b uses  $L = L_c$ . The intercepted flow ( $Q_i$ ) is then subtracted from the total flow ( $Q$ ) before evaluating grate inlet efficiency.

The runoff flow that encounters the grate inlet is considered as  $Q - Q_i$ . Equations (2.1) through (2.8) and equations (2.14) through (2.20) are used where applicable. Determining grate efficiency is followed by quantifying grate intercepted flow. Reviewed literature (Guo and MacKenzie, 2012) indicates that the sum of the individual curb-opening and grate inlet interceptions consistently overestimates the combination inlet’s actual interception capacity. This has led to the development of equation (2.21) to estimate final interception capacity through combination inlets shown.

$$Q_{combi} = Q_{curb} + Q_{grate} - K_u \sqrt{Q_{curb} Q_{grate}} \quad (2.21)$$

where:

$$\begin{aligned} K_u &= 0.37 \text{ for bar grates,} \\ Q_{combi} &= \text{Combination inlet interception capacity, } m^3/s \text{ (} ft^3/s \text{),} \\ Q_{curb} &= \text{Curb-opening interception capacity, } m^3/s \text{ (} ft^3/s \text{), and} \\ Q_{grate} &= \text{Grate inlet interception capacity, } \frac{m^3}{s} \left( \frac{ft^3}{s} \right). \end{aligned}$$

#### 2.2.4. Clogging Effect

Grate inlets and curb-opening inlets can get clogged with debris carried by incoming runoff. Previous clogging factors suggest using a 50% and 10% reduction of expected interception for grate inlets and curb-opening inlets respectively. The assumption of needing 8 grates due to clogging after calculating 4 grates had enough capacity is unrealistic, as well as needing a 10 m long curb-opening after calculating 5m.

Field studies and experiments have led to the development of a decaying clogging factor ( $C_g$ ) with equation (2.22), where an increase in the number of inlets ( $N$ ) decreases the effect of the clogging factor. Individual debris decay factors ( $e$ ) were experimentally obtained for grate and curb-opening inlets in Denver, Colorado, but their magnitude should be researched in areas with different climates. The recommended clogging factor for grates and curb-openings remain 0.50 and 0.10 respectively when analyzing a single-unit inlet, but the reduced factor when using 4 grates as an example results in 0.25. The result can be interpreted as 6 grates with average clogging having the same interception capacity as 4 completely unclogged grates. As well as the clogging factor for 4 curb-openings resulting in 0.04, which describes how a 5.2 m long opening with average clogging performs like a 5.0 m long unclogged opening.

$$C_g = C_o / [N(1 - e)] \quad (2.22)$$

where:

$$\begin{aligned} C_g &= \text{Multiple unit clogging factor, and} \\ C_o &= \text{Single-unit clogging factor 0.10 (For curb-opening inlets),} \\ &\quad 0.50 \text{ (For grate inlets),} \end{aligned}$$



$N$  = Number of units, and  
 $e$  = Debris decay ratio 0.25 (For curb-opening inlets),  
0.50 (For grate inlets).

The clogging factor is used in the empirically developed equation (2.23) to obtain an equivalent unclogged inlet length. The adjusted length should be applied when evaluating grate and curb-opening inlet efficiencies on equations (2.11), (2.13), (2.16), and (2.18). If evaluating a combination inlet, equation (2.21) already includes a reduction factor. This means evaluating the individual efficiencies of the grate and curb-opening inlets within a combination inlet does not require the use of an equivalent length ( $L_e$ ). The equivalent unclogged inlet lengths are given by:

$$\begin{aligned}
 L_e &= (1 - C_g)L && \text{(For multiple-unit inlet)} \\
 L_e &= (1 - C_o)L && \text{(For single-unit inlet)}
 \end{aligned}
 \tag{2.23}$$

where:

$L_e$  = Effective length of the inlet,  $m$  ( $ft$ ), and  
 $L$  = Grate inlet length,  $m$  ( $ft$ ).

A single grate is easily discernible, but the same cannot be said about curb-openings. Figure 11 shows how the equivalent length of the grate and curb-opening drainage inlets varies with the number of inlets installed. Since debris can get lodged on the vertical supports that hold the otherwise cantilever curb, the unit quantity of curb-opening inlets can be identified by the divisions caused by the vertical supports.

It should be noted that clogging patterns highly disturb the normal flow pattern which create significant uncertainties as how a clogged inlet will operate. This empirical consideration accounts for part of the uncertainties but distances its accuracy from clean inlet behavior.

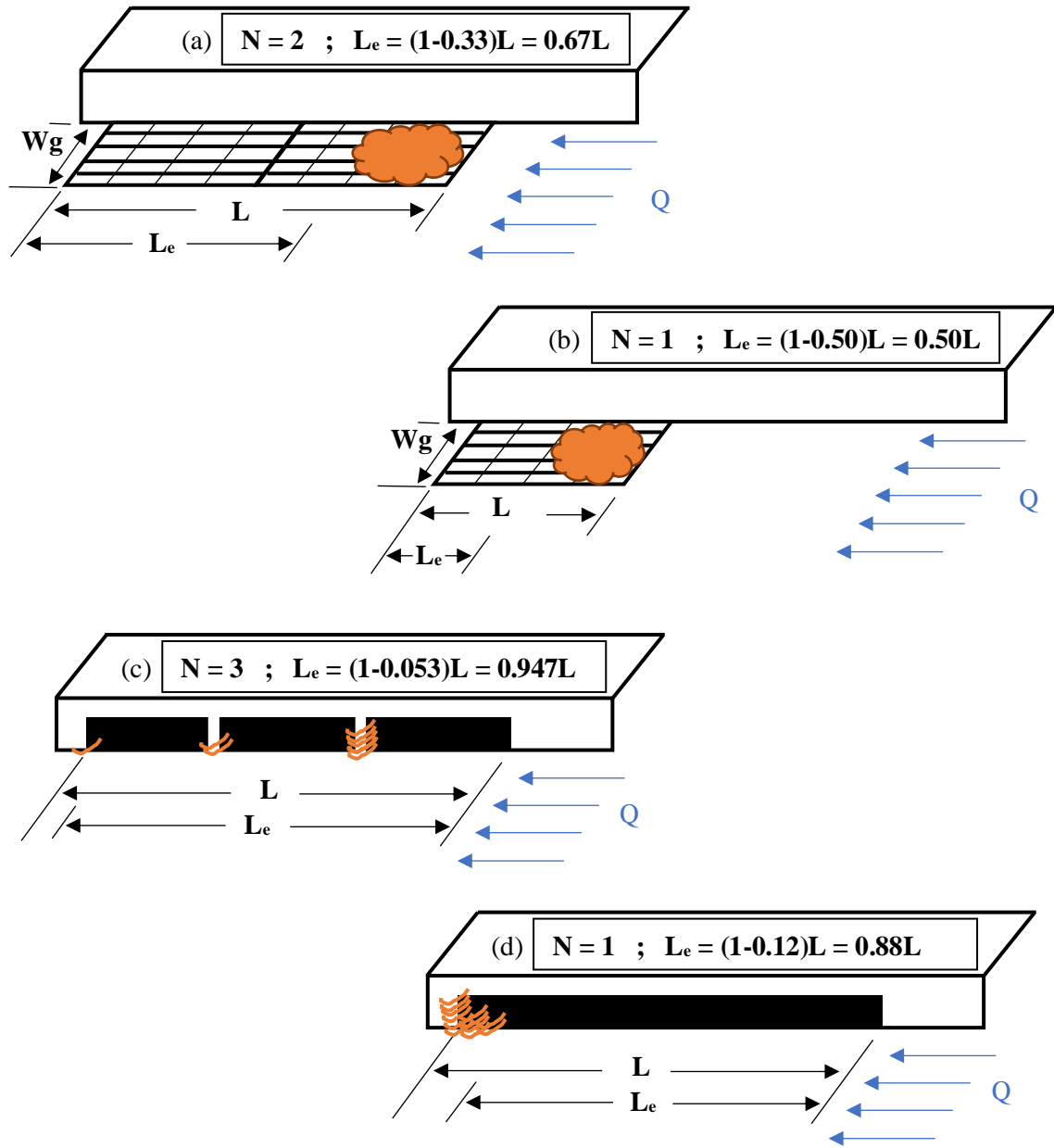


Figure 11. Inlet equivalent lengths from clogging factor. (a) Multi-unit grate inlet. (b) Single-unit grate inlet. (c) Multi-unit curb-opening inlet. (d) Single-unit curb-opening inlet.

### 3. HSM METHODOLOGY

#### 3.1. HSM Description

The new regulations for the Design, Operational Criteria, and Maintenance of Stormwater Systems in Puerto Rico (Junta de Planificación de Puerto Rico, 2022, in Spanish) require the procedures presented in the previous Chapter for the design of stormwater systems. Peak discharge and other criteria must be fulfilled. Finally, the regulations require computer simulations to verify and adjust the system components using design hydrographs. HSM will be a useful tool for this simulation phase.

A Visual Basic for Applications (VBA) macro developed for the HSM application has a user-friendly interface within MS Excel. The results from HSM are then inserted into EPA SWMM to continue the simulation process. The present version includes grate inlets, curb-opening inlets, and combinations inlets. Additional inlet types could be included as further expansion. The following steps describe the application of HSM in SWMM:

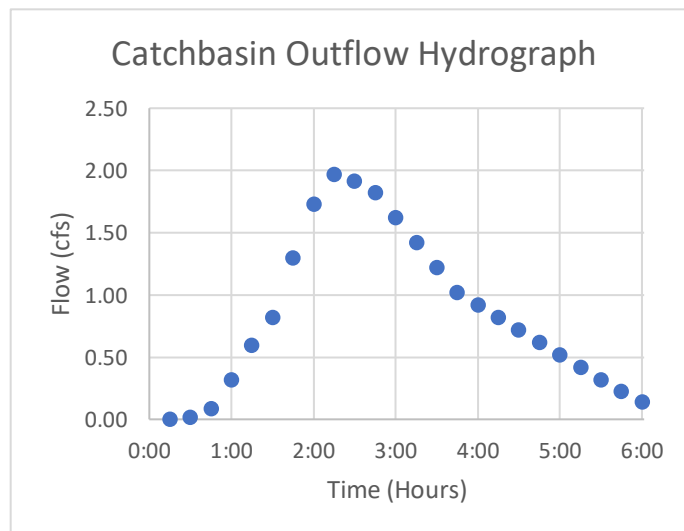


Figure 12. Hydrograph from first drainage zone.

1. **Input a total flow hydrograph:** A grate inlet is considered the exit point of an observed catch basin (i.e., a road segment). A total flow hydrograph is shown in Figure 12. This hydrograph could be generated from hydrologic models such as HEC-HMS (HEC, 2021), TR-20 (USDA, 1992), TR-55 (USDA, 1986), or SWMM (EPA, 2015) or any hydrograph provided by the designer. HSM is

applied to each of these hydrographs individually. If a layout of the stormwater system is available, the hydrographs from the drainage basins must be identified and assigned to the respective inlet and street location

2. **Compute the interception capacity of the inlet using the efficiency ( $E = Q_i/Q$ ), equation (2.7):**

The efficiency of a particular inlet is case-specific, depending on inlet type, total gutter flow, pavement roughness, longitudinal and cross slopes. After selecting a set of parameters, Figure 13 shows how interception efficiency varies with the runoff flows presented in the previous hydrograph. The inlet becomes less efficient as the gutter flow increases. It reached 75.9% at the peak discharge of 1.97cfs. These elements are used to determine the grate inflow, carryover flow and their respective hydrographs, as presented in Figure 14.

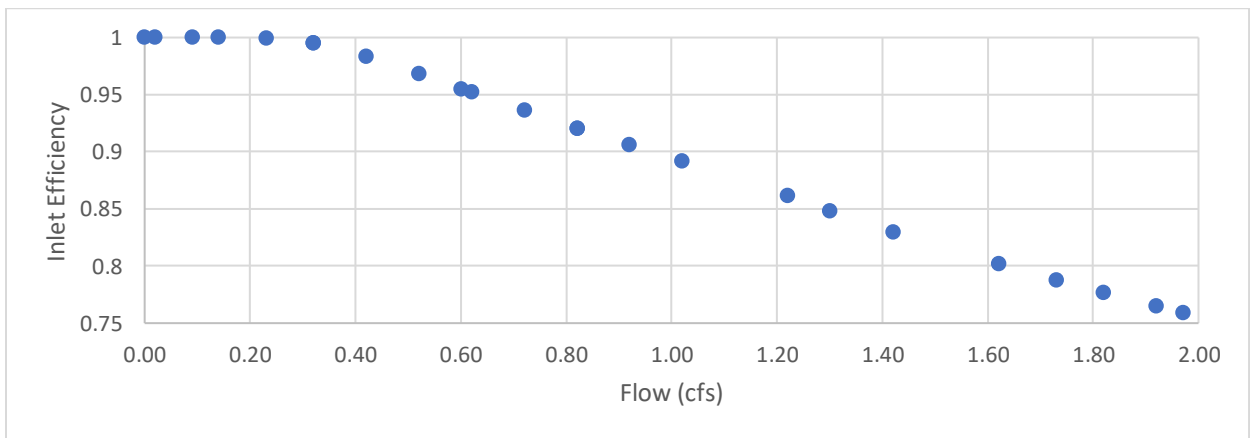


Figure 13. Efficiency versus Total Flow, derived from Figure 12 Efficiency at storm peak = 75.9%.

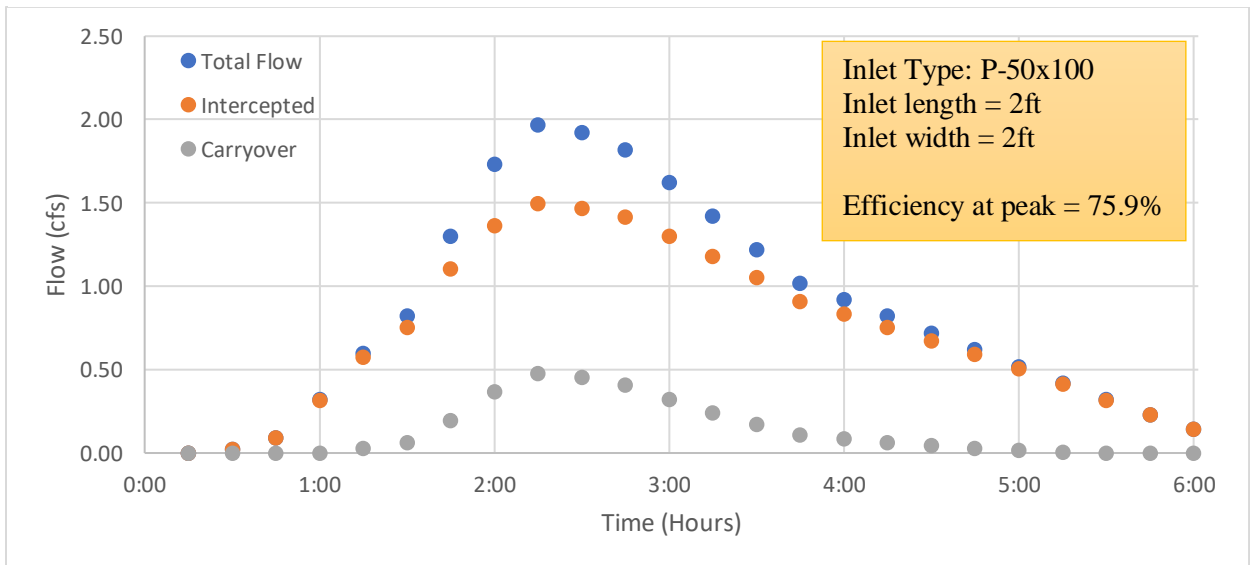


Figure 14. Separated hydrographs derived from Figure 12 and Figure 13.

3. **Insert hydrographs in SWMM:** The resulting hydrographs correspond to a drainage inlet location. These hydrographs are inserted into the corresponding SWMM nodes, allowing the

simulation of specific inlet types considered for installation. Two models are built independently. One for the minor system and the other for the major system. If required, both models could be joined at the project outset.

4. **Simulate the major and minor systems simultaneously as two separated systems:** In SWMM this is shown in Figure 15, starting from the point where the discharges were first separated. The major system is modeled as half the street cross-section as presented in Figure 16. The minor system is modeled as a circular pipe. Once the system interacts with another inlet downstream, repeat Step 2 and Step 3 to continue the hydrograph separation process and simulation in the next inlet node.

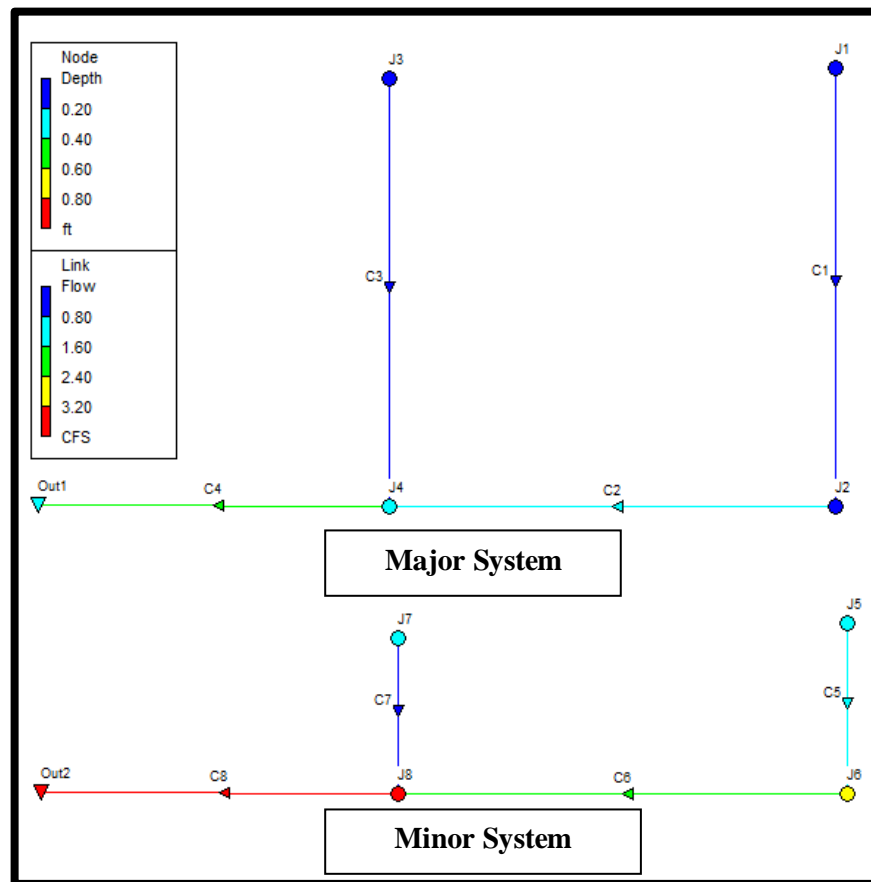


Figure 15. SWMM schematic for simulating a minor (bottom) and major system (top) of the same stormwater system.

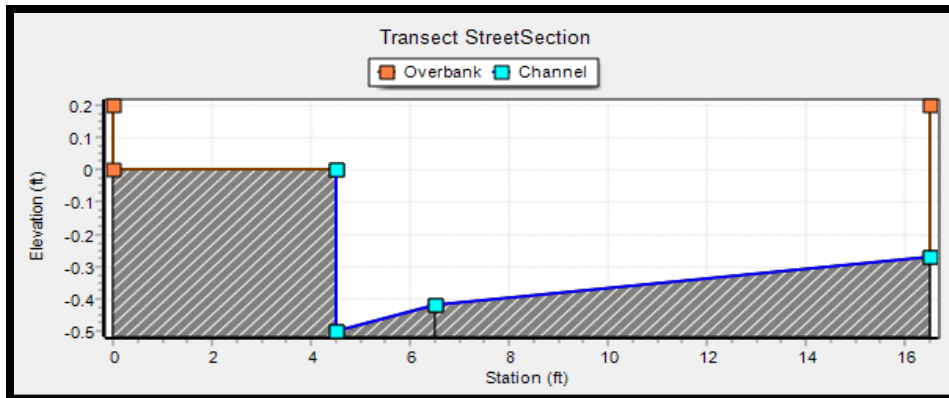


Figure 16. SWMM schematic for half a street-gutter cross section.

The following downstream portion receives runoff from its corresponding catch basin, as well as upstream flow obtained through the separated hydrographs. An 80% interception during peak discharge means 80% of peak flow enters the sewer system. The other 20% is added to the existing surface runoff downstream. A procedure without separation assumes 100% of upstream flow enters the downstream minor system, underestimating flooding, and overestimating pipe discharge.

5. **Repeat Steps 2 through Step 4** for all existing inlet nodes in the model until reaching the end of the system. The final road segment and pipe segment are shown as C4 and C8 respectively in Figure 15.

### 3.2. Description of VBA Program Interphase and Visualization of Results

The VBA user interphase is contained in a single Excel spreadsheet. Figure 17 contains columns A through E of the spreadsheet, which includes the space to input the runoff hydrograph to be analyzed. The input data is accepted in various formats of Date/Time/Value or Time/Value that are compatible with SWMM as exported text files. Figure 18 shows the gutter and inlet parameter input tables within columns G through P. The blue highlighted cells require user inputs, such as gutter slopes and inlets dimensions, while the green highlighted cells are calculated by the algorithm as it runs. Clicking on the button labeled as “Run HSM subroutine” would start the analysis and deliver the separated hydrographs.

Enter input table data as one of EPA SWMM accepted .txt formats:

;Date Time Value  
MM/DD/YYYY HH:mm:SS or HH:mm X

;Time Value  
(Empty) HH:mm:SS or HH:mm or HH.decimals X

	A	B	C	D	E		A	B	C	D	E
4						4					
5		Input Table:			Calculated Output:	5		Input Table:			Calculated Output:
6		Date	Hours	Inflow	Spread (T), [m or ft]	6		Date	Hours	Inflow	Spread (T), [m or ft]
7			0:15:00	0		7	4/15/2022	0:15:00	0		
8			0:30:00	0.02		8	4/15/2022	0:30:00	0.02		
9			0:45:00	0.09		9	4/15/2022	0:45:00	0.09		
10			1:00:00	0.32		10	4/15/2022	1:00:00	0.32		
11			1:15:00	0.6		11	4/15/2022	1:15:00	0.6		
12			1:30:00	0.82		12	4/15/2022	1:30:00	0.82		
13			1:45:00	1.3		13	4/15/2022	1:45:00	1.3		
14			2:00:00	1.73		14	4/15/2022	2:00:00	1.73		
15			2:15:00	1.97		15	4/15/2022	2:15:00	1.97		
16			2:30:00	1.92		16	4/15/2022	2:30:00	1.92		
17			2:45:00	1.82		17	4/15/2022	2:45:00	1.82		
18			3:00:00	1.62		18	4/15/2022	3:00:00	1.62		
19			3:15:00	1.42		19	4/15/2022	3:15:00	1.42		
20			3:30:00	1.22		20	4/15/2022	3:30:00	1.22		
21			3:45:00	1.02		21	4/15/2022	3:45:00	1.02		
22			4:00:00	0.92		22	4/15/2022	4:00:00	0.92		
23			4:15:00	0.82		23	4/15/2022	4:15:00	0.82		
24			4:30:00	0.72		24	4/15/2022	4:30:00	0.72		
25			4:45:00	0.62		25	4/15/2022	4:45:00	0.62		
26			5:00:00	0.52		26	4/15/2022	5:00:00	0.52		
27			5:15:00	0.42		27	4/15/2022	5:15:00	0.42		
28			5:30:00	0.32		28	4/15/2022	5:30:00	0.32		
29			5:45:00	0.23		29	4/15/2022	5:45:00	0.23		
30			6:00:00	0.14		30	4/15/2022	6:00:00	0.14		

Figure 17. VBA interphase runoff hydrograph input table. (Left) Time/Value format. (Right) Date/Time/Value format.

4	F	G	H	I	J	K	L	M	N	O	P	Q	R	S	T
5		Manual Input (Write below) =			Run HSM subroutine				Export Results		Protect/Unprotect HSMinput worksheet				
6		Calculated input =													
7															
8		Gutter Parameters List:			Create Hydrograph Plots				Inlet Parameters List:						
9		Gutter Geometry =							KL (PR, HEC) =		(Will adjust automatically)				
10		Units system =							Grate Unit Length (L) =		2 (Write as Meters or Feet)				
11		Kt =			(These coefficients depend on the Units System being used.)				Grate Unit Width (Wg) =		2 (Grate inlet exclusive. Write as Meters or Feet)				
12		Kv =							# of Grates =		1				
13		Krf =			They will adjust automatically when running the subroutine.)				Curb-Op Unit Length (L) =		2.5 (Write as Meters or Feet)				
14		Krs =							# of Curb-Openings =		4				
15		Manning's n =			0.016										
16		Longitudinal Slope (SL) =			0.015 (Not as percentage. Example, write 0.03 for 3%)										
17		Transverse Slope (Sx) =			0.055 (Not as percentage. Example, write 0.04 for 4%)										
18		Depression Depth (a) =			(Composite gutter only. Write as Meters or Feet)										
19		Depression Width (W) =			(Composite gutter only. Write as Meters or Feet)										
20		Depression Slope (Sw) =													
21															
22															
23		Is roadway symmetrical?			Non-Symmetrical (Use Figures d and e as reference)										
24															
25															
26															
27															
28		Max Resultant Spread (T) =													
29		Flow depth at gutter edge (H) =													
30															

Figure 18. VBA interphase parameter input tables and interactive buttons.

The windows in Figure 19 appear as soon as the algorithm runs. They allow the user to choose between the available gutter geometry options and the units of the input values, which determine the coefficient values. Once the algorithm concludes, Figure 20 shows the runoff input table together with each corresponding spread (T) value, while highlighting the peak spread of the storm event. The peak spread and the resulting flow depth (H) at the gutter edge are highlighted in Figure 21 together with the parameter tables to achieve an overview of the analysis that was performed.

Geometry Selection ✕

Select Intended Gutter Geometry:

☒ Uniform/Triangular Section (Figure a)

☐ Composite Section (Figure b)

Continue

Units Selection ✕

Select Intended Units System:

☐ Metric (CMS, Meters, etc.)

☒ Imperial (CFS, Feet, etc.)

Continue

Figure 19. Gutter geometry (Left) and Unit selection (Right) windows.

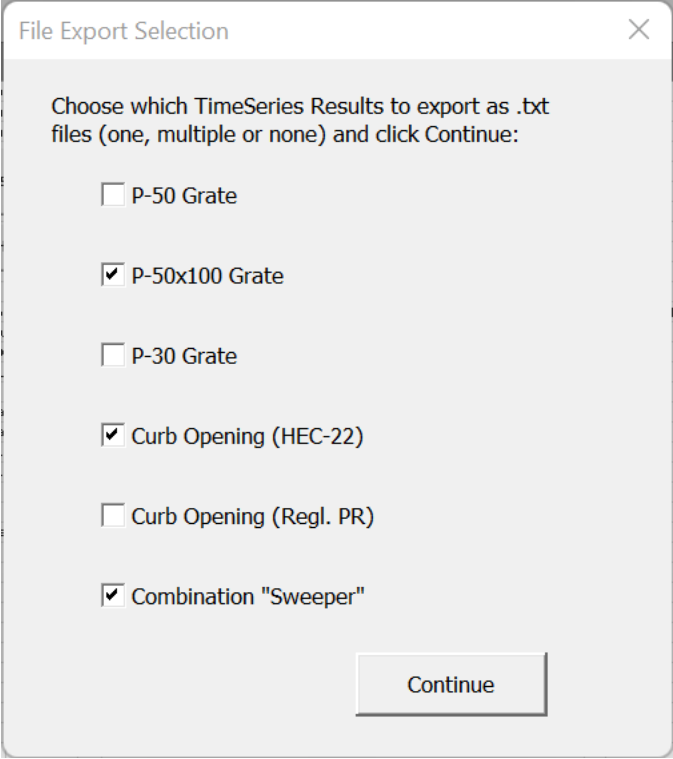
	A	B	C	D	E
4					
5		Input Table:			Calculated Output:
6		Date	Hours	Inflow	Spread (T), [m or ft]
7			0:15:00	0	0.0000
8			0:30:00	0.02	0.8217
9			0:45:00	0.09	1.4443
10			1:00:00	0.32	2.3240
11			1:15:00	0.6	2.9418
12			1:30:00	0.82	3.3074
13			1:45:00	1.3	3.9313
14			2:00:00	1.73	4.3760
15			2:15:00	1.97	4.5944
16			2:30:00	1.92	4.5503
17			2:45:00	1.82	4.4600
18			3:00:00	1.62	4.2695
19			3:15:00	1.42	4.0636
20			3:30:00	1.22	3.8388
21			3:45:00	1.02	3.5895
22			4:00:00	0.92	3.4532
23			4:15:00	0.82	3.3074
24			4:30:00	0.72	3.1500
25			4:45:00	0.62	2.9782
26			5:00:00	0.52	2.7881
27			5:15:00	0.42	2.5735
28			5:30:00	0.32	2.3240
29			5:45:00	0.23	2.0533
30			6:00:00	0.14	1.7045

Figure 20. Runoff hydrograph input table with spread (T) results after algorithm run. Maximum spread highlighted.





The option of exporting the results as text files is available through the “Export Results” button in Figure 21. The window in Figure 23 appears, allowing the user to choose one or multiple options to export as text files. For each option, the user is prompted with the chance to choose where to save an intercepted flow text file, as well as a carryover flow file. These can be inserted into SWMM or another modeling software.



The image shows a software dialog box titled "File Export Selection" with a close button (X) in the top right corner. The main text inside the dialog reads: "Choose which TimeSeries Results to export as .txt files (one, multiple or none) and click Continue:". Below this text are six checkboxes, each followed by a label. The first three are "P-50 Grate", "P-50x100 Grate", and "P-30 Grate". The last three are "Curb Opening (HEC-22)", "Curb Opening (Regl. PR)", and "Combination 'Sweeper'". The checkboxes for "P-50x100 Grate", "Curb Opening (HEC-22)", and "Combination 'Sweeper'" are checked, while the others are unchecked. At the bottom right of the dialog is a button labeled "Continue".

Option	Selected
P-50 Grate	<input type="checkbox"/>
P-50x100 Grate	<input checked="" type="checkbox"/>
P-30 Grate	<input type="checkbox"/>
Curb Opening (HEC-22)	<input checked="" type="checkbox"/>
Curb Opening (Regl. PR)	<input type="checkbox"/>
Combination "Sweeper"	<input checked="" type="checkbox"/>

*Figure 23. Export results window.*

## 4. MODEL APPLICATIONS

### 4.1. HSM Application Example 1

#### 4.1.1. Part 1: Initial Evaluation

Figure 17 includes a four-segment major system used to show the approach of simulating a small urban drainage system by applying HSM. The system represents two streets intersecting a road that contains the larger downstream pipe. The final network segment is named C4, and the drainage inlets would be installed on the nodes named J1, J2, J3, and J4. SWMM runoff module was used to simulate a storm event by providing a hyetograph. Figure 24 shows the hyetograph used as the storm for all sub-catchments in this simulation. SWMM kinematic wave approach was used. In general, any hydrographs could be used as input for HSM. Through the connections displayed in Figure 25, runoff is discharged along with the road network and a designer would consult these results together with construction codes to define the placement or removal of additional drainage inlets.

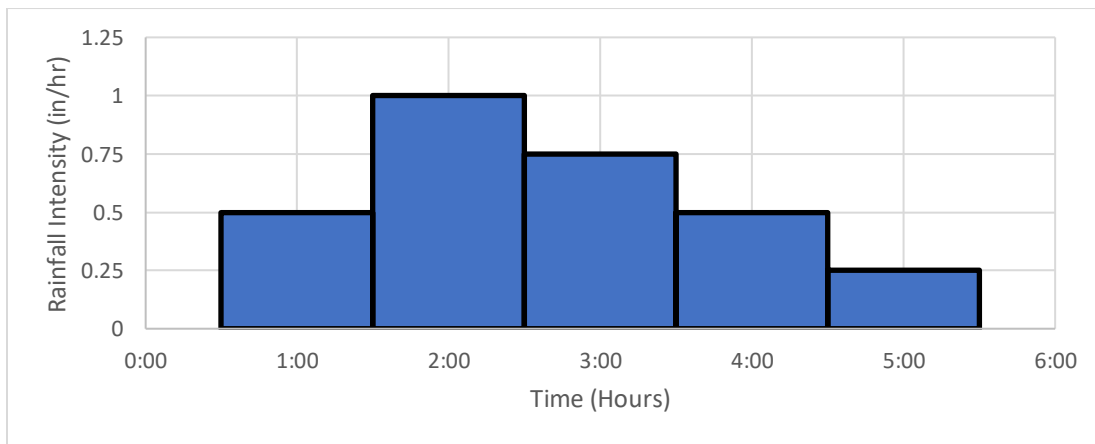


*Figure 24. Storm event hyetograph.*

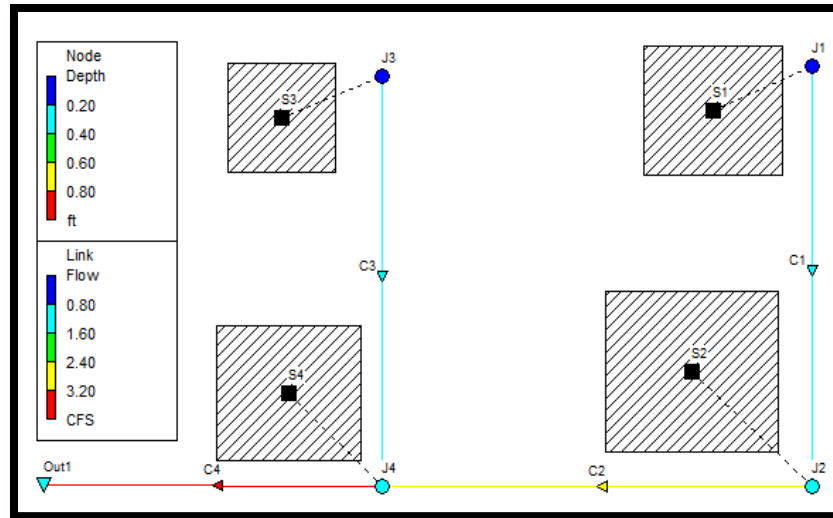


Figure 25. SWMM simulation without using HSM.

Other than requiring additional computational power to run both the major and minor systems simultaneously, the HSM allows the HEC-22 recommendations of determining inlet efficiency to be applied without adding too much effort by the designer. Introducing the runoff time series of each catchment into the VBA program, the user can shuffle through gutter and inlet parameters to obtain the hydrographs and their effects on intercepted and carryover flows for different types of inlets. Once the type of inlet is selected, the VBA macro will export the hydrographs into text files to be used as input into EPA SWMM or any other hydrologic simulation program

The uppermost inlets are represented as the J1 and J3 nodes, which had runoff originating from the S1 and S3 catchments respectively. After separating the hydrographs, HSM produces text files with the hydrographs that correspond to the major and minor system SWMM allows the user to open a “Properties” window for each node. Within, the “Inflow” option includes a “Time Series” flow where the user can input the HSM exported files, as shown in Figure 26.

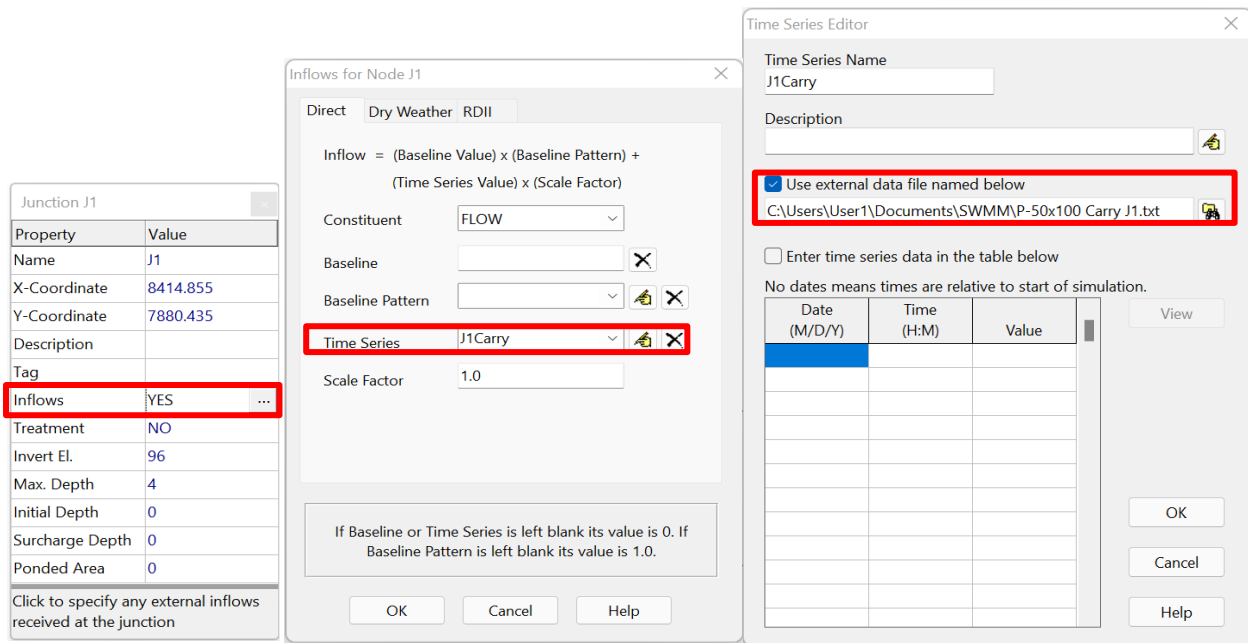


Figure 26. Screens from SWMM for the input of inlet and street hydrographs.

The model portrayed in Figure 27 now includes the minor system underneath. The only difference between them is that the major system is modeled as open channels equal to half the street, while the minor system is modeled as circular pipes. The carryover flow text file from S1 was used as input in the J1 inlet and the intercepted flow file was used in its respective node, J5. The S3 catchment was modeled equal to S1, and the same procedure was performed with the inlet on nodes J3 and J7. On both the J1 and J3 nodes, the chosen inlet was about 75% efficient during the storm peak, as shown previously in Figure 14. That intercepted flow hydrograph is introduced into nodes J5 and J7, while the other 25% carryover flow in J1 and J3.

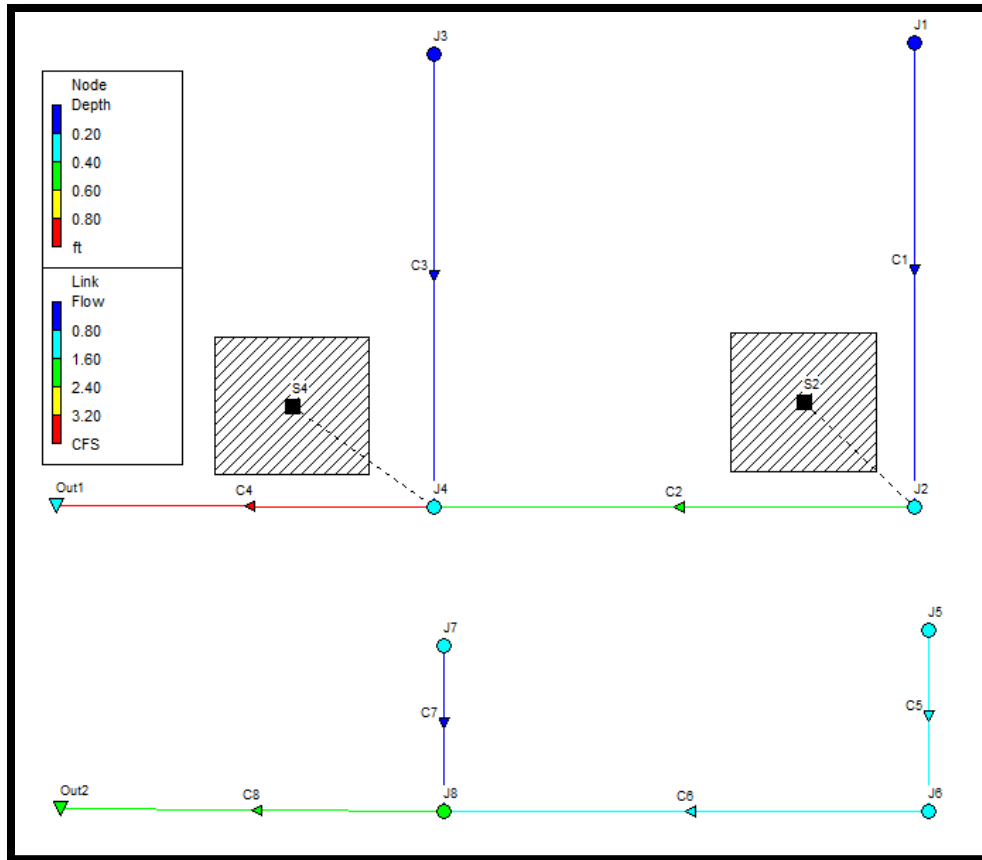


Figure 27. Major system (top) and minor system (bottom) after HSM in J1/J5 and J3/J7.

Similarly, the resulting discharge in J2 is inserted into the HSM program. Repeating the process without changing the inlet specifications in inlet J2 obtains the intercepted and carryover flows that correspond to J6 and J2 respectively, resulting in the Figure 28 system. Continuing with the procedure considers the effects of S4 runoff together with carryover flow from nodes J2 and J3 on inlet J4. Applying HSM to the final inlet, J4, with the same inlet parameters results in the previously presented Figure 15, which ends the HSM application for this system. An evaluation of the results allows the user to recognize if any alteration to the system design is required.

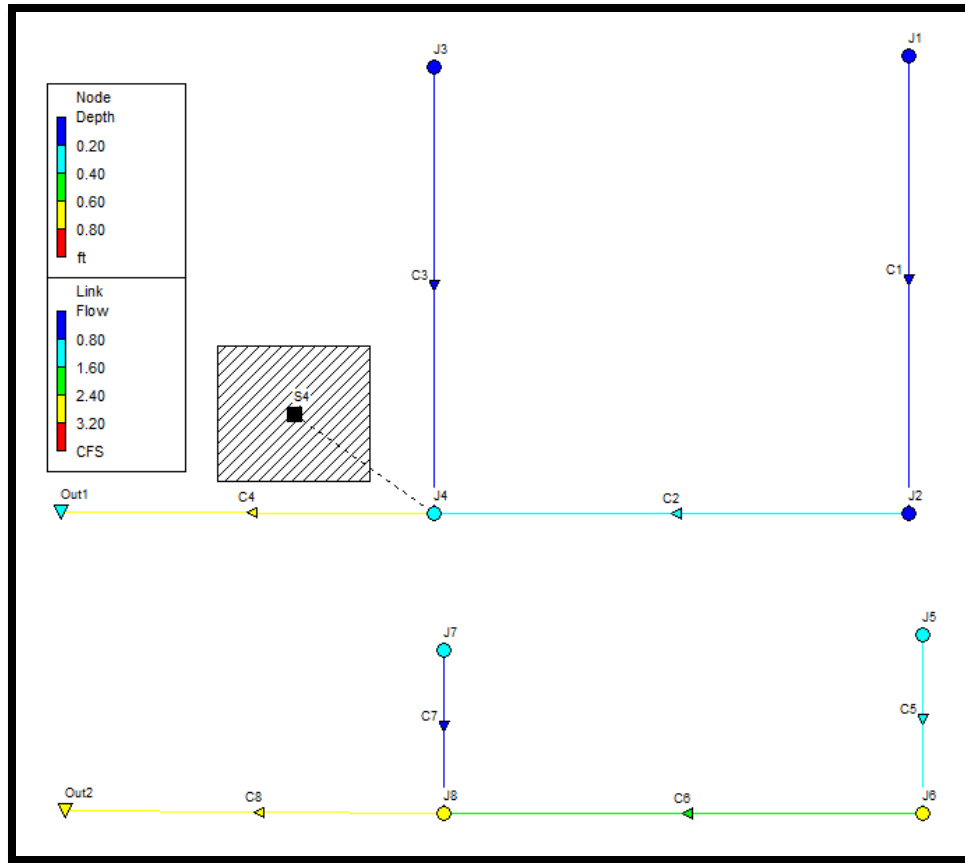


Figure 28. Systems after HSM in J2/J6.

The efficiency curve presented in Figure 29 gives a visual representation of how the current system would have managed the evaluated storm event. The hydrographs in Figure 30 show how the selected parameters achieve a 65/35 division between the intercepted flow (contained within the pipe system) and the carryover flow (potentially flooding the road) during the storm peak at the end of the system. The evaluation for this case suggests that either the inlets or gutter design should be improved to intercept additional flow or that additional inlets should be installed within the existing segments as extra nodes in the SWMM model.

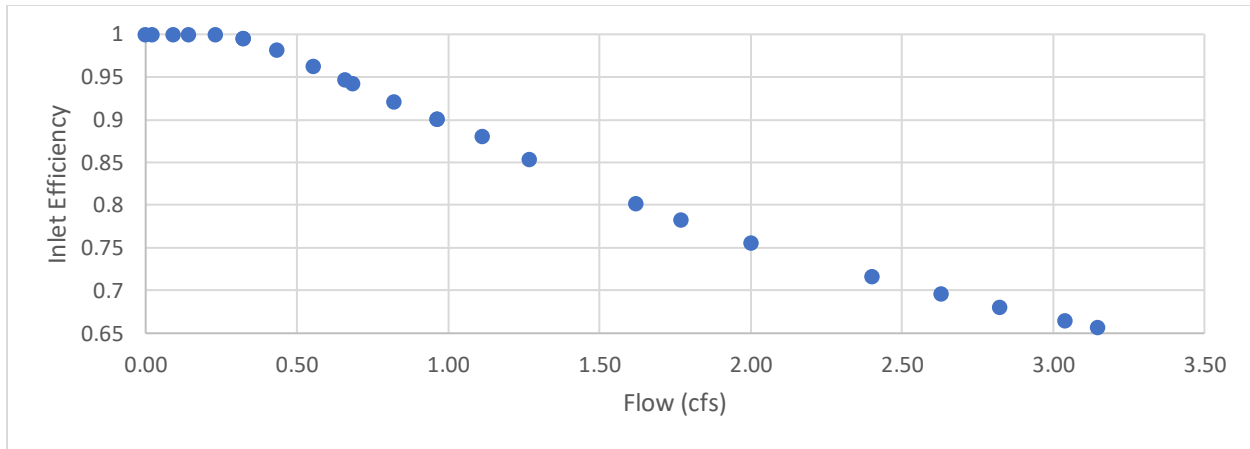


Figure 29. Efficiency vs Total Flow, derived from Figure 16. Efficiency at peak = 65.7%.

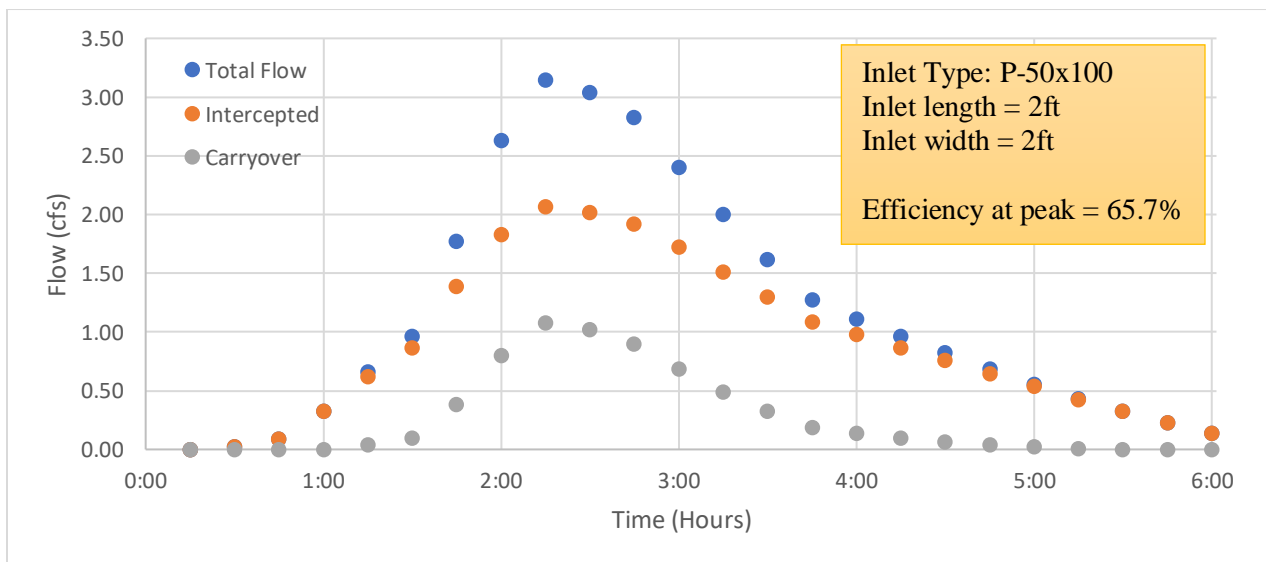


Figure 30. Resultant flows in the last portion of the systems (C4 roadway and C8 pipe).

#### 4.1.2. Part 2: Reevaluation by Improving Existing Inlets

An option for improving the system's performance is installing an extra grate in all the inlet locations. The HSM add-on helps evaluate this option. When maintaining the previous gutter parameters, Figure 31 shows how the upstream inlet's performance changed with adding an extra grate at the same location. Inlet interception improved from 75.9% to 81.9% during storm peak due to a change in inlet length from 2ft to 4ft. Other improvement effects include lesser flow spread (T) and depth (H).



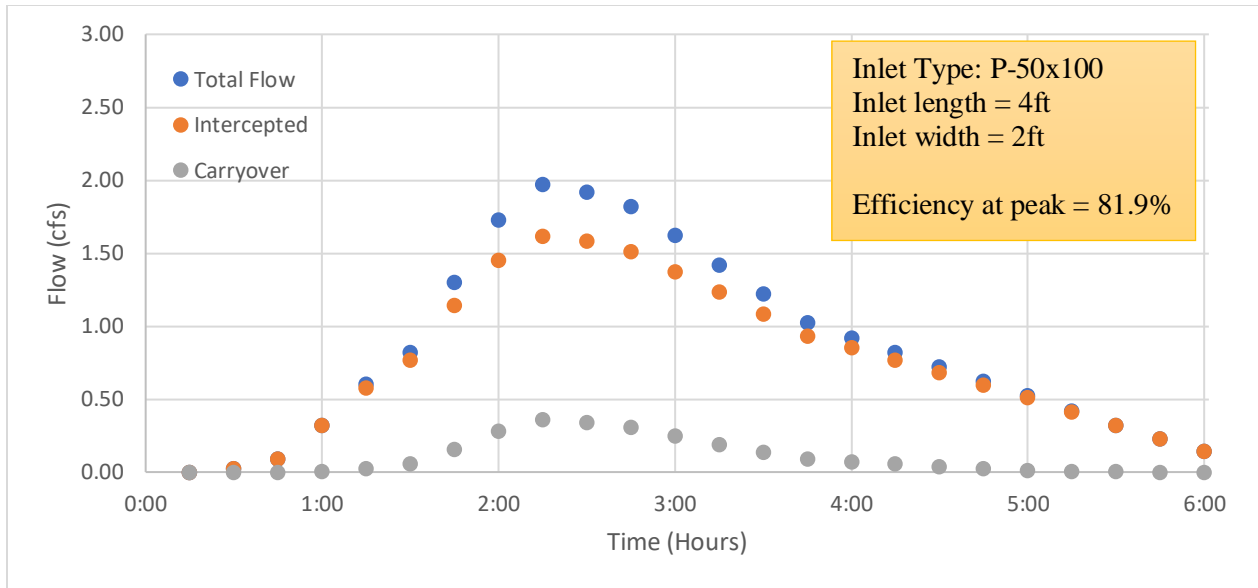


Figure 31. [Case 2] Separated hydrographs at upstream node, J1.

Having a 4ft inlet length by adding an extra grate in all inlet locations and repeating the process along the whole system yields Figure 32. Interception efficiency during the storm peak improved from 65.7% to 76.3%, as well as a reduction from the previously observed flow spread (T) and depth (H). This approach might have improved overall system performance, but some refinement could also yield an acceptable performance without altering the original system as much.

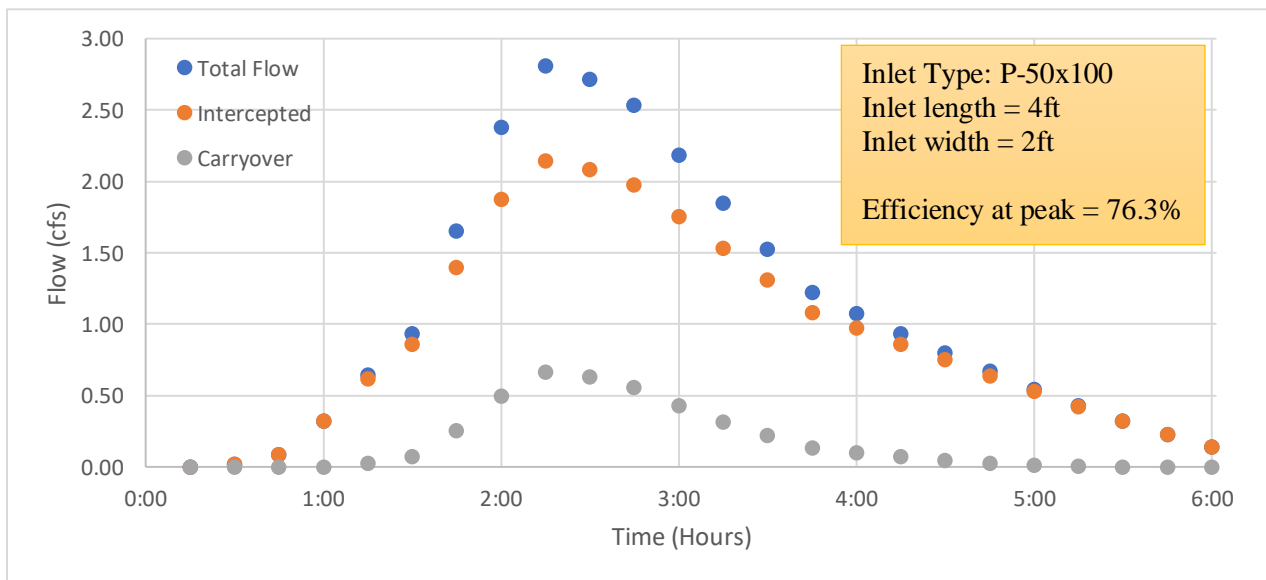


Figure 32. [Case 2] Separated hydrographs at end of system (C4 roadway and C8 pipe).

#### 4.1.3. Part 3: Reevaluation by Adding Inlet Locations

A different alternative to improving overall system performance includes adding inlet locations. Other stormwater drainage system design methods that explore suggestions for minimum inlet location spacing could be consulted. Figure 33 evaluates the option of installing an inlet (node J4) halfway between the inlets in nodes J3 and J5. All the inlets were analyzed with the original inlet length of 2ft, where Figure 14 described the interception capacity of nodes J1 and J3. The proposed inlet upstream of node J5 would reduce the runoff attributed to this inlet, as well as intercept carryover flow from node J3.

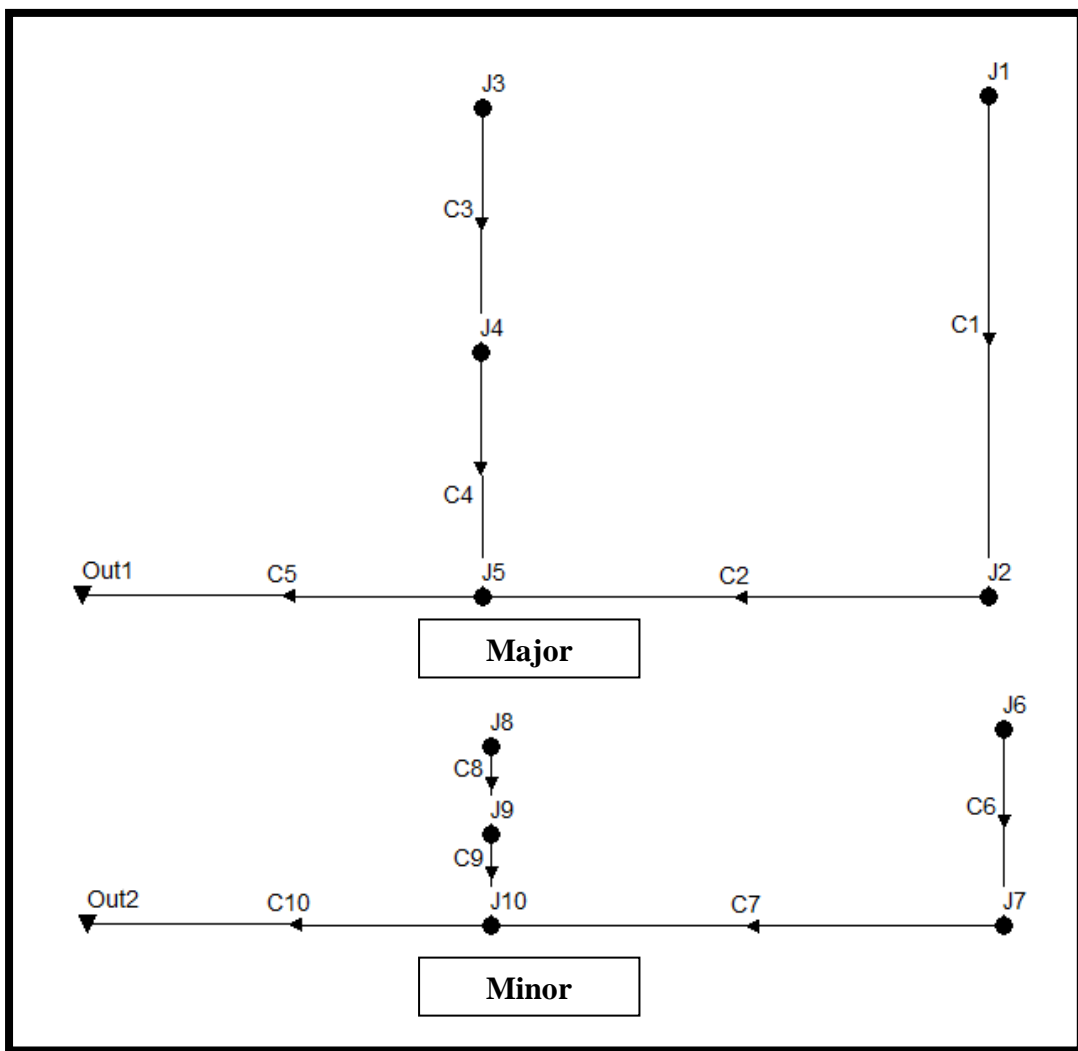


Figure 33. Redrawn system with an extra inlet location, J4/J9.

Figure 34 shows the end-of-system node (J5) performance, which results in a notable improvement from 65.7% to 76.2% interception efficiency during storm peak, as well as a reduction in flow spread (T) and depth (H) at this point. The interception efficiency at the end of the system using the previous option resulted in 76.3%, approximately the same as this option. The slight adjustment of installing a single grate halfway between nodes J3 and J5 gave a similar result at the end of the system as doubling the grate inlet length in all existing nodes.

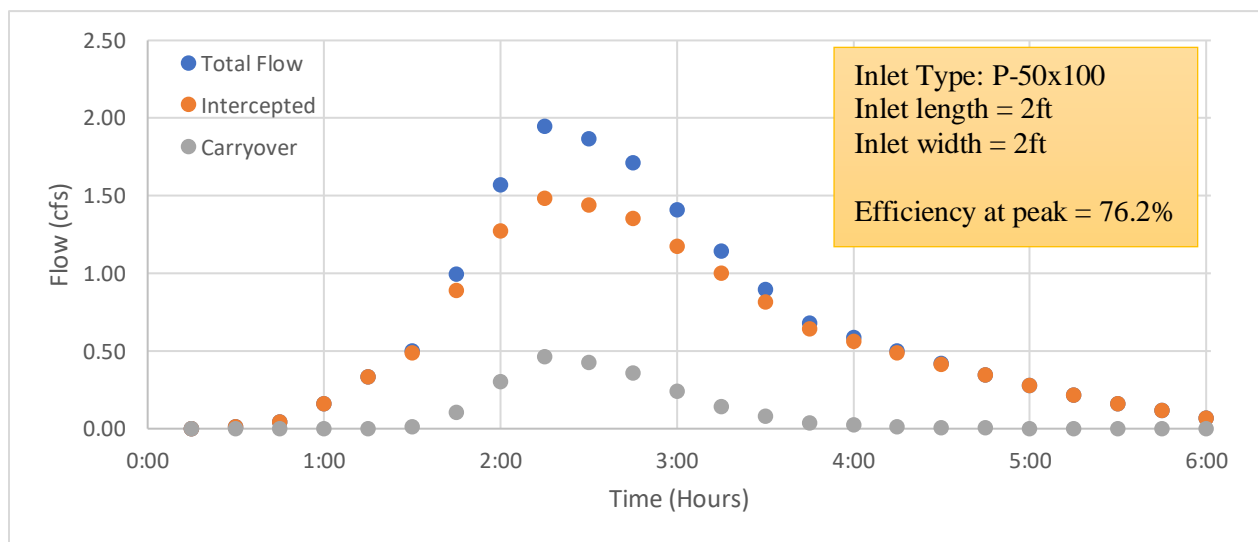


Figure 34. [Case 3] Separated hydrographs at end of system (C4 roadway and C8 pipe).

Unlike the previous adjustment of increasing inlet length everywhere in the system, the performance improvement only occurs in the final section. This option has no benefits for other upstream branches. The least efficient inlet is now on node J2, with an interception efficiency of 71.2% during the storm peak as shown in Figure 35. This option could still be within an acceptable range of regulation, but the specifics of the location should be evaluated before accepting the design. The original evaluation and both reevaluations could all be performed and compared smoothly by using the Hydrograph Separation Method (HSM) tool.

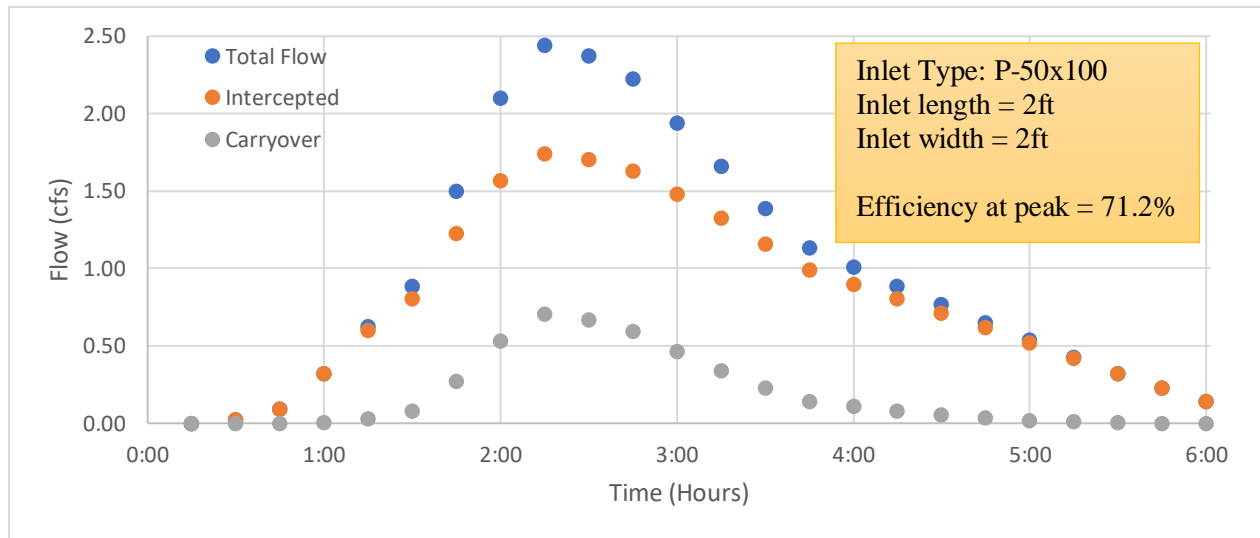


Figure 35. [Case 3] Separated hydrographs at upstream node, J1.

## 4.2. HSM Application Example 2

### 4.2.1. Part 1: Initial Evaluation

Cases, where on-grade 3 or 4-way intersections exist, can be evaluated by the HSM, such as the case in Figure 36. The system performance resulting when all the gutter and inlet parameters are considered is presented in Figures 37 and 38. Figure 37 shows the hydrograph separation and the minimum interception efficiency of 79.4% on the branched nodes; J1, J2, J4, and J5. Figure 38 shows how carryover flow affected inlet performance on the downstream node J6, reducing it to 69.8%.

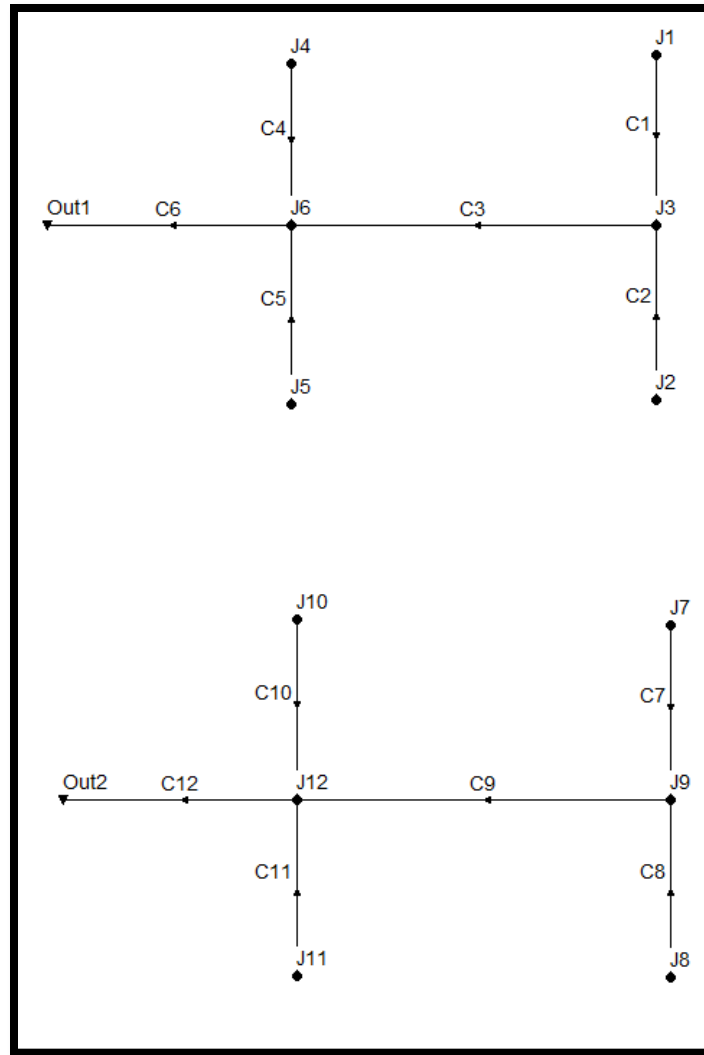


Figure 36. System with a 4-way intersection.

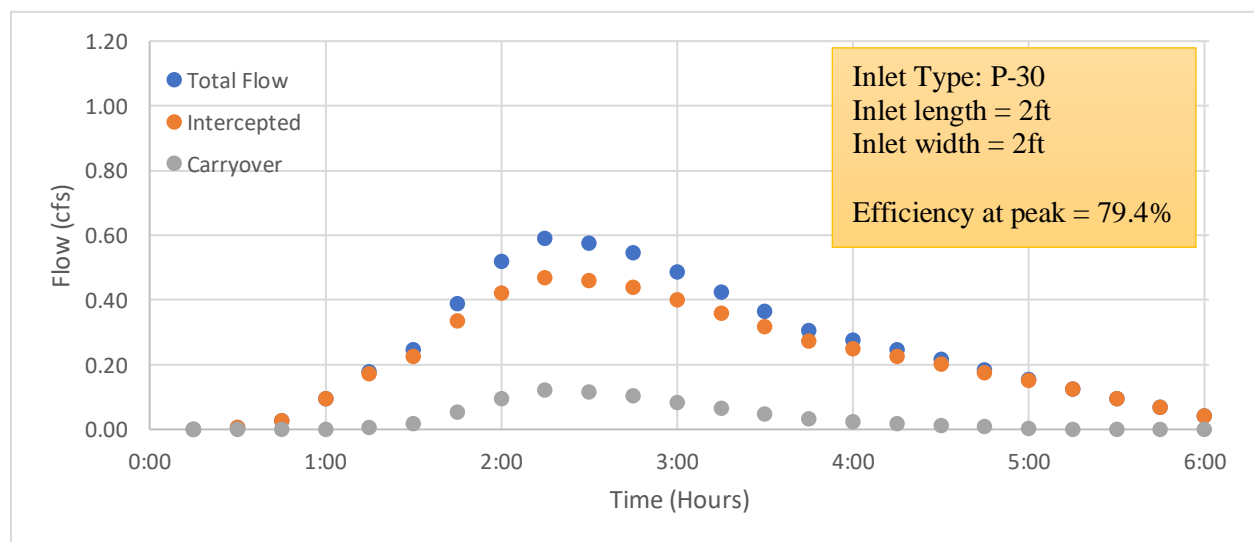


Figure 37. [Case 4] Separated hydrographs at upstream nodes; J1, J2, J4 and J5.

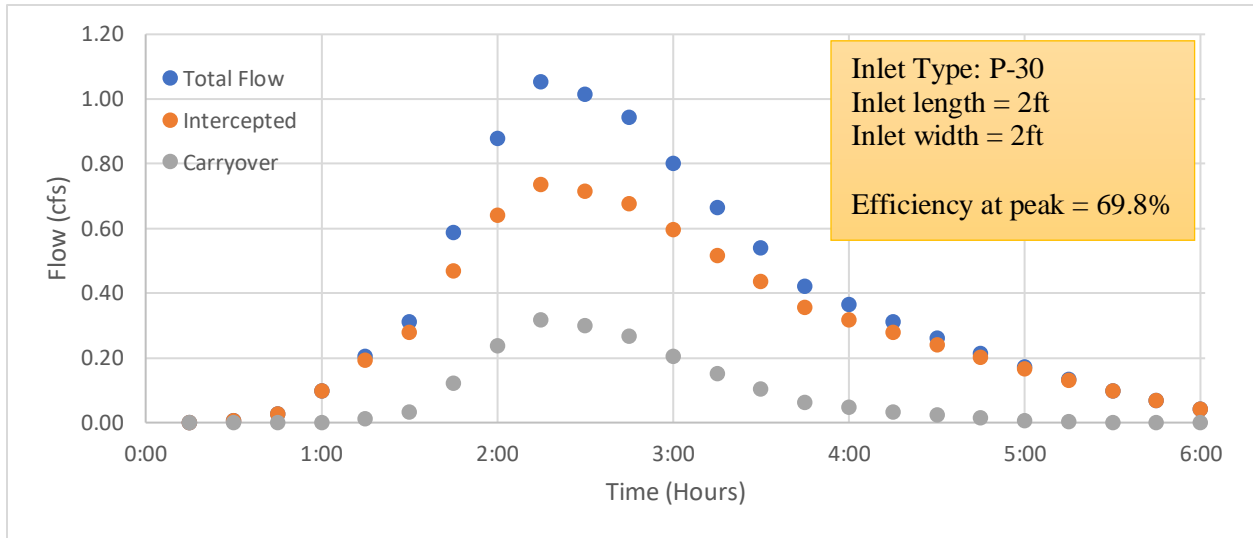


Figure 38. [Case 4] Separated hydrographs at the end of the system (C6 roadway and C12 pipe).

#### 4.2.2. Part 2: Evaluation by Varying Inlet Types

Another alternative made possible through HSM is being able to view the performance of different types of inlets simultaneously. The gutter parameters affect every inlet type differently, and a benefits/costs ratio would be part of the drainage system analysis. In this case, it is possible to keep the previously chosen grate inlets in the branched nodes while changing to better performing curb-opening inlets in nodes J3 and J6. With that alteration, Figure 39 shows the improved interception at the end of the system.

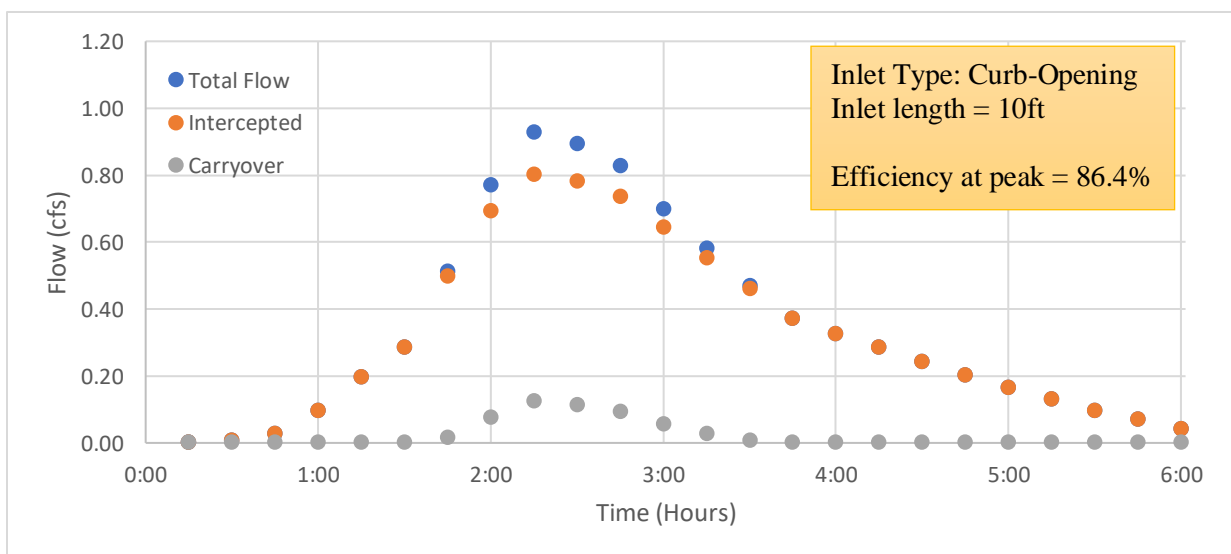


Figure 39. [Case 5] Separated hydrographs at end of system (C6 roadway and C12 pipe) using curb-opening inlets.

## 5. SENSITIVITY ANALYSIS AND DESIGN CURVES

Hydrologic models commonly depend on several parameters. For example, flow spread on a gutter depends on the discharge,  $Q$ , the pavement and gutter roughness,  $n$ , the longitudinal road slope,  $S_L$ , and the transverse or lateral slope,  $S_x$ . The general relation for this model would be:

$$T = f(Q, n, S_L, S_x) \quad (5.1)$$

The sensitivity analysis studies the variation in the results of a model caused by the change in the input variables. The analysis allows to understand how the result from the given model depends on the information provided by the different input variables (Hann, 2002). An evaluation of individual variable effects on results of interest leads to informed decision making in a design process. Relative sensitivity ( $S_r$ ) defined as equation (5.2) helps distinguish the relative effect of an individual input parameter,  $P$ , on the result,  $R$ . If parameter  $P$  has the higher magnitude in relative sensitivity ( $S_r$ ) that parameter has a greater effect on the result,  $R$ . A lower magnitude sensitivity describes a lower impact than the other parameters. The positive or negative indication describes the direction in which the parameter affects the result, either raising the value ( $R$ ) or lowering it.

$$S_r = (\partial R / \partial P)(P/R) \quad (5.2)$$

This chapter develops a local sensitivity analysis to determine how the variables involved in estimation of stormwater flow spread and inlet efficiency impact the results. Specifically, the relative sensitivity was obtained for parameters involved in triangular section spread (2.1), curb-opening efficiency (2.13), and grate inlet efficiency (2.19). This information will help designers providing which is the most sensitive parameter.

### 5.1. Relative Sensitivity of Flow Spread in Gutter Flow

Table 2 contains the relative sensitivity of  $Q$ ,  $n$ ,  $S_x$  and  $S_L$  on the triangular gutter spread ( $T$ ). Variables were defined in Section 2.1.1. Seventy-five (75) combinations including values of  $Q = (1, 2, 3, 4, 5)$  cfs,

$S_x = (0.015, 0.030, 0.045)$ ,  $S_L = (0.02, 0.04, 0.06, 0.08, 0.10)$  and Manning's  $n = 0.016$  were tested. The relative sensitivity equations for each individual parameter and the combination results are in Appendix A-1. They are summarized in Table 2.

*Table 2. Relative sensitivity on flow spread (T) with triangular sections.*

RELATIVE SENSITIVITY	Q	n	$S_x$	$S_L$
$(\partial T / \partial Q)(Q/T) =$	0.375			
$(\partial T / \partial n)(n/T) =$		0.375		
$(\partial T / \partial S_x)(S_x/T) =$			-0.626	
$(\partial T / \partial S_L)(S_L/T) =$				-0.188

The highest relative sensitivity is attributed to the cross-slope ( $S_x$ ) with a  $S_r = -0.626$ . This suggests that deviations on its value would have a greater effect on the resulting spread, when compared to changes caused by other parameters. This references the importance of selecting the cross slope or accurately shaping the “crown”/cross slope of a roadway. The Manning's  $n$  and gutter flow have the second largest relative sensitivity,  $S_r = 0.375$ . City guidelines tend to include suggested or recommended Manning's  $n$  values for drainage system designs, but multiple methods exist for estimating runoff discharges. The chosen gutter flows depend on the methods applied, considerably affecting the spread. The parameter with the lowest relative sensitivity for a triangular gutter section flow spread is the longitudinal slope ( $S_L$ ) with  $S_r = -0.188$ . This indicates that even large variations of  $S_L$  result in relatively similar flow spread.

Charts B1.1 through B1.6 in Appendix B-1 shows the estimated spread using the previously mentioned combinations. They provide a visual representation of parameter sensitivity, as well as an idea of how to build design curves for allowable flow spread (T) in a particular setting. Chart B1.1 contains resultant spread (T) and depth (H) in a triangular section for longitudinal slopes ( $S_L$ ) of 2%-10% and a constant cross slope ( $S_x$ ) of 1.5%. Chart B1.2 contains the same information but with a cross slope of 3%. Comparing them, flow spread at 5 cfs runoff and  $S_L = 2\%$ , is reduced from 14 ft to 10.25 ft when  $S_L$  increases to 10%, but it reduces to 8.75 ft when  $S_x = 3\%$  and  $S_L$  is still 2%. This support what is suggested in Table 2, that adjusting cross slope ( $S_x$ ) and longitudinal slope ( $S_L$ ) have a greater and lower impact respectively on the resulting spread. The plots show other visible tendencies, such as how an increased cross slope reduces



horizontal spread by increasing flow depth (H); and how longitudinal slope ( $S_L$ ) appears to have a greater effect on the spread when the gutter section is composite, instead of triangular.

Figures B1.4 through B1.6 in Appendix B-1 also show that the HEC-22 equations for calculating gutter flow in a composite section perform erratically in small gutter flow magnitudes. These equations were adjusted using empirical coefficients and exponents suggesting that their precision encompasses a limited range of parameter combinations that are not explicitly provided by HEC-22. Design procedures tend to use storm events significantly larger than those affected by the encountered limitations. Therefore, the situation present in low gutter flow cases should pose no problem to regular urban drainage design applications.

## 5.2. Relative Sensitivity of Curb-Opening Efficiency

Interception efficiency of a curb-opening is dependent on  $Q$ ,  $n$ ,  $S_x$ ,  $S_L$ , and  $L$ . Variables were defined in Section 2.2.1. A total of 150 combinations including  $Q = (1, 2, 3, 4, 5)$  cfs,  $S_x = (0.015, 0.030, 0.045)$ ,  $S_L = (0.02, 0.04, 0.06, 0.08, 0.10)$ , Manning's  $n = 0.016$ , and  $L = (3, 9)$  ft in triangular sections were evaluated for efficiency, equation (2.13). Variations in the values of relative sensitivities were obtained when varying the parameter combinations. Table 3 contains the minimum and maximum  $S_r$  values across all 75 combinations of  $L = 3$  ft, while Table 4 contains the 75 combinations that correspond to  $L = 9$  ft. Appendix A-2 includes each individual combination result for in-depth comparisons.

Table 3. Relative sensitivity on curb-opening efficiency with triangular sections. Inlet length,  $L = 3$  ft.

RELATIVE SENSITIVITY	$Q$		$n$		$S_x$		$S_L$		$L$	
	Min	Max	Min	Max	Min	Max	Min	Max	Min	Max
$(\partial E / \partial Q)(Q/E) =$	-0.336	-0.395								
$(\partial E / \partial n)(n/E) =$			0.509	0.599						
$(\partial E / \partial S_x)(S_x/E) =$					0.509	0.599				
$(\partial E / \partial S_L)(S_L/E) =$							-0.090	-0.106		
$(\partial E / \partial L)(L/E) =$									0.902	1.062

Table 4. Relative sensitivity on curb-opening efficiency with triangular sections. Inlet length,  $L = 9\text{ft}$ .

RELATIVE SENSITIVITY	Q		n		S <sub>x</sub>		S <sub>L</sub>		L	
	Min	Max	Min	Max	Min	Max	Min	Max	Min	Max
$(\partial E / \partial Q)(Q/E) =$	-0.138	-0.337								
$(\partial E / \partial n)(n/E) =$			0.209	0.512						
$(\partial E / \partial S_x)(S_x/E) =$					0.209	0.512				
$(\partial E / \partial S_L)(S_L/E) =$							-0.037	-0.091		
$(\partial E / \partial L)(L/E) =$									0.371	0.907

Although the difference between sensitivities varied with each parameter combination, the order in which parameters had greater impact mostly remained the same. In  $L = 3\text{ft}$  combinations, inlet length ( $L$ ) was the parameter with the greatest effect on curb-opening efficiency ( $S_r = [0.902, 1.062]$ ). Suggesting that although other parameters could improve performance, the short inlet length overpowered the system response and did not allow efficiency to increase. This is evident in the design efficiency curves in Appendix B-2 with the “Curb 2019” (“Curb Regl”) curves in Charts B2.1, B2.2, and B2.3. They show how curb-opening efficiency generally improves when only raising  $S_x$  or only lowering  $S_L$ , but also how improvements are more noticeable when an increased inlet length is the only varying parameter. Appendix A-2 Table A2.13 shows how inlet length relative sensitivity declines when increasing  $S_x$ , but that the decline is far greater with a longer inlet length. This allows other parameters to have an increased effect on inlet efficiency response when inlet length is larger.

In all combinations, Manning’s  $n$  and  $S_x$  are the second most impactful parameters ( $S_r = [0.209, 0.599]$ ), quantifying the importance of roadway geometry construction, and surface material selection and maintenance. Gutter flow ( $Q$ ) is the next most impactful parameter ( $|S_r| = [0.138, 0.395]$ ). And although its relative impact can reduce when inlet length is larger, the results give considerable value to accurate storm runoff estimates. Longitudinal slope ( $S_L$ ) relative sensitivity shows the least effect ( $|S_r| = [0.037, 0.106]$ ). This conclusion is supported by results from Appendix B-2 with design efficiency Charts B2.1 through B2.12, where “Curb 2019” (“Curb Regl”) curves are grouped in each figure. The same figures show how  $S_L$  sensitivity would be greater using the HEC-22 curb-opening efficiency of equation (2.11), as the curves are more spaced apart, especially with composite sections. The difference between the effects of  $S_x$  and  $S_L$ ,

quantified by their sensitivities, continues to be staggering. Like the flow spread relative sensitivities, Charts B2.7 and B2.8 show how efficiency improves by 10% with a 5cfs runoff either by increasing  $S_x$  slightly from 1.5% to 3% or by increasing  $S_L$  five times from 2% to 10%.

### 5.3. Relative Sensitivity of Grate Inlet Efficiency

The interception efficiency of a grate inlet is dependent on  $T$ ,  $n$ ,  $S_x$ ,  $S_L$ ,  $W_g$ , and  $L$ . A total of 150 combinations between  $Q = (1, 2, 3, 4, 5)$ cfs,  $S_x = (0.015, 0.030, 0.045)$ ,  $S_L = (0.02, 0.04, 0.06, 0.08, 0.10)$ , Manning's  $n = 0.016$ ,  $W_g = 2$ ft,  $L = (2, 6)$ ft = (1, 3) grates, and grate type = P-50 in triangular sections were evaluated for the grate inlet efficiency equation (2.19). Like the curb-opening sensitivities, the results did not remain constant throughout parameter combinations. Table 5 contains the minimum and maximum  $S_r$  values across all 75 combinations of  $L = 2$ ft = 1 grate, while Table 6 contains the 75 combinations that correspond to  $L = 6$ ft = 3 grates. Appendix A-3 includes each combination result for in-depth comparisons. The differences between minimum and maximum grate parameter sensitivities are much larger than the curb-opening sensitivities. The efficiency of these inlets is affected by several parameters which depend on other variables, such as the splash-over velocity and the clogging effect. These variables are expressed by empirical equations and combined with the frontal and side flow efficiencies making the model difficult to analyze with the relative sensitivity method only. The interaction between all the factors present in grate inlet hydrodynamics guarantees further research.

Table 5. Relative sensitivity on (P-50) grate inlet efficiency with triangular sections. Inlet length,  $L = 2$ ft.

RELATIVE SENSITIVITY	$T$		$n$		$S_x$		$S_L$		$L$		$W_g$	
	Min	Max	Min	Max	Min	Max	Min	Max	Min	Max	Min	Max
$(\partial E / \partial T)(T/E) =$	-2.449	-201.0										
$(\partial E / \partial n)(n/E) =$			0.310	0.996								
$(\partial E / \partial S_x)(S_x/E) =$					-0.121	-0.646						
$(\partial E / \partial S_L)(S_L/E) =$							-0.155	-0.498				
$(\partial E / \partial W_g)(W_g/E) =$									0.392	0.590		
$(\partial E / \partial L)(L/E) =$											0.297	1.176

Table 6. Relative sensitivity on (P-50) grate inlet efficiency with triangular sections. Inlet length,  $L = 6\text{ft}$ .

RELATIVE SENSITIVITY	T		n		$S_x$		$S_L$		L		$W_g$	
	Min	Max	Min	Max	Min	Max	Min	Max	Min	Max	Min	Max
$(\partial E / \partial T)(T/E) =$	-3.533	-217.9										
$(\partial E / \partial n)(n/E) =$			0.306	0.839								
$(\partial E / \partial S_x)(S_x/E) =$					-0.077	-0.459						
$(\partial E / \partial S_L)(S_L/E) =$							-0.153	-0.419				
$(\partial E / \partial W_g)(W_g/E) =$									1.423	1.824		
$(\partial E / \partial L)(L/E) =$											0.371	1.262

The present analysis suggests that flow spread (T) is the most sensitive parameter ( $|S_r| = [2.449, 217.9]$ ) and had the most variation in sensitivity computations. Spread sensitivity magnitude decreased when parameters that lowered spread increased. Appendix A-3 Tables A3.4 and A3.11 show how increasing  $S_x$  or  $S_L$  lower sensitivity magnitude and improves efficiency response while increasing Q or L increase sensitivity. Although increasing gutter flow (Q) and inlet length (L) decrease and improve efficiency respectively.

The inlet length relative sensitivity ( $S_r = [0.392, 0.590]$ ) varied its position throughout the combinations when using a single grate. It could become the 2<sup>nd</sup> most impactful parameter and almost the least. It suggests that when installing a single or small grate inlet, the other parameters must be chosen carefully to achieve adequate performance. Grate length (L) placed it as the 2<sup>nd</sup> most important parameter ( $S_r = [1.423, 1.824]$ ) that controlled inlet efficiency. In these cases, constructing more favorable slopes improved performance by low increments because increasing inlet length overwhelmingly improved the efficiency response. After considering inlet length and flow spread, inlet width ( $W_g$ ) was consistently the parameter with the largest effect ( $|S_r| = [0.297, 1.262]$ ). Like inlet length, this suggests that increasing grate width reduces the effects of roadway geometry variations on overall inlet efficiency response. Although roadway geometry still requires dedicated attention installing a road-wide grate is impractical and unsafe in most locations.

Appendix A-3 Charts A3.5 and A3.12 show how Manning's n (n) sensitivity ( $S_r = [0.306, 0.996]$ ) increases significantly with steeper slopes, as surface roughness directly affects surface friction, runoff velocity, and its ability to "splash-over" grates. Cross slope ( $S_x$ ) sensitivity ( $|S_r| = [0.153, 0.646]$ ) does not

reflect its impact on flow spread, where it was the most critical parameter and thus, requires careful consideration to comply with design guidelines. Limiting spread is shown here to be the most important aspect of managing interception performance for grate inlets. Cross slope sensitivity did increase as inlet length increased, describing its effect on side flow interception. Longitudinal slope ( $S_L$ ) falls as the least impactful parameter again ( $|S_r| = [0.153, 0.498]$ ). Supported by Appendix B-3 Charts B3.1 through B3.9, efficiency curves are grouped. Increasing gutter flow does increase  $S_L$  sensitivity where velocity begins to increase “splash-over” occurrence. Charts B3.10 through B3.15 show this sensitivity is greater for composite sections.

Grate efficiency requires more in-depth evaluations. Many empirical equations are interconnected and used during the procedure to determine grate efficiency, but their individual development and researched adjustments are somewhat independent of each other. Many more parameter combinations exist for grate inlet installations, as they exist in many shapes and sizes. Grate width ( $W_g$ ) or another parameter could overtake  $L$  and  $T$  sensitivities as the most impactful parameter within other existing combinations. Several nuances exist that require grate inlet designs to be studied carefully.

Appendix B-3 contains the grate efficiency design curves for the evaluated combinations, although using the average efficiency between P-50, P-50x100 and P-30 grate types. These figures show how increasing cross slope improves efficiency response in lower flow rates more than in higher flows. Longitudinal slopes appear to have a negligible effect on triangular sections, while composite sections contain considerable change when  $S_L$  varies. Although, the effect of “splash-over” from increasing flow velocities due to steeper longitudinal slopes can still be observed as efficiency drops below those from lower slopes. The difficulties in low composite flow calculations previously discussed seem to be least apparent in higher inlet lengths as well. Generally, grate efficiency design curves should be developed in a case-by-case manner to foresee the specific nuances from a particular setting.

Inlet width was kept constant ( $W_g = 2\text{ft}$ ) through the relative sensitivity analysis but Table 7 suggests that increasing grate width would have a greater impact on inlet efficiency rather than increasing inlet length. Longitudinal slope and cross slope were kept at 2% and 1.5% respectively, while grate dimension combinations of  $L = (2, 4)\text{ft} = (1, 2)$  grates and  $W_g = (0.5, 1.0, 1.5, 2, 2.5)\text{ft}$  were evaluated. The increase of efficiency was considerable when marginally increasing grate width ( $W_g$ ) when compared to doubling grate length ( $L$ ). Additional risk-based and cost/benefit analyses would help confirm a suggested method to improve and standardize grate inlet installations.

Table 7. Grate Inlet Efficiency (E%) when varying Inlet Dimensions (Length (L) and Width ( $W_g$ )).

		Grate Inlet Efficiency (E%)									
L(ft)=		2					4				
$W_g(\text{ft}) =$		0.5	1.0	1.5	2.0	2.5	0.5	1.0	1.5	2.0	2.5
Q(cfs) =	1	18.4	32.8	45.5	56.5	66.2	24.9	38.2	49.9	60.1	68.9
	2	14.4	26.0	36.6	46.2	54.9	19.5	30.4	40.4	49.4	57.6
	3	12.4	22.6	32.1	40.8	48.7	16.8	26.5	35.5	43.7	51.3
	4	11.1	20.5	29.1	37.2	44.7	15.1	24.0	32.3	40.0	47.1
	5	10.3	18.9	27.0	34.6	41.7	13.9	22.2	30.0	37.2	44.0

## **6. SUMMARY OF RESULTS**

### **6.1. Capabilities of the Hydrograph Separation Method (HSM)**

The Hydrograph Separation Method (HSM) is an urban stormwater drainage system design process improvement tool made to explicitly identify intercepted and carryover flows, and to obtain better approximations of runoff magnitude in on-grade sections of major and minor systems. The HSM tool can be used together with EPA SWMM and other modeling software to achieve improved drainage designs in all types of urban environments. However, it could be used to separate any single or continuous event hydrograph developed from other rainfall-runoff simulators. The quantified separation between runoff flow that is intercepted by the minor system and flow that continues to affect the major system downstream can more accurately allow the designer to understand and interpret the drainage system's response to a particular storm event.

Two small drainage systems were analyzed and reevaluated by changing inlet specifications and exploring possible variations. SWMM Version 5.1 was used in these examples. EPA SWMM is a tool that facilitates the design process of infrastructure in various types of urban and environmental settings (Rossman, 2014). Its main application is in stormwater drainage system design. The use of HSM in these evaluations helped identify areas of the drainage system that required additional attention and reevaluation. The ability to evaluate singular locations in a complex system individually also helped catch nuances that would not have been observed by using a singular expansive model by itself. This process assisted in successfully describing systems that would perform successfully to the design storm event within its design criteria or conditions.

The design equations for stormwater systems proposed by the Federal Highway Administration and the Planning Board of Puerto Rico (Junta de Planificación de Puerto Rico, 2022, in Spanish) were implemented into a user-friendly interactable software to ease HSM application. The HSM tool allows a user to insert a runoff hydrograph, followed by picking and choosing the gutter and inlet parameters that could be implemented into their design. Then see how these affect the efficiency response of various stormwater

drainage inlets through visually separated hydrographs while highlighting the response during the storm peak. This allows a user to quickly identify if their design complies with guideline conditions and regulations, and quickly test how other parameter configurations could achieve the result they intend.

## **6.2. Results of the Relative Sensitivity Analysis**

A relative sensitivity analysis of the parameters that affect these equations identified the importance of carefully shaping the roadway geometry during the construction phase and of choosing adequate runoff estimation methods. Understanding the effects that parameters have on each other can avoid unintended results. Manning's  $n$  values considerably affected all evaluated equations; thus, careful consideration should be given to choosing a value of Manning's  $n$  for a design. Increasing its magnitude showed also increased overall inlet efficiency, but at the cost of increasing horizontal flow spread ( $T$ ) as well. This leads a designer to find a balance between all parameters to achieve the intended results.

Variability in longitudinal slopes ( $S_L$ ) did not alter the resulting flow spread ( $T$ ) and inlet efficiency ( $E$ ) greatly when compared to changing other parameters. Its effect was even less in triangular section gutters compared to composite sections. However, the increased flow velocities of higher flows on steeper slopes did show to cause more “splash-over” and decrease efficiency when using shorter grate lengths.

Unlike longitudinal slopes, slight differences between a design and constructed cross slope ( $S_x$ ) were shown to significantly alter the spread ( $T$ ) magnitude. This suggests paying attention when constructing the “crown”/cross slope of a roadway. Especially since flow spread was the most sensitive parameter for grate inlet efficiency, and the cross slope was the most impactful for limiting flow spread.

Increasing inlet length ( $L$ ) for all inlet types and also inlet width ( $W_g$ ) for grate inlets was shown to increase their sensitivity for managing interception efficiency. Suggesting that increasing inlet size improves inlet interception. Although an orifice-style discharge capacity analysis should then be performed on the pipe installed underneath to complete the actual interception capacity of the inlet during intense storm events.



Different parameter combinations were shown to vary inlet efficiency parameter sensitivities to different degrees and case-by-case evaluations are generally recommended. Grate inlets in particular require more in-depth evaluations regarding interception efficiency. Many empirical equations are interconnected and used during the procedure to determine grate efficiency, but their individual development and researched adjustments are somewhat independent of each other. This possibly leads to undesired effects on other equations in the chain.

The HSM tool helps designers speed up the process of evaluating alternatives and proposing modifications to stormwater drainage infrastructure. The ability to quickly evaluate alternatives also allows for statistical analyses that can help quantify the effects of individual parameters, helping to further understand the nuances of stormwater drainage inlet hydrodynamics. As additional research offers adjustments to drainage hydrodynamic relations, the HSM tool can be updated and expanded upon as well, allowing the further study and application of HSM.

## 7. CONCLUSIONS AND RECOMMENDATIONS

### 7.1. Conclusions

The main objective of developing a methodology for urban stormwater drainage systems that facilitates the separation of a catch basin hydrograph into the individual hydrographs that correspond to the inflow intercepted by a storm drain inlet and carryover flow that continues within the street gutter was achieved. The Hydrograph Separation Method (HSM) and the software to estimate it facilitate the creation of individual hydrographs that correspond to the inflow intercepted by a storm drain inlet and the carryover flow that continues within the street gutter. The benefits of having the separated hydrographs include predicting the surface flood levels on the street and estimating the size of the minor system's elements with more precision, keeping flows over the streets under control, and improving the overall design process.

The methodology was programmed in MS Excel Visual Basic for Applications (VBA) facilitates the design process of drainage systems and allows the analysis of different alternatives and their impact on the system's performance. Quick and easy alterations to the gutter and inlet parameters can be done within the VBA HSM tool, allowing the user to visually see the effects of their proposed alternatives.

The HSM tool permitted an in-depth evaluation of inlet design parameter relative sensitivity. This analysis demonstrated how the HSM tool could also be used to perform an in-depth statistical analysis of a particular system's response. This analysis concluded that roadway longitudinal slope ( $S_L$ ) is not a sensitive parameter, resulting for most cases in similar magnitudes of flow spread ( $T$ ) and inlet efficiency ( $E$ ) when using a longitudinal slope range of 2%-10%. The opposite was shown to be true for cross slopes ( $S_x$ ), having a high sensitivity throughout all the parameter combinations. Changing between 1.5%, 3%, and 4.5% cross slopes resulted in noticeable differences in estimated flow spreads and inlet efficiencies. This suggests that cross slopes, in particular, have to be carefully shaped during the construction phase of a project, with little room for error.

Although the combinations included in the grate efficiency relative sensitivity analysis did not vary grate width ( $W_g$ ), the increase in inlet length ( $L$ ) sensitivity from its magnitude suggested a similar reaction for

$W_g$  sensitivity. Table 7 was constructed to evaluate how varying  $L$  compared to varying  $W_g$  on the resulting grate interception efficiency. This showed how 6-inch increments in grate width did improve interception efficiency much more than doubling grate length from 2ft to 4ft. This suggests that whenever the option of installing a rectangular grate exists and civilian safety is not affected, the best and most efficient grate orientation is to have  $W_g$  be greater than  $L$ .

The HSM tool can export the results the user is interested in as text files. These results are incorporated in stormwater simulation programs, such as EPA SWMM, as a wide variety of programs accept hydrographs inputs as time series tables. Stormwater levels on the streets will be estimated with higher precision and, the minor system design will be improved by having better estimates of inlet discharges and pipe diameters. Design of low-impact development (LID) measures will benefit from the HSM by having better estimates of flows into areas with vegetation or infiltration sites. HSM can also incorporate new relations for inlet capacity or LID flows for better designs for the urban environment. As drainage design research continues, HSM applications could be expanded by incorporating regulations criteria contained in specific design manuals.

## **7.2. Recommendations**

The recommended use for HSM is together with other drainage inlet design methods and not as a standalone tool. Determining the distance between inlets is critical when designing drainage systems. Although HSM does not evaluate this parameter, its effect on carryover flow and inlet/pipe sizing is considerable. HSM could be used as support for inlet spacing methods by confirming required inlet efficiencies, evaluating possible adjustments and supporting cost/benefit analyses.

The overall street geometry could also be designed together with HSM. Total spread ( $T$ ) and flow depth ( $H$ ) at the curb edge are limiting factors affected by surface roughness ( $n$ ), longitudinal slope ( $S_L$ ), and cross slopes ( $S_x$ ) which are mainly chosen when designing the roadway, but as the relative sensitivity analysis concluded, the effects of each parameter vary greatly. Another recommendation stemming from

the relative sensitivity analysis is the existence of a more efficient orientation when using grate inlets, installing them wider than longer proving to intercept more runoff.

HSM use is aimed at supporting the general design process, facilitating repetitive calculations that are not evaluated in large-scale simulation software but required in finished designs. Additional statistical analyses using HSM could also support general guideline updates. By using the relative sensitivity results, the suggested Manning's  $n$  within drainage guidelines could be controlled as an implicit safety factor if deemed necessary. The minimum suggested cross slopes ( $S_x$ ) could be raised to avoid undesired flooding because the design and constructed slopes can differ considerably, maintaining other security conditions under control. Other similar types of adjustments could also be evaluated with the help of HSM, to improve the process and results of stormwater drainage systems.

## REFERENCES

- The City of San Diego. (2017). Drainage Design Manual. Transportation & Storm Water Design Manuals. 3-1.
- Federal Highway Administration (FHWA). Rev. 2013. Urban Drainage Design Manual. Hydraulic Engineering Circular 22. Washington, DC: Federal Highway Administration.
- Gómez, M., & Russo, B. (2005). Comparative study of methodologies to determine inlet efficiency from test data: HEC-12 methodology vs UPC method. *WIT Transactions on Ecology and the Environment*, 80.
- Gómez, M., & Russo, B. (2011, February). Methodology to estimate hydraulic efficiency of drain inlets. In *Proceedings of the institution of civil engineers-water management* (Vol. 164, No. 2, pp. 81-90). Thomas Telford Ltd. <https://doi.org/10.1680/wama.900070>
- Guo, J. C. (2006). Design of street curb opening inlets using a decay-based clogging factor. *Journal of hydraulic engineering*, 132(11), 1237-1241. DOI: 10.1061/ASCE0733-94292006132:111237
- Guo, J. C., & MacKenzie, K. (2012). Hydraulic efficiency of grate and curb-opening inlets under clogging effect (No.CDOT-2012-3). Colorado. DTD Applied Research and Innovation Branch.
- Hann, C. T., (2002). *Statistical Methods in Hydrology*, Iowa State Press.
- Hydrologic Engineering Center. (2021). HEC-HMS User's Manual version 4.9. Viewing Results for the Current Run. Retrieved May 26, 2022, from <https://www.hec.usace.army.mil/confluence/hmsdocs/hmsum/4.9>
- Izzard, C. F. (1949). Tentative results on capacity of curb opening inlets. 29th Annual Conference of the Highway Research Board, 11–13.
- Junta de Planificación de Puerto Rico. (2022). Reglamento para el Diseño, Criterios de Operación y Mantenimiento de Sistemas de Alcantarillados Pluviales en Puerto Rico. (Para aprobación por el gobernador de Puerto Rico).
- Li, X., Fang, X., Li, J., Manoj, K. C., Gong, Y., & Chen, G. (2018). Estimating time of concentration for overland flow on pervious surfaces by particle tracking method. *Water (Switzerland)*, 10(4). <https://doi.org/10.3390/w10040379>
- Li, X., Fang, X., Chen, G., Gong, Y., Wang, J., & Li, J. (2019). Evaluating curb inlet efficiency for urban drainage and road bioretention facilities. *Water*, 11(4), 851.
- Mogenfelt, P. (2017). Modeling LID-units in SWMM-A review of the current approach with suggestions for improvement.[www.tvrl.lth.se](http://www.tvrl.lth.se)
- Rossman, L. A. (2014). *SWMM-CAT User's Guide* (EPA/600/R-14/428) (Issue September).
- Rossman, L. A. (2010). Modeling low impact development alternatives with SWMM. *Journal of Water Management Modeling*.
- Senior, M., Scheckenberger, R., & Bishop, B. (2018). Modeling Catchbasins and Inlets in SWMM. *Journal of Water Management Modeling*, 2018. <https://doi.org/10.14796/JWMM.C435>

- US Department of Agriculture. (1992). Technical Release 20 (TR-20). Computer Program for Project Formulation Hydrology.
- US Department of Agriculture. (1986). Technical Release 55 (TR-55). Urban Hydrology for Small Watersheds.
- USA Environmental Protection Agency. (2015). Storm Water Management Model (SWMM). Storm Water Management Model. <https://www.epa.gov/water-research/storm-water-management-model-swmm>
- Uyumaz, A. H. (1992). Discharge Capacity for Curb-opening Inlets. *Journal of Hydraulic Engineering*, 118(7), 1048–1051.

## APPENDIX A

### List of Contents

<b>Appendix A-1</b>	<b>Spread Relative Sensitivity (<math>S_r</math>)</b>	<b>57</b>
Equations A1.1	Equations for Spread Relative Sensitivity ( $S_r$ )	57
Table A1.2	Resultant Spread (T) in a Triangular Section	58
Table A1.3	Gutter Flow (Q) $S_r$ Results	58
Table A1.4	Manning's n (n) $S_r$ Results	58
Table A1.5	Cross Slope ( $S_x$ ) $S_r$ Results	58
Table A1.6	Longitudinal Slope ( $S_L$ ) $S_r$ Results	58
<b>Appendix A-2</b>	<b>Curb-Opening Efficiency Relative Sensitivity (1 Curb-Opening: L = 3ft)</b>	<b>59</b>
Equations A2.1	Equations for Curb-Opening Efficiency Relative Sensitivity ( $S_r$ )	59
Table A2.2	Curb-Opening Efficiency (E%) Results with L = 3ft in a Triangular Section	60
Table A2.3	Gutter Flow (Q) $S_r$ Results with L = 3ft	60
Table A2.4	Manning's n (n) $S_r$ Results with L = 3ft	60
Table A2.5	Cross Slope ( $S_x$ ) $S_r$ Results with L = 3ft	61
Table A2.6	Longitudinal Slope ( $S_L$ ) $S_r$ Results with L = 3ft	61
Table A2.7	Inlet Length (L) $S_r$ Results with L = 3ft	61
Table A2.8	Curb-Opening Efficiency (E%) Results with L = 9ft in a Triangular Section	61
Table A2.9	Gutter Flow (Q) $S_r$ Results with L = 9ft	61
Table A2.10	Manning's n (n) $S_r$ Results with L = 9ft	62
Table A2.11	Cross Slope ( $S_x$ ) $S_r$ Results with L = 9ft	62
Table A2.12	Longitudinal Slope ( $S_L$ ) $S_r$ Results with L = 9ft	62
Table A2.13	Inlet Length (L) $S_r$ Results with L = 9ft	62
<b>Appendix A-3</b>	<b>Grate Inlet Efficiency Relative Sensitivity (1 Grate: L = 2ft x <math>W_g</math> = 2ft)</b>	<b>63</b>
Equations A3.1	Equations for Grate Inlet Efficiency Relative Sensitivity ( $S_r$ )	63
Table A3.2	Resultant Spread (T) in a Triangular Section	64
Table A3.3	Grate Inlet Efficiency (E%) Results with L = 2ft in a Triangular Section	65
Table A3.4	Spread (T) $S_r$ Results with L = 2ft	65
Table A3.5	Manning's n (n) $S_r$ Results with L = 2ft	65
Table A3.6	Cross Slope ( $S_x$ ) $S_r$ Results with L = 2ft	65
Table A3.7	Longitudinal Slope ( $S_L$ ) $S_r$ Results with L = 2ft	65
Table A3.8	Inlet Length (L) $S_r$ Results with L = 2ft	66
Table A3.9	Inlet Width ( $W_g$ ) $S_r$ Results with L = 2ft	66
Table A3.10	Grate Inlet Efficiency (E%) Results with L = 6ft in a Triangular Section	66
Table A3.11	Spread (T) $S_r$ Results with L = 6ft	66
Table A3.12	Manning's n (n) $S_r$ Results with L = 6ft	66
Table A3.13	Cross Slope ( $S_x$ ) $S_r$ Results with L = 6ft	67
Table A3.14	Longitudinal Slope ( $S_L$ ) $S_r$ Results with L = 6ft	67
Table A3.15	Inlet Length (L) $S_r$ Results with L = 6ft	67
Table A3.16	Inlet Width ( $W_g$ ) $S_r$ Results with L = 6ft	67

## APPENDIX A-1

### Spread Relative Sensitivity ( $S_r$ )

**Equations A1.1** – Equations for Spread Relative Sensitivity ( $S_r$ )

$$T = [(Qn)/(K_T S_x^{1.67} S_L^{0.5})]^{0.375}$$

$$S_{r\ T/Q} = \left(\frac{\partial T}{\partial Q}\right) \left(\frac{Q}{T}\right)$$

$$\left(\frac{\partial T}{\partial Q}\right) = \frac{0.375\ T}{Q}$$

$$S_{r\ T/n} = \left(\frac{\partial T}{\partial n}\right) \left(\frac{n}{T}\right)$$

$$\left(\frac{\partial T}{\partial n}\right) = \frac{0.375\ T}{n}$$

$$S_{r\ T/S_x} = \left(\frac{\partial T}{\partial S_x}\right) \left(\frac{S_x}{T}\right)$$

$$\left(\frac{\partial T}{\partial S_x}\right) = \frac{-0.62625\ T}{S_x}$$

$$S_{r\ T/S_L} = \left(\frac{\partial T}{\partial S_L}\right) \left(\frac{S_L}{T}\right)$$

$$\left(\frac{\partial T}{\partial S_L}\right) = \frac{-0.1875\ T}{S_L}$$



**Table A1.2 - Resultant Spread (T) in a Triangular Section**

		Resultant Spread (T) [ft]														
		0.015					0.03					0.045				
Sx =	SL =	0.02	0.04	0.06	0.08	0.1	0.02	0.04	0.06	0.08	0.1	0.02	0.04	0.06	0.08	0.1
Q(cfs) =	1	7.62	6.69	6.20	5.87	5.63	4.93	4.33	4.02	3.80	3.65	3.83	3.36	3.12	2.95	2.83
	2	9.88	8.67	8.04	7.62	7.30	6.40	5.62	5.21	4.93	4.73	4.96	4.36	4.04	3.83	3.67
	3	11.50	10.10	9.36	8.87	8.50	7.45	6.54	6.06	5.74	5.51	5.78	5.07	4.70	4.46	4.27
	4	12.81	11.25	10.42	9.88	9.47	8.30	7.29	6.75	6.40	6.14	6.44	5.65	5.24	4.96	4.76
	5	13.93	12.23	11.33	10.74	10.30	9.02	7.92	7.34	6.96	6.67	7.00	6.15	5.70	5.40	5.18

**Table A1.3 – Gutter Flow (Q) S<sub>r</sub> Results**

		Gutter Flow (Q) S <sub>r</sub> Results														
		0.015					0.03					0.045				
Sx =	SL =	0.02	0.04	0.06	0.08	0.1	0.02	0.04	0.06	0.08	0.1	0.02	0.04	0.06	0.08	0.1
Q(cfs) =	1	0.375	0.375	0.375	0.375	0.375	0.375	0.375	0.375	0.375	0.375	0.375	0.375	0.375	0.375	0.375
	2	0.375	0.375	0.375	0.375	0.375	0.375	0.375	0.375	0.375	0.375	0.375	0.375	0.375	0.375	0.375
	3	0.375	0.375	0.375	0.375	0.375	0.375	0.375	0.375	0.375	0.375	0.375	0.375	0.375	0.375	0.375
	4	0.375	0.375	0.375	0.375	0.375	0.375	0.375	0.375	0.375	0.375	0.375	0.375	0.375	0.375	0.375
	5	0.375	0.375	0.375	0.375	0.375	0.375	0.375	0.375	0.375	0.375	0.375	0.375	0.375	0.375	0.375

**Table A1.4 – Manning's n (n) S<sub>r</sub> Results**

		Manning's n (n) S <sub>r</sub> Results														
		0.015					0.03					0.045				
Sx =	SL =	0.02	0.04	0.06	0.08	0.1	0.02	0.04	0.06	0.08	0.1	0.02	0.04	0.06	0.08	0.1
Q(cfs) =	1	0.375	0.375	0.375	0.375	0.375	0.375	0.375	0.375	0.375	0.375	0.375	0.375	0.375	0.375	0.375
	2	0.375	0.375	0.375	0.375	0.375	0.375	0.375	0.375	0.375	0.375	0.375	0.375	0.375	0.375	0.375
	3	0.375	0.375	0.375	0.375	0.375	0.375	0.375	0.375	0.375	0.375	0.375	0.375	0.375	0.375	0.375
	4	0.375	0.375	0.375	0.375	0.375	0.375	0.375	0.375	0.375	0.375	0.375	0.375	0.375	0.375	0.375
	5	0.375	0.375	0.375	0.375	0.375	0.375	0.375	0.375	0.375	0.375	0.375	0.375	0.375	0.375	0.375

**Table A1.5 – Cross Slope (S<sub>x</sub>) S<sub>r</sub> Results**

		Cross Slope (S <sub>x</sub> ) S <sub>r</sub> Results														
		0.015					0.03					0.045				
Sx =	SL =	0.02	0.04	0.06	0.08	0.1	0.02	0.04	0.06	0.08	0.1	0.02	0.04	0.06	0.08	0.1
Q(cfs) =	1	-0.626	-0.626	-0.626	-0.626	-0.626	-0.626	-0.626	-0.626	-0.626	-0.626	-0.626	-0.626	-0.626	-0.626	-0.626
	2	-0.626	-0.626	-0.626	-0.626	-0.626	-0.626	-0.626	-0.626	-0.626	-0.626	-0.626	-0.626	-0.626	-0.626	-0.626
	3	-0.626	-0.626	-0.626	-0.626	-0.626	-0.626	-0.626	-0.626	-0.626	-0.626	-0.626	-0.626	-0.626	-0.626	-0.626
	4	-0.626	-0.626	-0.626	-0.626	-0.626	-0.626	-0.626	-0.626	-0.626	-0.626	-0.626	-0.626	-0.626	-0.626	-0.626
	5	-0.626	-0.626	-0.626	-0.626	-0.626	-0.626	-0.626	-0.626	-0.626	-0.626	-0.626	-0.626	-0.626	-0.626	-0.626

**Table A1.6 – Longitudinal Slope (S<sub>L</sub>) S<sub>r</sub> Results**

		Longitudinal Slope (S <sub>L</sub> ) S <sub>r</sub> Results														
		0.015					0.03					0.045				
Sx =	SL =	0.02	0.04	0.06	0.08	0.1	0.02	0.04	0.06	0.08	0.1	0.02	0.04	0.06	0.08	0.1
Q(cfs) =	1	-0.188	-0.188	-0.188	-0.188	-0.188	-0.188	-0.188	-0.188	-0.188	-0.188	-0.188	-0.188	-0.188	-0.188	-0.188
	2	-0.188	-0.188	-0.188	-0.188	-0.188	-0.188	-0.188	-0.188	-0.188	-0.188	-0.188	-0.188	-0.188	-0.188	-0.188
	3	-0.188	-0.188	-0.188	-0.188	-0.188	-0.188	-0.188	-0.188	-0.188	-0.188	-0.188	-0.188	-0.188	-0.188	-0.188
	4	-0.188	-0.188	-0.188	-0.188	-0.188	-0.188	-0.188	-0.188	-0.188	-0.188	-0.188	-0.188	-0.188	-0.188	-0.188
	5	-0.188	-0.188	-0.188	-0.188	-0.188	-0.188	-0.188	-0.188	-0.188	-0.188	-0.188	-0.188	-0.188	-0.188	-0.188

## APPENDIX A-2

### Curb-Opening Efficiency Relative Sensitivity (1 Curb-Opening: L = 3ft)

**Equations A2.1** – Equations for Curb-Opening Efficiency Relative Sensitivity ( $S_r$ )

$$L_T = K_{LT} Q^{0.372} S_L^{0.1} \left( \frac{1}{n S_x} \right)^{0.564}$$

$$E = 1 - \left[ 1 - \left( L/L_T \right) \right]^{2.42} = 1 - \left[ 1 - \left( \frac{L}{K_{LT} Q^{0.372} S_L^{0.1} \left( \frac{1}{n S_x} \right)^{0.564}} \right) \right]^{2.42}$$

$$S_{r E/Q} = \left( \frac{\partial E}{\partial Q} \right) \left( \frac{Q}{E} \right)$$

$$\left( \frac{\partial E}{\partial Q} \right) = \frac{-0.90024 L \left[ 1 - \left( L/L_T \right) \right]^{1.42}}{Q L_T}$$

$$S_{r E/n} = \left( \frac{\partial E}{\partial n} \right) \left( \frac{n}{E} \right)$$

$$\left( \frac{\partial E}{\partial n} \right) = \frac{1.36488 L \left[ 1 - \left( L/L_T \right) \right]^{1.42}}{S_x n^2 L_T}$$

$$S_{r E/S_x} = \left( \frac{\partial E}{\partial S_x} \right) \left( \frac{S_x}{E} \right)$$

$$\left( \frac{\partial E}{\partial S_x} \right) = \frac{1.36488 L \left[ 1 - \left( L/L_T \right) \right]^{1.42}}{S_x^2 n L_T}$$

$$S_{r\ E/SL} = \left(\frac{\partial E}{\partial S_L}\right) \left(\frac{S_L}{E}\right)$$

$$\left(\frac{\partial E}{\partial S_L}\right) = \frac{-0.242\ L \left[1 - \left(L/L_T\right)\right]^{1.42}}{S_L\ L_T}$$

$$S_{r\ E/L} = \left(\frac{\partial E}{\partial L}\right) \left(\frac{L}{E}\right)$$

$$\left(\frac{\partial E}{\partial L}\right) = \frac{2.42\ L \left[1 - \left(L/L_T\right)\right]^{1.42}}{L_T}$$

**Table A2.2 - Curb-Opening Efficiency (E%) Results with L = 3ft in a Triangular Section**

		Curb-Opening Efficiency (E%)														
Sx =		0.015					0.03					0.045				
SL =		0.02	0.04	0.06	0.08	0.1	0.02	0.04	0.06	0.08	0.1	0.02	0.04	0.06	0.08	0.1
Q(cfs) =	1	24.1	22.6	21.8	21.2	20.8	34.3	32.2	31.1	30.3	29.7	41.7	39.3	38.0	37.1	36.4
	2	19.0	17.8	17.1	16.6	16.3	27.2	25.5	24.6	24.0	23.5	33.4	31.4	30.3	29.5	28.9
	3	16.4	15.4	14.8	14.4	14.1	23.7	22.2	21.4	20.8	20.4	29.2	27.4	26.4	25.7	25.2
	4	14.9	13.9	13.4	13.0	12.7	21.5	20.1	19.4	18.9	18.5	26.5	24.9	24.0	23.3	22.8
	5	13.7	12.8	12.3	12.0	11.8	19.9	18.6	17.9	17.4	17.1	24.6	23.0	22.2	21.6	21.2

**Table A2.3 – Gutter Flow (Q) S<sub>r</sub> Results with L = 3ft**

		Gutter Flow (Q) S <sub>r</sub> Results														
Sx =		0.015					0.03					0.045				
SL =		0.02	0.04	0.06	0.08	0.1	0.02	0.04	0.06	0.08	0.1	0.02	0.04	0.06	0.08	0.1
Q(cfs) =	1	-0.373	-0.376	-0.377	-0.378	-0.379	-0.352	-0.357	-0.359	-0.361	-0.362	-0.336	-0.341	-0.344	-0.346	-0.348
	2	-0.382	-0.385	-0.386	-0.387	-0.387	-0.367	-0.370	-0.372	-0.373	-0.374	-0.354	-0.358	-0.361	-0.362	-0.364
	3	-0.387	-0.389	-0.390	-0.390	-0.391	-0.374	-0.377	-0.378	-0.379	-0.380	-0.363	-0.367	-0.369	-0.370	-0.371
	4	-0.390	-0.391	-0.392	-0.393	-0.393	-0.378	-0.380	-0.382	-0.383	-0.383	-0.368	-0.372	-0.373	-0.374	-0.377
	5	-0.392	-0.393	-0.394	-0.394	-0.395	-0.381	-0.383	-0.384	-0.385	-0.386	-0.372	-0.375	-0.377	-0.378	-0.378

**Table A2.4 – Manning's n (n) S<sub>r</sub> Results with L = 3ft**

		Manning's n (n) S <sub>r</sub> Results														
Sx =		0.015					0.03					0.045				
SL =		0.02	0.04	0.06	0.08	0.1	0.02	0.04	0.06	0.08	0.1	0.02	0.04	0.06	0.08	0.1
Q(cfs) =	1	0.566	0.570	0.572	0.574	0.575	0.534	0.541	0.545	0.547	0.549	0.509	0.517	0.522	0.525	0.527
	2	0.580	0.583	0.585	0.586	0.587	0.556	0.561	0.564	0.566	0.567	0.537	0.544	0.547	0.549	0.551
	3	0.587	0.589	0.591	0.592	0.593	0.567	0.571	0.573	0.575	0.576	0.550	0.556	0.559	0.561	0.562
	4	0.591	0.593	0.595	0.596	0.596	0.573	0.577	0.579	0.580	0.581	0.559	0.563	0.566	0.568	0.572
	5	0.594	0.596	0.597	0.598	0.599	0.577	0.581	0.583	0.584	0.585	0.564	0.569	0.571	0.573	0.574

**Table A2.5 – Cross Slope ( $S_x$ )  $S_r$  Results with  $L = 3$  ft**

		Cross Slope ( $S_x$ ) $S_r$ Results														
		$S_x =$					0.015					0.03				
		$S_L =$					0.02	0.04	0.06	0.08	0.1	0.02	0.04	0.06	0.08	0.1
$Q(cfs) =$	1	0.566	0.570	0.572	0.574	0.575	0.534	0.541	0.545	0.547	0.549	0.509	0.517	0.522	0.525	0.527
	2	0.580	0.583	0.585	0.586	0.587	0.556	0.561	0.564	0.566	0.567	0.537	0.544	0.547	0.549	0.551
	3	0.587	0.589	0.591	0.592	0.593	0.567	0.571	0.573	0.575	0.576	0.550	0.556	0.559	0.561	0.562
	4	0.591	0.593	0.595	0.596	0.596	0.573	0.577	0.579	0.580	0.581	0.559	0.563	0.566	0.568	0.572
	5	0.594	0.596	0.597	0.598	0.599	0.577	0.581	0.583	0.584	0.585	0.564	0.569	0.571	0.573	0.574

**Table A2.6 – Longitudinal Slope ( $S_L$ )  $S_r$  Results with  $L = 3$  ft**

		Longitudinal Slope ( $S_L$ ) $S_r$ Results														
		$S_x =$					0.015					0.03				
		$S_L =$					0.02	0.04	0.06	0.08	0.1	0.02	0.04	0.06	0.08	0.1
$Q(cfs) =$	1	-0.100	-0.101	-0.101	-0.102	-0.102	-0.095	-0.096	-0.097	-0.097	-0.097	-0.090	-0.092	-0.093	-0.093	-0.094
	2	-0.103	-0.103	-0.104	-0.104	-0.104	-0.099	-0.100	-0.100	-0.100	-0.101	-0.095	-0.096	-0.097	-0.097	-0.098
	3	-0.104	-0.104	-0.105	-0.105	-0.105	-0.100	-0.101	-0.102	-0.102	-0.102	-0.098	-0.099	-0.099	-0.099	-0.100
	4	-0.105	-0.105	-0.105	-0.106	-0.106	-0.102	-0.102	-0.103	-0.103	-0.103	-0.099	-0.100	-0.100	-0.101	-0.101
	5	-0.105	-0.106	-0.106	-0.106	-0.106	-0.102	-0.103	-0.103	-0.104	-0.104	-0.100	-0.101	-0.101	-0.102	-0.102

**Table A2.7 – Inlet Length ( $L$ )  $S_r$  Results with  $L = 3$  ft**

		Inlet Length ( $L$ ) $S_r$ Results														
		$S_x =$					0.015					0.03				
		$S_L =$					0.02	0.04	0.06	0.08	0.1	0.02	0.04	0.06	0.08	0.1
$Q(cfs) =$	1	1.003	1.010	1.014	1.017	1.019	0.947	0.959	0.965	0.970	0.973	0.902	0.917	0.925	0.931	0.935
	2	1.028	1.034	1.037	1.039	1.041	0.986	0.995	1.000	1.003	1.006	0.952	0.964	0.970	0.974	0.977
	3	1.040	1.045	1.048	1.050	1.051	1.005	1.012	1.016	1.019	1.021	0.976	0.985	0.991	0.994	0.997
	4	1.048	1.052	1.054	1.056	1.057	1.016	1.023	1.026	1.029	1.031	0.990	0.999	1.003	1.007	1.013
	5	1.053	1.057	1.059	1.060	1.062	1.024	1.030	1.033	1.035	1.037	1.000	1.008	1.012	1.015	1.017

**Table A2.8 - Curb-Opening Efficiency ( $E\%$ ) Results with  $L = 9$  ft in a Triangular Section**

		Curb-Opening Efficiency ( $E\%$ )														
		$S_x =$					0.015					0.03				
		$S_L =$					0.02	0.04	0.06	0.08	0.1	0.02	0.04	0.06	0.08	0.1
$Q(cfs) =$	1	63.8	60.7	58.9	57.6	56.6	81.9	78.8	76.9	75.6	74.5	91.4	88.7	87.1	85.9	84.9
	2	52.5	49.7	48.1	47.0	46.1	70.0	66.7	64.9	63.6	62.5	80.6	77.4	75.5	74.2	73.2
	3	46.5	43.9	42.5	41.4	40.7	63.0	59.9	58.1	56.8	55.9	73.6	70.4	68.5	67.1	66.1
	4	42.6	40.1	38.8	37.8	37.1	58.2	55.2	53.5	52.3	51.4	68.6	65.4	63.5	62.2	61.2
	5	39.7	37.4	36.1	35.2	34.5	54.6	51.7	50.1	48.9	48.1	64.8	61.6	59.8	58.5	57.5

**Table A2.9 – Gutter Flow ( $Q$ )  $S_r$  Results with  $L = 9$  ft**

		Gutter Flow ( $Q$ ) $S_r$ Results														
		$S_x =$					0.015					0.03				
		$S_L =$					0.02	0.04	0.06	0.08	0.1	0.02	0.04	0.06	0.08	0.1
$Q(cfs) =$	1	-0.269	-0.278	-0.283	-0.287	-0.289	-0.199	-0.214	-0.223	-0.228	-0.232	-0.138	-0.158	-0.170	-0.177	-0.183
	2	-0.300	-0.306	-0.310	-0.312	-0.314	-0.249	-0.260	-0.266	-0.270	-0.273	-0.206	-0.220	-0.228	-0.234	-0.238
	3	-0.313	-0.319	-0.322	-0.324	-0.326	-0.272	-0.281	-0.286	-0.289	-0.291	-0.236	-0.248	-0.254	-0.259	-0.262
	4	-0.322	-0.327	-0.329	-0.331	-0.333	-0.285	-0.293	-0.297	-0.300	-0.302	-0.254	-0.264	-0.270	-0.274	-0.277
	5	-0.328	-0.332	-0.335	-0.336	-0.337	-0.295	-0.302	-0.305	-0.308	-0.310	-0.266	-0.276	-0.281	-0.284	-0.287

**Table A2.10** – Manning's n (n) S<sub>r</sub> Results with L = 9ft

		Manning's n (n) S <sub>r</sub> Results														
S <sub>x</sub> =		0.015					0.03					0.045				
S <sub>L</sub> =		0.02	0.04	0.06	0.08	0.1	0.02	0.04	0.06	0.08	0.1	0.02	0.04	0.06	0.08	0.1
Q(cfs) =	1	0.408	0.422	0.430	0.435	0.439	0.302	0.325	0.338	0.346	0.352	0.209	0.240	0.257	0.269	0.277
	2	0.454	0.464	0.470	0.474	0.476	0.378	0.394	0.403	0.409	0.414	0.312	0.334	0.346	0.354	0.360
	3	0.475	0.484	0.488	0.491	0.494	0.412	0.426	0.433	0.438	0.442	0.358	0.376	0.386	0.393	0.398
	4	0.488	0.495	0.499	0.502	0.504	0.432	0.444	0.451	0.455	0.458	0.385	0.401	0.410	0.415	0.420
	5	0.497	0.503	0.507	0.510	0.512	0.447	0.457	0.463	0.467	0.470	0.404	0.418	0.426	0.431	0.435

**Table A2.11** – Cross Slope (S<sub>x</sub>) S<sub>r</sub> Results with L = 9ft

		Cross Slope (S <sub>x</sub> ) S <sub>r</sub> Results														
S <sub>x</sub> =		0.015					0.03					0.045				
S <sub>L</sub> =		0.02	0.04	0.06	0.08	0.1	0.02	0.04	0.06	0.08	0.1	0.02	0.04	0.06	0.08	0.1
Q(cfs) =	1	0.408	0.422	0.430	0.435	0.439	0.302	0.325	0.338	0.346	0.352	0.209	0.240	0.257	0.269	0.277
	2	0.454	0.464	0.470	0.474	0.476	0.378	0.394	0.403	0.409	0.414	0.312	0.334	0.346	0.354	0.360
	3	0.475	0.484	0.488	0.491	0.494	0.412	0.426	0.433	0.438	0.442	0.358	0.376	0.386	0.393	0.398
	4	0.488	0.495	0.499	0.502	0.504	0.432	0.444	0.451	0.455	0.458	0.385	0.401	0.410	0.415	0.420
	5	0.497	0.503	0.507	0.510	0.512	0.447	0.457	0.463	0.467	0.470	0.404	0.418	0.426	0.431	0.435

**Table A2.12** – Longitudinal Slope (S<sub>L</sub>) S<sub>r</sub> Results with L = 9ft

		Longitudinal Slope (S <sub>L</sub> ) S <sub>r</sub> Results														
S <sub>x</sub> =		0.015					0.03					0.045				
S <sub>L</sub> =		0.02	0.04	0.06	0.08	0.1	0.02	0.04	0.06	0.08	0.1	0.02	0.04	0.06	0.08	0.1
Q(cfs) =	1	-0.072	-0.075	-0.076	-0.077	-0.078	-0.054	-0.058	-0.060	-0.061	-0.062	-0.037	-0.043	-0.046	-0.048	-0.049
	2	-0.081	-0.082	-0.083	-0.084	-0.084	-0.067	-0.070	-0.072	-0.073	-0.073	-0.055	-0.059	-0.061	-0.063	-0.064
	3	-0.084	-0.086	-0.087	-0.087	-0.088	-0.073	-0.075	-0.077	-0.078	-0.078	-0.063	-0.067	-0.068	-0.070	-0.070
	4	-0.087	-0.088	-0.089	-0.089	-0.089	-0.077	-0.079	-0.080	-0.081	-0.081	-0.068	-0.071	-0.073	-0.074	-0.074
	5	-0.088	-0.089	-0.090	-0.090	-0.091	-0.079	-0.081	-0.082	-0.083	-0.083	-0.072	-0.074	-0.076	-0.076	-0.077

**Table A2.13** – Inlet Length (L) S<sub>r</sub> Results with L = 9ft

		Inlet Length (L) S <sub>r</sub> Results														
S <sub>x</sub> =		0.015					0.03					0.045				
S <sub>L</sub> =		0.02	0.04	0.06	0.08	0.1	0.02	0.04	0.06	0.08	0.1	0.02	0.04	0.06	0.08	0.1
Q(cfs) =	1	0.724	0.749	0.762	0.771	0.778	0.535	0.576	0.599	0.614	0.625	0.371	0.426	0.456	0.476	0.492
	2	0.806	0.823	0.833	0.840	0.845	0.670	0.699	0.715	0.726	0.734	0.553	0.592	0.614	0.628	0.639
	3	0.843	0.857	0.866	0.871	0.875	0.731	0.755	0.768	0.777	0.783	0.634	0.667	0.684	0.696	0.705
	4	0.865	0.878	0.885	0.890	0.894	0.767	0.788	0.799	0.807	0.813	0.683	0.711	0.726	0.737	0.744
	5	0.881	0.893	0.899	0.904	0.907	0.792	0.811	0.821	0.828	0.833	0.716	0.741	0.755	0.765	0.772

### APPENDIX A-3

#### Grate Inlet Efficiency Relative Sensitivity (1 Grate: L = 2ft x W<sub>g</sub> = 2ft)

**Equations A3.1** – Equations for Grate Inlet Efficiency Relative Sensitivity (S<sub>r</sub>)

$$\begin{aligned}
 E_o &= 1 - [1 - (W_g/T)]^{2.67} \\
 V &= (K_V/n) S_x^{0.67} S_L^{0.5} T^{0.67} \\
 R_s &= 1 / \left( 1 + \frac{K_{Rs} V^{1.8}}{S_x L^{2.3}} \right) = 1 / \left( 1 + \frac{K_{Rs} [(K_V/n) S_x^{0.67} S_L^{0.5} T^{0.67}]^{1.8}}{S_x L^{2.3}} \right) \\
 V_o &= \alpha + \beta L - \gamma L^2 + \eta L^3 ; V_{oP-50} = 2.22 + 4.03L - 0.65L^2 + 0.06L^3 \\
 R_f &= 1 - K_{Rf}(V - V_o) = 1 - K_{Rf}[(K_V/n) S_x^{0.67} S_L^{0.5} T^{0.67}] - [\alpha + \beta L - \gamma L^2 + \eta L^3]
 \end{aligned}$$

$$\begin{aligned}
 E &= R_f E_o + R_s (1 - E_o) \\
 E &= \left\{ 1 - K_{Rf} \left( \left[ \left( \frac{K_V}{n} \right) S_x^{0.67} S_L^{0.5} T^{0.67} \right] - [\alpha + \beta L - \gamma L^2 + \eta L^3] \right) \right\} \{ 1 - [1 - (W_g/T)]^{2.67} \} \\
 &\quad + \left\{ 1 / \left( 1 + \frac{K_{Rs} \left[ \left( \frac{K_V}{n} \right) S_x^{0.67} S_L^{0.5} T^{0.67} \right]^{1.8}}{S_x L^{2.3}} \right) \right\} (1 - \{ 1 - [1 - (W_g/T)]^{2.67} \})
 \end{aligned}$$

$$\begin{aligned}
 S_{r E/T} &= \left( \frac{\partial E}{\partial T} \right) \left( \frac{T}{E} \right) \\
 \left( \frac{\partial E}{\partial T} \right) &= \frac{-1.206 K_{Rs} V^{1.8} R_s^2 (1 - E_o)}{L^{2.3} S_x T} + \frac{2.67 W_g R_s \left( 1 - W_g/T \right)^{1.67}}{T^2} - 2.67 W_g R_f \left( 1 - W_g/T \right)^{1.67} \\
 &\quad - \frac{0.67 K_{Rf} V E_o}{T}
 \end{aligned}$$

$$\begin{aligned}
 S_{r E/n} &= \left( \frac{\partial E}{\partial n} \right) \left( \frac{n}{E} \right) \\
 \left( \frac{\partial E}{\partial n} \right) &= \frac{1.8 K_{Rs} V^{1.8} R_s^2 (1 - E_o)}{L^{2.3} n S_x} + \frac{K_{Rf} V E_o}{n}
 \end{aligned}$$

$$S_{r\ E/Sx} = \left( \frac{\partial E}{\partial S_x} \right) \left( \frac{S_x}{E} \right)$$

$$\left( \frac{\partial E}{\partial S_x} \right) = \frac{0.206\ R_s^2\ K_{Rs}\ V^{1.8} (1 - E_o)}{L^{2.3}\ S_x^2} - \frac{0.67\ K_{Rf}\ V\ E_o}{S_x}$$

$$S_{r\ E/SL} = \left( \frac{\partial E}{\partial S_L} \right) \left( \frac{S_L}{E} \right)$$

$$\left( \frac{\partial E}{\partial S_L} \right) = \frac{-0.9\ R_s^2\ K_{Rs}\ V^{1.8} (1 - E_o)}{L^{2.3}\ S_x\ S_L} - \frac{K_{Rf}\ V\ E_o}{2\ S_L}$$

$$S_{r\ E/L} = \left( \frac{\partial E}{\partial L} \right) \left( \frac{L}{E} \right)$$

$$\left( \frac{\partial E}{\partial L} \right) = \frac{2.3\ R_s^2\ K_{Rs}\ V^{1.8} (1 - E_o)}{L^{3.3}\ S_x} + K_{Rf}\ E_o (\beta - 2\gamma L + 3\eta L^2)$$

$$S_{r\ E/Wg} = \left( \frac{\partial E}{\partial W_g} \right) \left( \frac{W_g}{E} \right)$$

$$\left( \frac{\partial E}{\partial W_g} \right) = \frac{2.67\ (R_f - R_s)}{T} \left( 1 - W_g/T \right)^{1.67}$$

**Table A3.2 - Resultant Spread (T) in a Triangular Section**

		Resultant Spread (T) [ft]														
Sx =		0.015					0.03					0.045				
SL =		0.02	0.04	0.06	0.08	0.1	0.02	0.04	0.06	0.08	0.1	0.02	0.04	0.06	0.08	0.1
Q(cfs) =	1	7.62	6.69	6.20	5.87	5.63	4.93	4.33	4.02	3.80	3.65	3.83	3.36	3.12	2.95	2.83
	2	9.88	8.67	8.04	7.62	7.30	6.40	5.62	5.21	4.93	4.73	4.96	4.36	4.04	3.83	3.67
	3	11.50	10.10	9.36	8.87	8.50	7.45	6.54	6.06	5.74	5.51	5.78	5.07	4.70	4.46	4.27
	4	12.81	11.25	10.42	9.88	9.47	8.30	7.29	6.75	6.40	6.14	6.44	5.65	5.24	4.96	4.76
	5	13.93	12.23	11.33	10.74	10.30	9.02	7.92	7.34	6.96	6.67	7.00	6.15	5.70	5.40	5.18



**Table A3.3 - Grate Inlet Efficiency (E%) Results with L = 2ft in a Triangular Section**

		Grate Inlet Efficiency (E%)														
		S <sub>x</sub> =					0.015					0.03				
		S <sub>L</sub> =					0.02	0.04	0.06	0.08	0.1	0.02	0.04	0.06	0.08	0.1
Q(cfs) =	1	56.6	61.8	65.0	67.4	69.2	75.8	81.2	84.4	86.5	88.1	86.7	91.3	93.7	95.2	96.3
	2	46.2	50.8	53.8	55.9	57.7	64.1	69.6	72.9	75.3	75.2	75.5	80.9	84.1	83.3	80.7
	3	40.8	45.0	47.7	49.7	51.3	57.4	62.7	66.0	66.0	64.5	68.6	74.2	75.1	72.5	69.8
	4	37.2	41.2	43.7	45.6	46.0	52.9	58.0	60.2	58.7	57.1	63.8	69.3	67.4	64.7	62.0
	5	34.6	38.3	40.8	42.1	41.6	49.6	54.5	54.9	53.3	51.6	60.1	64.3	61.6	58.8	56.0

**Table A3.4 – Spread (T) S<sub>r</sub> Results with L = 2ft**

		Spread (T) S <sub>r</sub> Results														
		S <sub>x</sub> =					0.015					0.03				
		S <sub>L</sub> =					0.02	0.04	0.06	0.08	0.1	0.02	0.04	0.06	0.08	0.1
Q(cfs) =	1	-56.2	-39.9	-32.3	-27.6	-24.3	-18.6	-12.4	-9.5	-7.8	-6.7	-8.7	-5.3	-3.8	-3.0	-2.4
	2	-99.0	-70.9	-57.6	-49.3	-43.6	-35.1	-24.1	-18.9	-15.8	-14.0	-18.0	-11.8	-9.0	-7.6	-6.7
	3	-136.2	-97.5	-79.1	-67.7	-59.7	-49.4	-34.1	-26.9	-23.4	-21.3	-26.1	-17.4	-13.8	-12.1	-11.0
	4	-169.8	-121.4	-98.3	-84.0	-75.8	-62.4	-43.1	-34.6	-30.8	-28.2	-33.4	-22.4	-18.6	-16.5	-15.0
	5	-201.0	-143.4	-115.9	-99.9	-92.0	-74.5	-51.4	-42.4	-38.0	-34.9	-40.2	-27.5	-23.3	-20.7	-19.0

**Table A3.5 – Manning's n (n) S<sub>r</sub> Results with L = 2ft**

		Manning's n (n) S <sub>r</sub> Results														
		S <sub>x</sub> =					0.015					0.03				
		S <sub>L</sub> =					0.02	0.04	0.06	0.08	0.1	0.02	0.04	0.06	0.08	0.1
Q(cfs) =	1	0.329	0.334	0.356	0.380	0.404	0.314	0.352	0.392	0.428	0.460	0.310	0.369	0.419	0.463	0.500
	2	0.388	0.396	0.424	0.453	0.481	0.386	0.428	0.473	0.515	0.566	0.388	0.451	0.508	0.577	0.655
	3	0.423	0.435	0.467	0.500	0.532	0.430	0.476	0.526	0.592	0.668	0.436	0.504	0.584	0.684	0.782
	4	0.448	0.464	0.500	0.536	0.585	0.462	0.512	0.575	0.665	0.755	0.472	0.544	0.657	0.775	0.893
	5	0.468	0.488	0.527	0.572	0.638	0.487	0.541	0.627	0.730	0.833	0.501	0.587	0.722	0.858	0.996

**Table A3.6 – Cross Slope (S<sub>x</sub>) S<sub>r</sub> Results with L = 2ft**

		Cross Slope (S <sub>x</sub> ) S <sub>r</sub> Results														
		S <sub>x</sub> =					0.015					0.03				
		S <sub>L</sub> =					0.02	0.04	0.06	0.08	0.1	0.02	0.04	0.06	0.08	0.1
Q(cfs) =	1	-0.121	-0.170	-0.202	-0.227	-0.249	-0.155	-0.208	-0.245	-0.274	-0.299	-0.176	-0.233	-0.273	-0.305	-0.332
	2	-0.145	-0.202	-0.240	-0.270	-0.296	-0.182	-0.246	-0.290	-0.325	-0.363	-0.207	-0.276	-0.324	-0.375	-0.429
	3	-0.161	-0.224	-0.266	-0.299	-0.327	-0.201	-0.272	-0.321	-0.372	-0.427	-0.228	-0.305	-0.369	-0.441	-0.509
	4	-0.173	-0.241	-0.286	-0.322	-0.361	-0.216	-0.292	-0.350	-0.417	-0.482	-0.244	-0.327	-0.413	-0.498	-0.580
	5	-0.184	-0.255	-0.303	-0.344	-0.394	-0.228	-0.309	-0.382	-0.458	-0.532	-0.258	-0.352	-0.453	-0.550	-0.646

**Table A3.7 – Longitudinal Slope (S<sub>L</sub>) S<sub>r</sub> Results with L = 2ft**

		Longitudinal Slope (S <sub>L</sub> ) S <sub>r</sub> Results														
		S <sub>x</sub> =					0.015					0.03				
		S <sub>L</sub> =					0.02	0.04	0.06	0.08	0.1	0.02	0.04	0.06	0.08	0.1
Q(cfs) =	1	-0.165	-0.167	-0.178	-0.190	-0.202	-0.157	-0.176	-0.196	-0.214	-0.230	-0.155	-0.185	-0.210	-0.231	-0.250
	2	-0.194	-0.198	-0.212	-0.227	-0.241	-0.193	-0.214	-0.237	-0.257	-0.283	-0.194	-0.225	-0.254	-0.289	-0.327
	3	-0.212	-0.218	-0.234	-0.250	-0.266	-0.215	-0.238	-0.263	-0.296	-0.334	-0.218	-0.252	-0.292	-0.342	-0.391
	4	-0.224	-0.232	-0.250	-0.268	-0.293	-0.231	-0.256	-0.287	-0.332	-0.377	-0.236	-0.272	-0.329	-0.388	-0.447
	5	-0.234	-0.244	-0.263	-0.286	-0.319	-0.243	-0.270	-0.313	-0.365	-0.417	-0.250	-0.294	-0.361	-0.429	-0.498



**Table A3.8 – Inlet Length (L) S<sub>r</sub> Results with L = 2ft**

		Inlet Length (L) S <sub>r</sub> Results														
S <sub>x</sub> =		0.015					0.03					0.045				
S <sub>L</sub> =		0.02	0.04	0.06	0.08	0.1	0.02	0.04	0.06	0.08	0.1	0.02	0.04	0.06	0.08	0.1
Q(cfs) =	1	0.542	0.471	0.444	0.430	0.421	0.474	0.430	0.415	0.407	0.402	0.436	0.409	0.399	0.395	0.392
	2	0.568	0.486	0.456	0.439	0.429	0.507	0.450	0.429	0.418	0.422	0.469	0.428	0.413	0.420	0.436
	3	0.579	0.493	0.461	0.444	0.433	0.523	0.460	0.436	0.439	0.453	0.488	0.439	0.434	0.454	0.475
	4	0.586	0.497	0.464	0.446	0.446	0.533	0.466	0.448	0.462	0.480	0.500	0.446	0.459	0.482	0.508
	5	0.590	0.499	0.465	0.452	0.462	0.540	0.470	0.465	0.483	0.503	0.508	0.460	0.480	0.508	0.538

**Table A3.9 – Inlet Width (W<sub>g</sub>) S<sub>r</sub> Results with L = 2ft**

		Inlet Width (W <sub>g</sub> ) S <sub>r</sub> Results														
S <sub>x</sub> =		0.015					0.03					0.045				
S <sub>L</sub> =		0.02	0.04	0.06	0.08	0.1	0.02	0.04	0.06	0.08	0.1	0.02	0.04	0.06	0.08	0.1
Q(cfs) =	1	1.063	1.001	0.949	0.906	0.870	0.809	0.714	0.644	0.589	0.544	0.606	0.488	0.407	0.346	0.297
	2	1.133	1.069	1.016	0.973	0.935	0.931	0.843	0.777	0.724	0.697	0.772	0.668	0.593	0.553	0.530
	3	1.159	1.090	1.035	0.989	0.950	0.978	0.889	0.822	0.795	0.786	0.839	0.737	0.683	0.665	0.649
	4	1.170	1.098	1.040	0.992	0.974	1.002	0.911	0.854	0.849	0.844	0.875	0.771	0.748	0.736	0.726
	5	1.176	1.100	1.039	0.999	1.001	1.016	0.922	0.890	0.888	0.887	0.897	0.805	0.795	0.787	0.782

**Table A3.10 – Grate Inlet Efficiency (E%) Results with L = 6ft in a Triangular Section**

		Grate Inlet Efficiency (E%)														
S <sub>x</sub> =		0.015					0.03					0.045				
S <sub>L</sub> =		0.02	0.04	0.06	0.08	0.1	0.02	0.04	0.06	0.08	0.1	0.02	0.04	0.06	0.08	0.1
Q(cfs) =	1	71.3	71.1	71.9	72.9	73.8	86.1	87.2	88.5	89.6	90.6	93.0	94.5	95.6	96.5	97.2
	2	60.9	60.2	60.8	61.7	62.5	76.8	77.4	78.5	79.7	80.7	85.4	86.7	88.0	89.2	90.2
	3	54.9	54.1	54.6	55.3	56.0	70.8	71.0	72.1	73.2	74.2	80.0	81.0	82.3	83.5	84.6
	4	50.8	49.9	50.3	50.9	51.7	66.4	66.5	67.5	68.5	69.5	75.8	76.6	77.9	79.1	80.2
	5	47.7	46.7	47.1	47.7	48.4	63.0	62.9	63.8	64.9	65.8	72.5	73.1	74.4	75.6	76.6

**Table A3.11 – Spread (T) S<sub>r</sub> Results with L = 6ft**

		Spread (T) S <sub>r</sub> Results														
S <sub>x</sub> =		0.015					0.03					0.045				
S <sub>L</sub> =		0.02	0.04	0.06	0.08	0.1	0.02	0.04	0.06	0.08	0.1	0.02	0.04	0.06	0.08	0.1
Q(cfs) =	1	-64.9	-51.1	-43.4	-38.2	-34.4	-23.8	-16.9	-13.5	-11.3	-9.8	-11.6	-7.5	-5.5	-4.3	-3.5
	2	-110.5	-89.4	-76.9	-68.4	-62.0	-43.3	-32.6	-26.8	-23.1	-20.4	-23.5	-16.6	-13.1	-10.9	-9.4
	3	-149.6	-122.3	-105.8	-94.2	-85.6	-59.9	-45.9	-38.3	-33.2	-29.5	-33.5	-24.4	-19.7	-16.7	-14.5
	4	-185.0	-152.1	-131.8	-117.5	-106.8	-74.7	-57.9	-48.5	-42.3	-37.7	-42.4	-31.4	-25.6	-21.8	-19.1
	5	-217.9	-179.7	-155.8	-139.0	-126.3	-88.5	-69.0	-58.0	-50.6	-45.1	-50.7	-37.9	-31.0	-26.5	-23.3

**Table A3.12 – Manning's n (n) S<sub>r</sub> Results with L = 6ft**

		Manning's n (n) S <sub>r</sub> Results														
S <sub>x</sub> =		0.015					0.03					0.045				
S <sub>L</sub> =		0.02	0.04	0.06	0.08	0.1	0.02	0.04	0.06	0.08	0.1	0.02	0.04	0.06	0.08	0.1
Q(cfs) =	1	0.434	0.474	0.492	0.505	0.517	0.329	0.392	0.433	0.465	0.493	0.306	0.380	0.431	0.473	0.509
	2	0.587	0.618	0.628	0.636	0.645	0.448	0.518	0.560	0.594	0.623	0.404	0.490	0.547	0.593	0.633
	3	0.687	0.708	0.711	0.716	0.724	0.532	0.603	0.644	0.678	0.708	0.477	0.569	0.629	0.677	0.719
	4	0.761	0.773	0.771	0.774	0.781	0.597	0.667	0.708	0.742	0.772	0.535	0.630	0.692	0.741	0.785
	5	0.819	0.823	0.818	0.819	0.825	0.651	0.719	0.759	0.793	0.824	0.583	0.681	0.743	0.794	0.839

**Table A3.13 – Cross Slope ( $S_x$ )  $S_r$  Results with  $L = 6$  ft**

		Cross Slope ( $S_x$ ) $S_r$ Results														
		$S_x =$					0.015					0.03				
		$S_L =$					0.02	0.04	0.06	0.08	0.1	0.02	0.04	0.06	0.08	0.1
$Q(cfs) =$	1	-0.077	-0.127	-0.163	-0.193	-0.217	-0.130	-0.187	-0.227	-0.259	-0.285	-0.162	-0.223	-0.265	-0.299	-0.327
	2	-0.076	-0.138	-0.183	-0.220	-0.250	-0.138	-0.206	-0.256	-0.295	-0.328	-0.176	-0.250	-0.302	-0.344	-0.379
	3	-0.077	-0.147	-0.198	-0.239	-0.273	-0.142	-0.219	-0.275	-0.319	-0.356	-0.184	-0.267	-0.326	-0.373	-0.412
	4	-0.078	-0.154	-0.210	-0.254	-0.291	-0.146	-0.230	-0.290	-0.338	-0.379	-0.190	-0.280	-0.344	-0.395	-0.437
	5	-0.079	-0.161	-0.221	-0.268	-0.307	-0.149	-0.239	-0.303	-0.354	-0.397	-0.194	-0.290	-0.359	-0.413	-0.459

**Table A3.14 – Longitudinal Slope ( $S_L$ )  $S_r$  Results with  $L = 6$  ft**

		Longitudinal Slope ( $S_L$ ) $S_r$ Results														
		$S_x =$					0.015					0.03				
		$S_L =$					0.02	0.04	0.06	0.08	0.1	0.02	0.04	0.06	0.08	0.1
$Q(cfs) =$	1	-0.217	-0.237	-0.246	-0.252	-0.258	-0.165	-0.196	-0.216	-0.233	-0.247	-0.153	-0.190	-0.216	-0.236	-0.255
	2	-0.293	-0.309	-0.314	-0.318	-0.323	-0.224	-0.259	-0.280	-0.297	-0.312	-0.202	-0.245	-0.274	-0.297	-0.316
	3	-0.343	-0.354	-0.356	-0.358	-0.362	-0.266	-0.301	-0.322	-0.339	-0.354	-0.238	-0.284	-0.314	-0.338	-0.359
	4	-0.380	-0.386	-0.386	-0.387	-0.390	-0.298	-0.334	-0.354	-0.371	-0.386	-0.267	-0.315	-0.346	-0.371	-0.392
	5	-0.410	-0.412	-0.409	-0.410	-0.413	-0.325	-0.360	-0.379	-0.396	-0.412	-0.292	-0.340	-0.372	-0.397	-0.419

**Table A3.15 – Inlet Length ( $L$ )  $S_r$  Results with  $L = 6$  ft**

		Inlet Length ( $L$ ) $S_r$ Results														
		$S_x =$					0.015					0.03				
		$S_L =$					0.02	0.04	0.06	0.08	0.1	0.02	0.04	0.06	0.08	0.1
$Q(cfs) =$	1	1.491	1.572	1.586	1.584	1.578	1.423	1.481	1.494	1.497	1.496	1.424	1.462	1.470	1.472	1.471
	2	1.606	1.673	1.671	1.658	1.643	1.471	1.536	1.547	1.546	1.541	1.436	1.489	1.499	1.500	1.498
	3	1.689	1.739	1.724	1.702	1.681	1.519	1.583	1.588	1.582	1.573	1.462	1.519	1.528	1.527	1.522
	4	1.754	1.787	1.762	1.733	1.707	1.562	1.620	1.620	1.609	1.597	1.490	1.547	1.553	1.549	1.543
	5	1.807	1.824	1.790	1.756	1.726	1.600	1.652	1.646	1.631	1.617	1.516	1.571	1.574	1.568	1.559

**Table A3.16 – Inlet Width ( $W_g$ )  $S_r$  Results with  $L = 6$  ft**

		Inlet Width ( $W_g$ ) $S_r$ Results														
		$S_x =$					0.015					0.03				
		$S_L =$					0.02	0.04	0.06	0.08	0.1	0.02	0.04	0.06	0.08	0.1
$Q(cfs) =$	1	0.975	1.057	1.079	1.081	1.075	0.803	0.783	0.749	0.713	0.678	0.632	0.547	0.477	0.419	0.371
	2	1.027	1.141	1.178	1.189	1.188	0.900	0.929	0.919	0.900	0.877	0.780	0.750	0.710	0.670	0.633
	3	1.050	1.176	1.218	1.230	1.230	0.938	0.988	0.988	0.973	0.954	0.837	0.834	0.806	0.773	0.741
	4	1.063	1.195	1.238	1.251	1.250	0.959	1.020	1.025	1.012	0.994	0.868	0.879	0.858	0.829	0.799
	5	1.072	1.208	1.250	1.262	1.260	0.973	1.040	1.047	1.035	1.017	0.887	0.908	0.890	0.863	0.834

## APPENDIX B

### List of Contents

<b>Appendix B-1</b>	<b>Spread Design Curves</b>	<b>69</b>
Chart B1.1	Triangular Section Spread with Cross Slope ( $S_x$ ) = 0.015	69
Chart B1.2	Triangular Section Spread with Cross Slope ( $S_x$ ) = 0.030	70
Chart B1.3	Triangular Section Spread with Cross Slope ( $S_x$ ) = 0.045	70
Chart B1.4	Composite Section Spread with Cross Slope ( $S_x$ ) = 0.015	71
Chart B1.5	Composite Section Spread with Cross Slope ( $S_x$ ) = 0.030	71
Chart B1.6	Composite Section Spread with Cross Slope ( $S_x$ ) = 0.045	72
<b>Appendix B-2</b>	<b>Curb-Opening Efficiency Design Curves (1 Curb-Opening: L = 3ft)</b>	<b>73</b>
Chart B2.1	Triangular Section 3ft Curb-Opening with Cross Slope ( $S_x$ ) = 0.015	74
Chart B2.2	Triangular Section 3ft Curb-Opening with Cross Slope ( $S_x$ ) = 0.030	74
Chart B2.3	Triangular Section 3ft Curb-Opening with Cross Slope ( $S_x$ ) = 0.045	75
Chart B2.4	Triangular Section 6ft Curb-Opening with Cross Slope ( $S_x$ ) = 0.015	75
Chart B2.5	Triangular Section 6ft Curb-Opening with Cross Slope ( $S_x$ ) = 0.030	76
Chart B2.6	Triangular Section 6ft Curb-Opening with Cross Slope ( $S_x$ ) = 0.045	76
Chart B2.7	Triangular Section 9ft Curb-Opening with Cross Slope ( $S_x$ ) = 0.015	77
Chart B2.8	Triangular Section 9ft Curb-Opening with Cross Slope ( $S_x$ ) = 0.030	77
Chart B2.9	Triangular Section 9ft Curb-Opening with Cross Slope ( $S_x$ ) = 0.045	78
Chart B2.10	Composite Section (W = 2ft, a = 2in) 3ft Curb-Opening with Cross Slope ( $S_x$ ) = 0.015	78
Chart B2.11	Composite Section (W = 2ft, a = 2in) 3ft Curb-Opening with Cross Slope ( $S_x$ ) = 0.030	79
Chart B2.12	Composite Section (W = 2ft, a = 2in) 3ft Curb-Opening with Cross Slope ( $S_x$ ) = 0.045	79
Chart B2.13	Composite Section (W = 2ft, a = 2in) 9ft Curb-Opening with Cross Slope ( $S_x$ ) = 0.015	80
Chart B2.14	Composite Section (W = 2ft, a = 2in) 9ft Curb-Opening with Cross Slope ( $S_x$ ) = 0.030	80
Chart B2.15	Composite Section (W = 2ft, a = 2in) 9ft Curb-Opening with Cross Slope ( $S_x$ ) = 0.045	81
<b>Appendix B-3</b>	<b>Grate Inlet Efficiency Design Curves (1 Grate: L = 2ft x W<sub>g</sub> = 2ft)</b>	<b>82</b>
Chart B3.1	Triangular Section 1 Grate with Cross Slope ( $S_x$ ) = 0.015	82
Chart B3.2	Triangular Section 1 Grate with Cross Slope ( $S_x$ ) = 0.030	83
Chart B3.3	Triangular Section 1 Grate with Cross Slope ( $S_x$ ) = 0.045	83
Chart B3.4	Triangular Section 2 Grates with Cross Slope ( $S_x$ ) = 0.015	84
Chart B3.5	Triangular Section 2 Grates with Cross Slope ( $S_x$ ) = 0.030	84
Chart B3.6	Triangular Section 2 Grates with Cross Slope ( $S_x$ ) = 0.045	85
Chart B3.7	Triangular Section 3 Grates with Cross Slope ( $S_x$ ) = 0.015	85
Chart B3.8	Triangular Section 3 Grates with Cross Slope ( $S_x$ ) = 0.030	86
Chart B3.9	Triangular Section 3 Grates with Cross Slope ( $S_x$ ) = 0.045	86
Chart B3.10	Composite Section (W = 2ft, a = 2in) 1 Grate with Cross Slope ( $S_x$ ) = 0.015	87
Chart B3.11	Composite Section (W = 2ft, a = 2in) 1 Grate with Cross Slope ( $S_x$ ) = 0.030	87
Chart B3.12	Composite Section (W = 2ft, a = 2in) 1 Grate with Cross Slope ( $S_x$ ) = 0.045	88
Chart B3.13	Composite Section (W = 2ft, a = 2in) 3 Grates with Cross Slope ( $S_x$ ) = 0.015	88
Chart B3.14	Composite Section (W = 2ft, a = 2in) 3 Grates with Cross Slope ( $S_x$ ) = 0.030	89
Chart B3.15	Composite Section (W = 2ft, a = 2in) 3 Grates with Cross Slope ( $S_x$ ) = 0.045	89

## APPENDIX B-1

### Spread Design Curves

#### LEGEND:

- SL = 0.02 (line): Resultant spread (T) when longitudinal slope is 0.02 = 2%.
- SL = 0.04 (line): Resultant spread (T) when longitudinal slope is 0.04 = 4%.
- SL = 0.06 (line): Resultant spread (T) when longitudinal slope is 0.06 = 6%.
- SL = 0.08 (line): Resultant spread (T) when longitudinal slope is 0.08 = 8%.
- SL = 0.10 (line): Resultant spread (T) when longitudinal slope is 0.10 = 10%.
- H2 (circular marker): Resultant depth (H) when longitudinal slope is 0.02 = 2%.
- H4 (circular marker): Resultant depth (H) when longitudinal slope is 0.04 = 4%.
- H6 (circular marker): Resultant depth (H) when longitudinal slope is 0.06 = 6%.
- H8 (circular marker): Resultant depth (H) when longitudinal slope is 0.08 = 8%.
- H10 (circular marker): Resultant depth (H) when longitudinal slope is 0.10 = 10%.

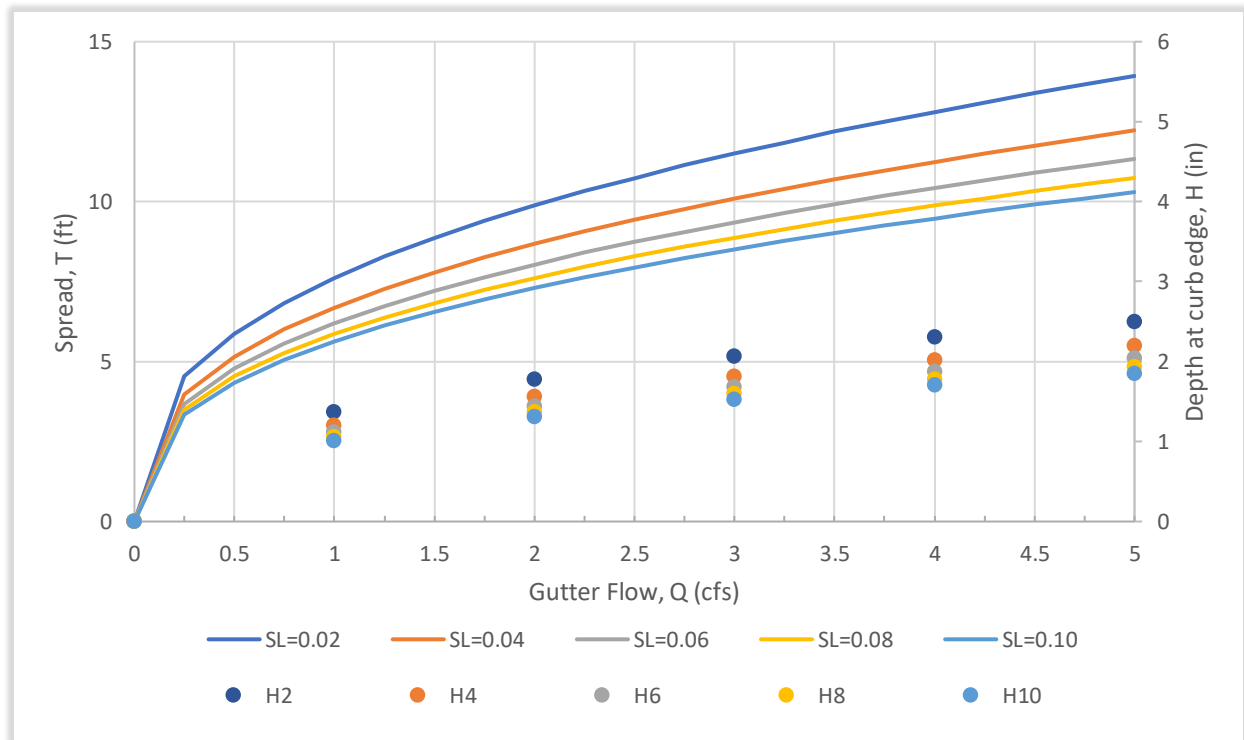


**Chart B1.1** - Triangular Section Spread with Cross Slope ( $S_x$ ) = 0.015.

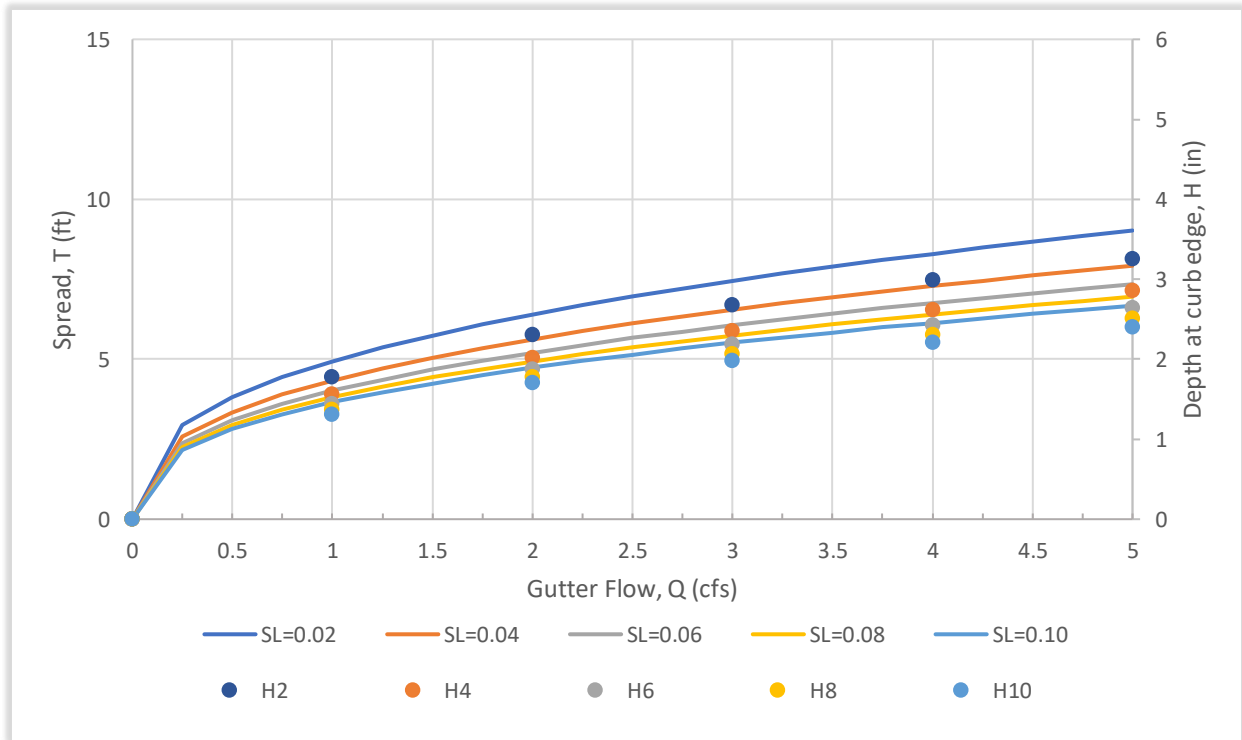


**Chart B1.2** - Triangular Section Spread with Cross Slope ( $S_x$ ) = 0.030.

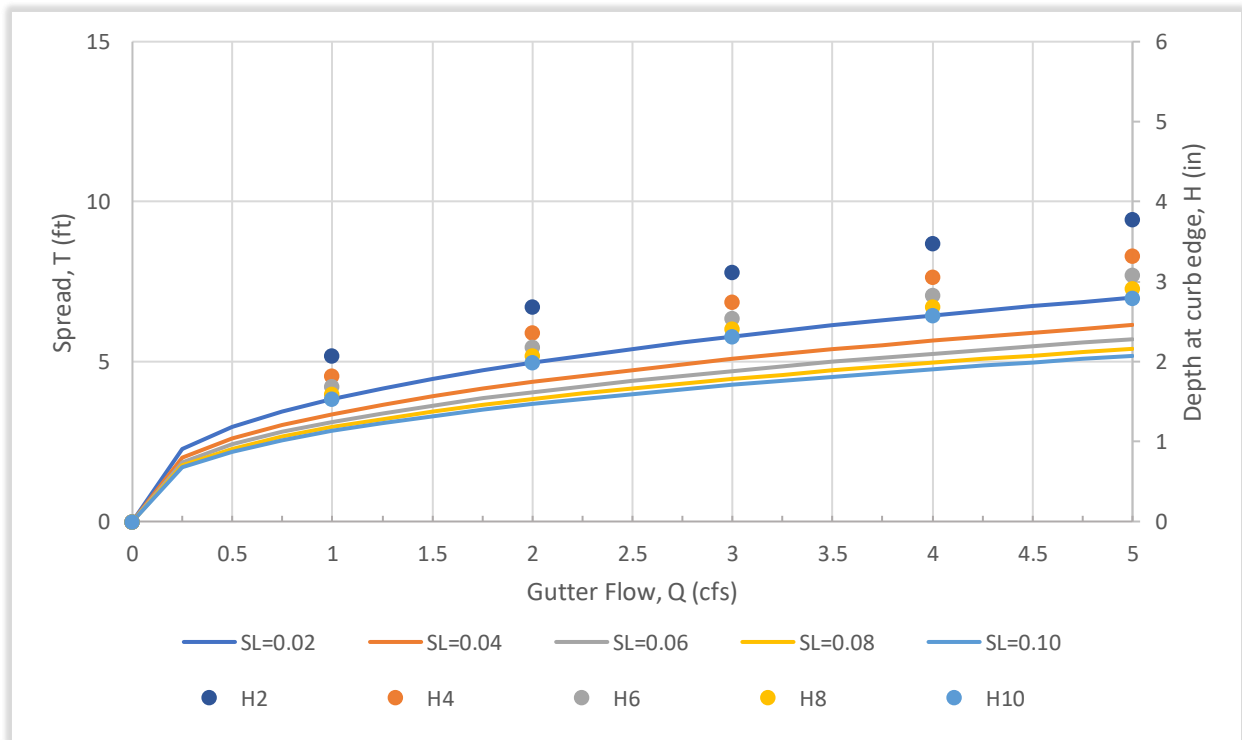


**Chart B1.3** - Triangular Section Spread with Cross Slope ( $S_x$ ) = 0.045.

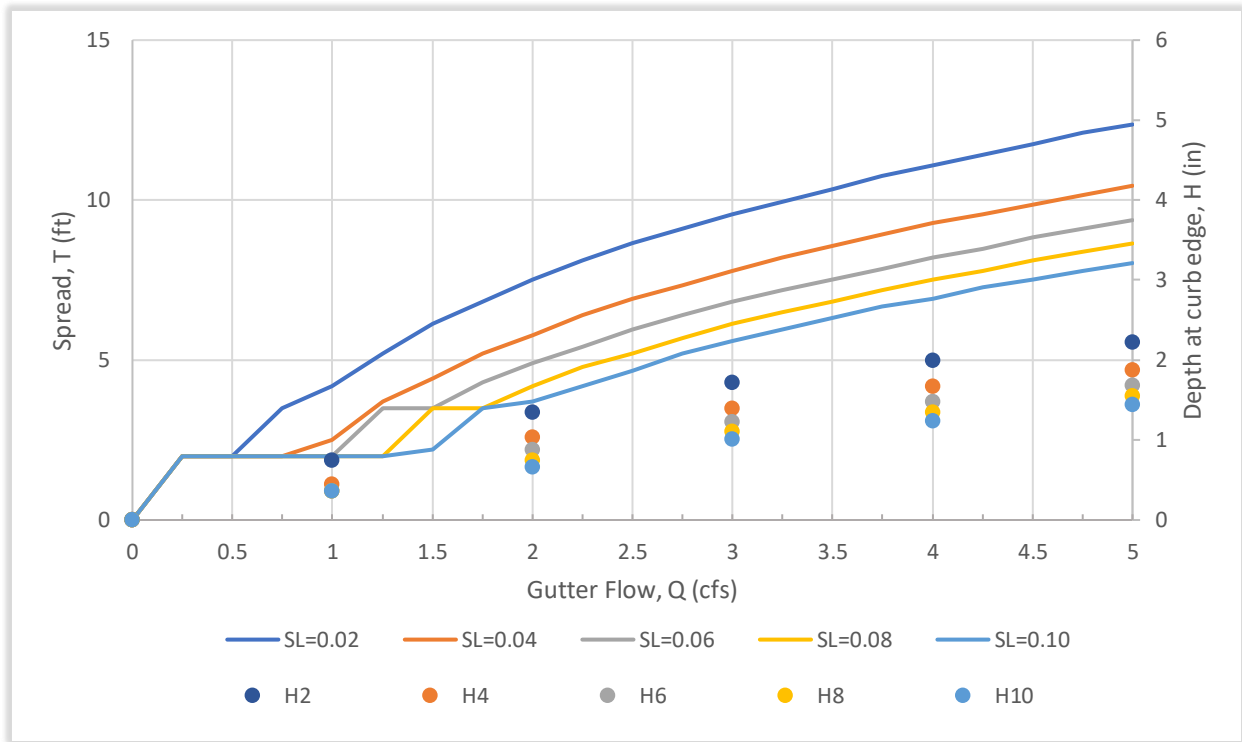


**Chart B1.4** – Composite Section Spread with Cross Slope ( $S_x$ ) = 0.015.

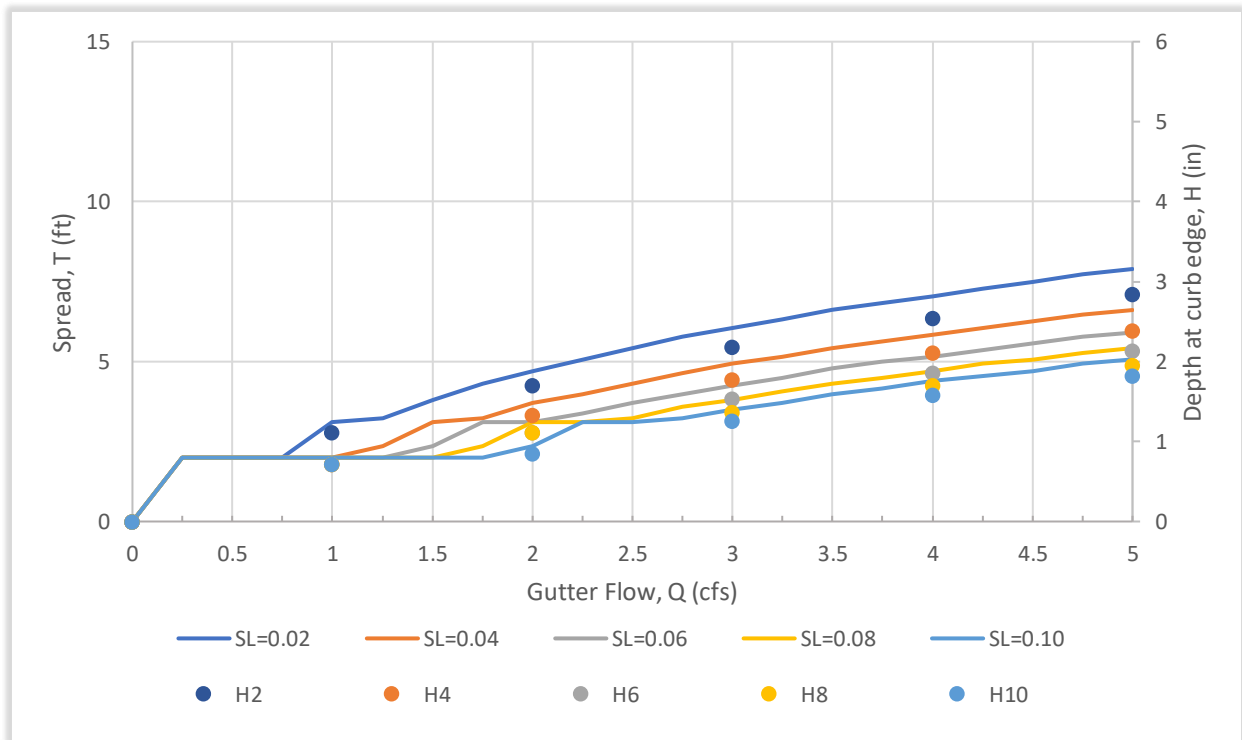


**Chart B1.5** – Composite Section Spread with Cross Slope ( $S_x$ ) = 0.030.

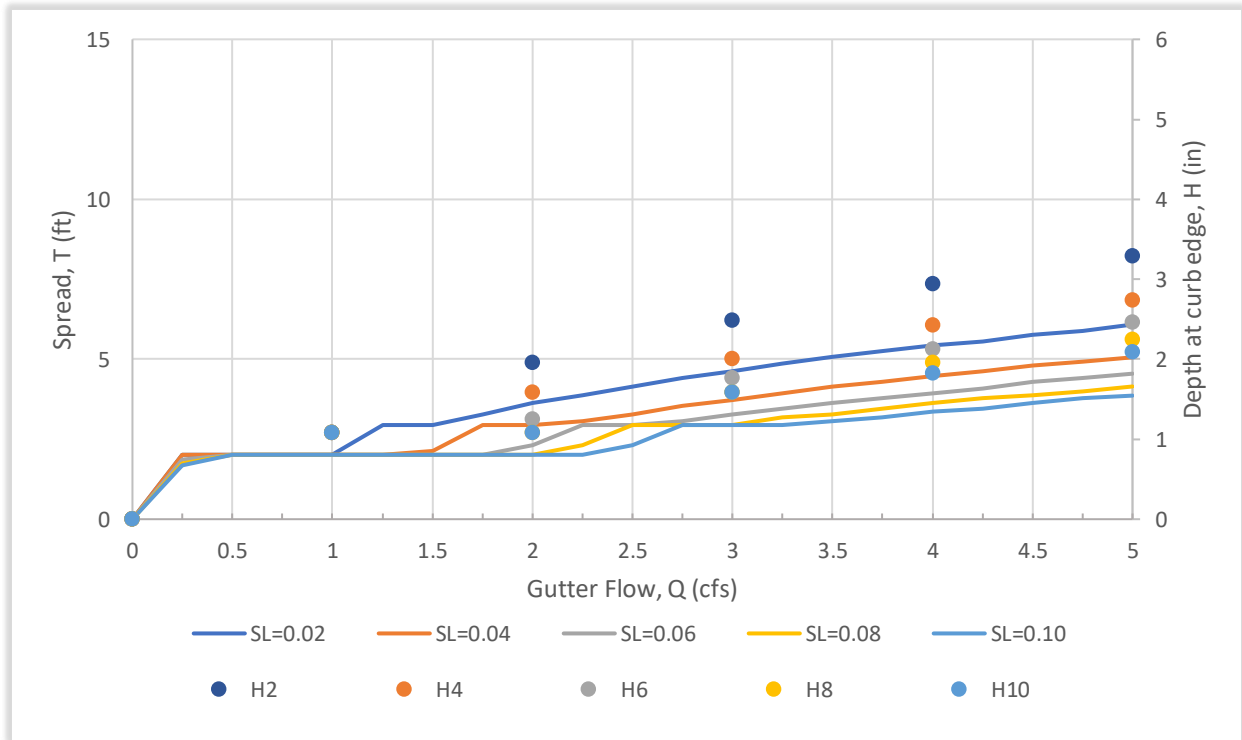


**Chart B1.6** – Composite Section Spread with Cross Slope ( $S_x$ ) = 0.045.

## APPENDIX B-2

### Curb-Opening Efficiency Design Curves (1 Curb-Opening: L = 3ft)

#### LEGEND:

- Curb 2013 SL = 0.02 (line): Interception efficiency (E) of curb-opening inlets with longitudinal slope of 0.02 = 2% when using the HEC-22 (2013) equations (2.9) and (2.11).
- Curb 2013 SL = 0.04 (line): Interception efficiency (E) of curb-opening inlets with longitudinal slope of 0.04 = 4% when using the HEC-22 (2013) equations (2.9) and (2.11).
- Curb 2013 SL = 0.06 (line): Interception efficiency (E) of curb-opening inlets with longitudinal slope of 0.06 = 6% when using the HEC-22 (2013) equations (2.9) and (2.11).
- Curb 2013 SL = 0.08 (line): Interception efficiency (E) of curb-opening inlets with longitudinal slope of 0.08 = 8% when using the HEC-22 (2013) equations (2.9) and (2.11).
- Curb 2013 SL = 0.10 (line): Interception efficiency (E) of curb-opening inlets with longitudinal slope of 0.10 = 10% when using the HEC-22 (2013) equations (2.9) and (2.11).
  
- Curb 2019 SL = 0.02 (line with cross marker): Interception efficiency (E) of curb-opening inlets with longitudinal slope of 0.02 = 2% when using the Li et al. (2019) equations (2.13) and (2.14).
- Curb 2019 SL = 0.04 (line with cross marker): Interception efficiency (E) of curb-opening inlets with longitudinal slope of 0.04 = 4% when using the Li et al. (2019) equations (2.13) and (2.14).
- Curb 2019 SL = 0.06 (line with cross marker): Interception efficiency (E) of curb-opening inlets with longitudinal slope of 0.06 = 6% when using the Li et al. (2019) equations (2.13) and (2.14).
- Curb 2019 SL = 0.08 (line with cross marker): Interception efficiency (E) of curb-opening inlets with longitudinal slope of 0.08 = 8% when using the Li et al. (2019) equations (2.13) and (2.14).
- Curb 2019 SL = 0.10 (line with cross marker): Interception efficiency (E) of curb-opening inlets with longitudinal slope of 0.10 = 10% when using the Li et al. (2019) equations (2.13) and (2.14).
  
- Comb SL = 0.02 (line with circular marker): Interception efficiency (E) of “sweeper” combination inlets with longitudinal slope of 0.02 = 2% when using the Guo and MacKenzie (2012) equation (2.21).
- Comb SL = 0.04 (line with circular marker): Interception efficiency (E) of “sweeper” combination inlets with longitudinal slope of 0.04 = 4% when using the Guo and MacKenzie (2012) equation (2.21).
- Comb SL = 0.06 (line with circular marker): Interception efficiency (E) of “sweeper” combination inlets with longitudinal slope of 0.06 = 6% when using the Guo and MacKenzie (2012) equation (2.21).
- Comb SL = 0.08 (line with circular marker): Interception efficiency (E) of “sweeper” combination inlets with longitudinal slope of 0.08 = 8% when using the Guo and MacKenzie (2012) equation (2.21).
- Comb SL = 0.10 (line with circular marker): Interception efficiency (E) of “sweeper” combination inlets with longitudinal slope of 0.10 = 10% when using the Guo and MacKenzie (2012) equation (2.21).



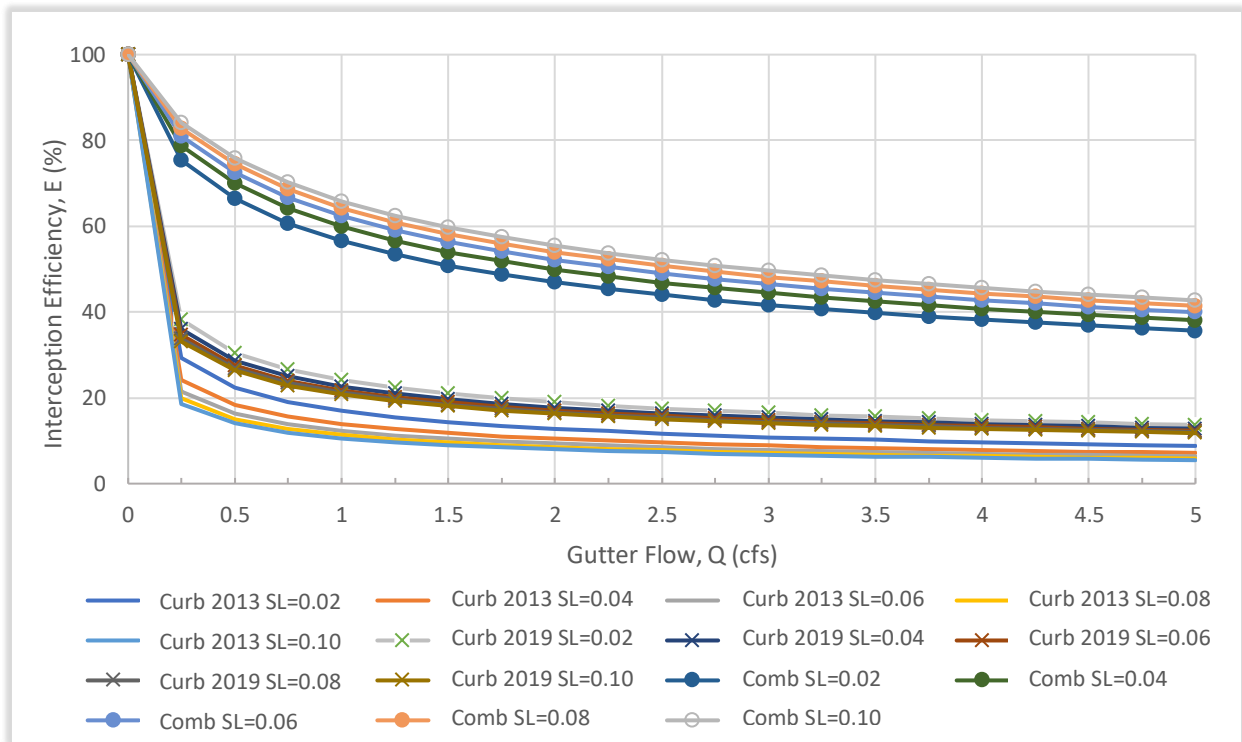


**Chart B2.1** – Triangular Section 3ft Curb-Opening with Cross Slope ( $S_x$ ) = 0.015.

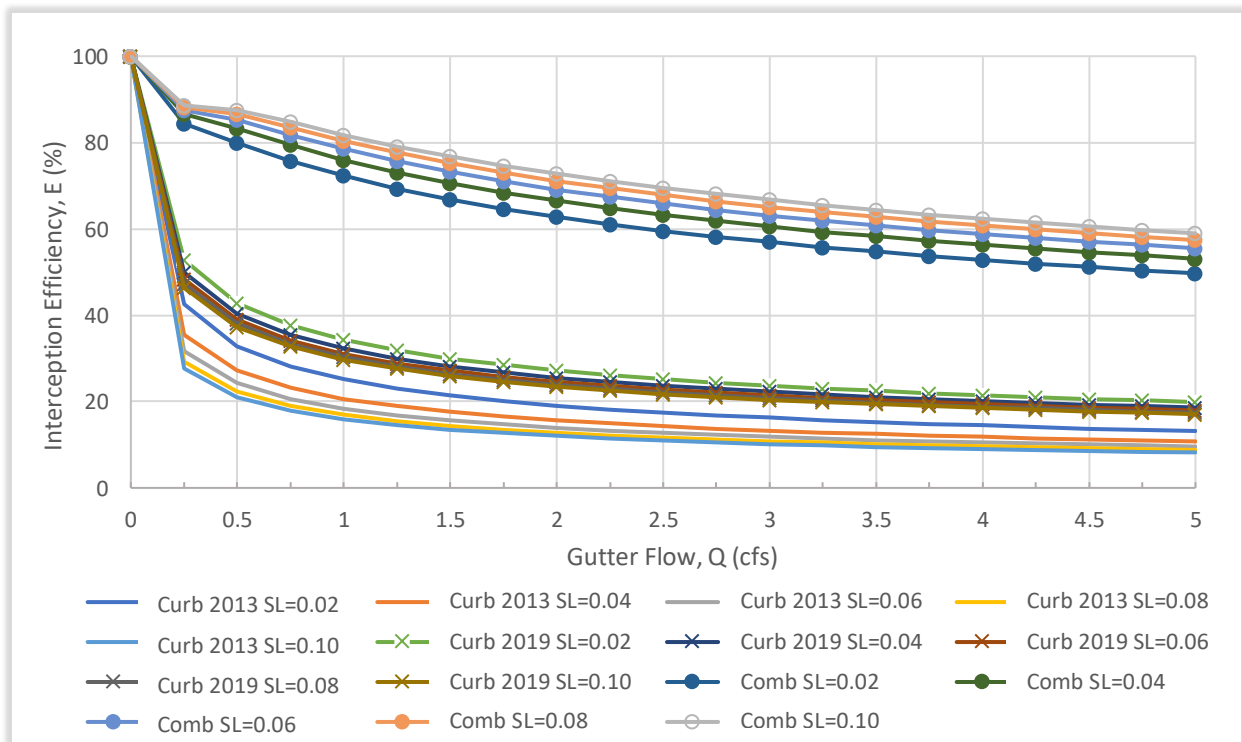


**Chart B2.2** – Triangular Section 3ft Curb-Opening with Cross Slope ( $S_x$ ) = 0.030.

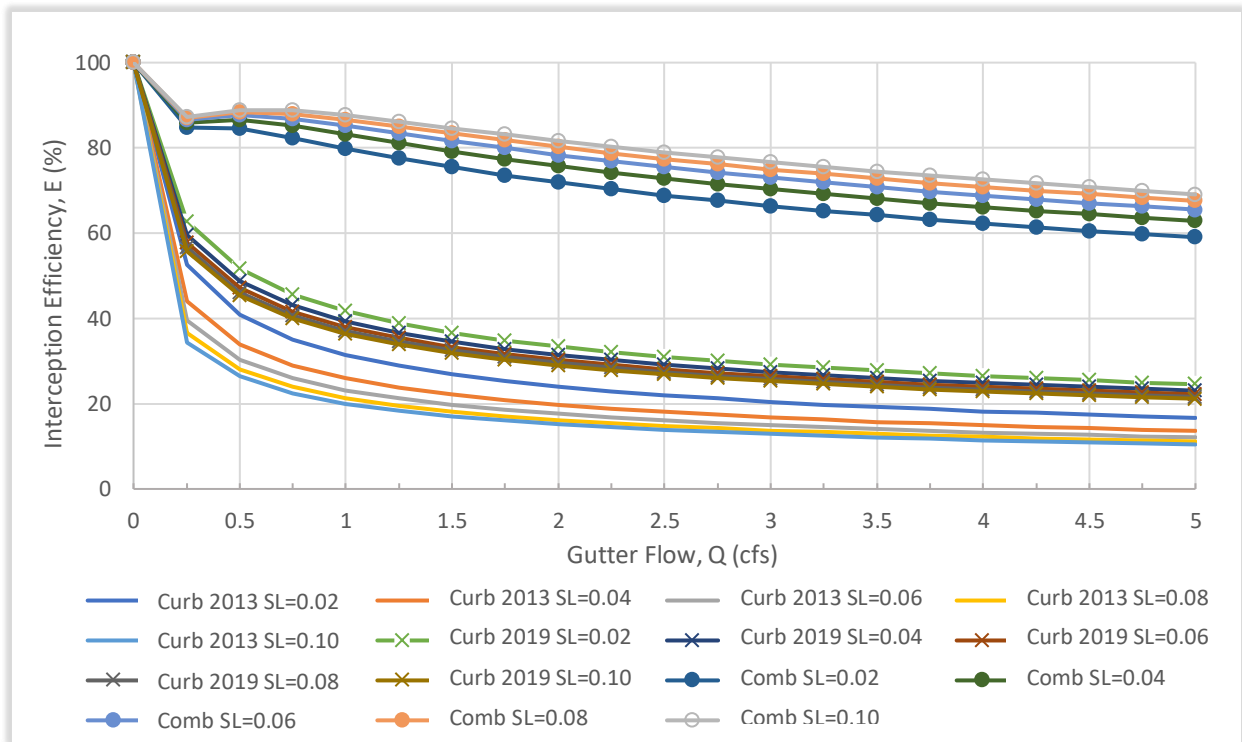


**Chart B2.3** – Triangular Section 3ft Curb-Opening with Cross Slope ( $S_x$ ) = 0.045.

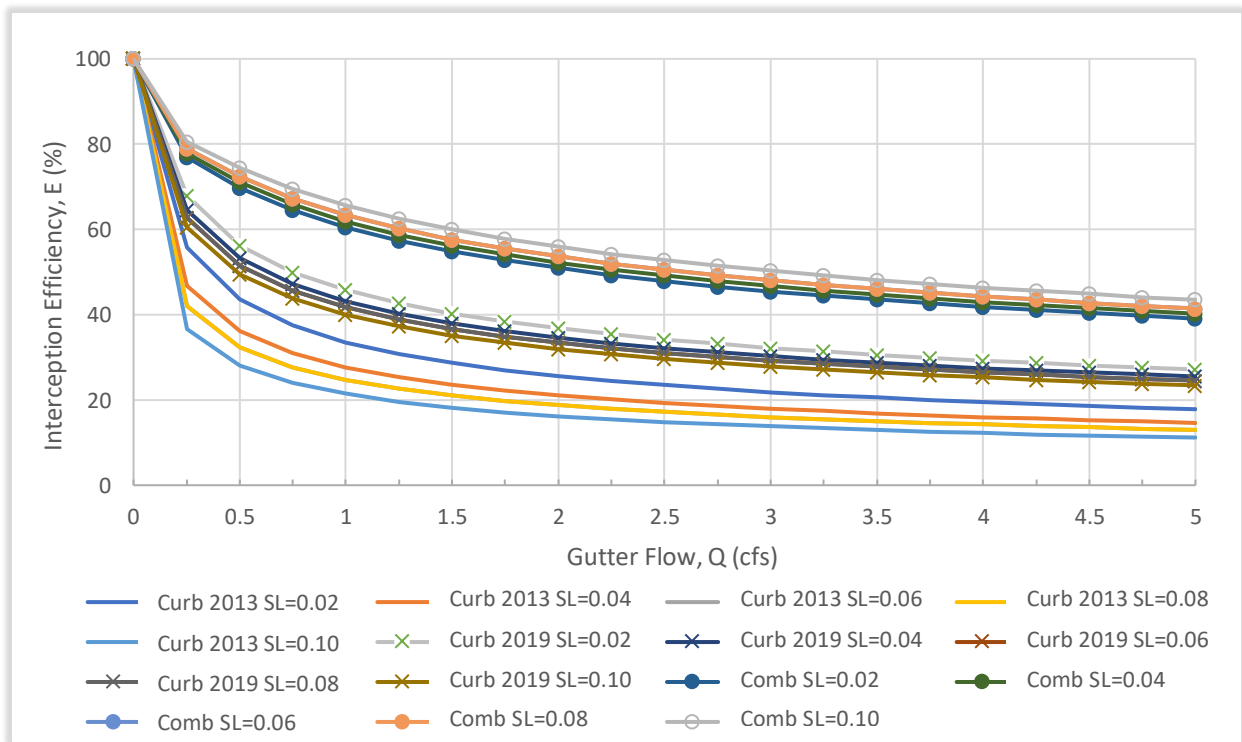


**Chart B2.4** – Triangular Section 6ft Curb-Opening with Cross Slope ( $S_x$ ) = 0.015.

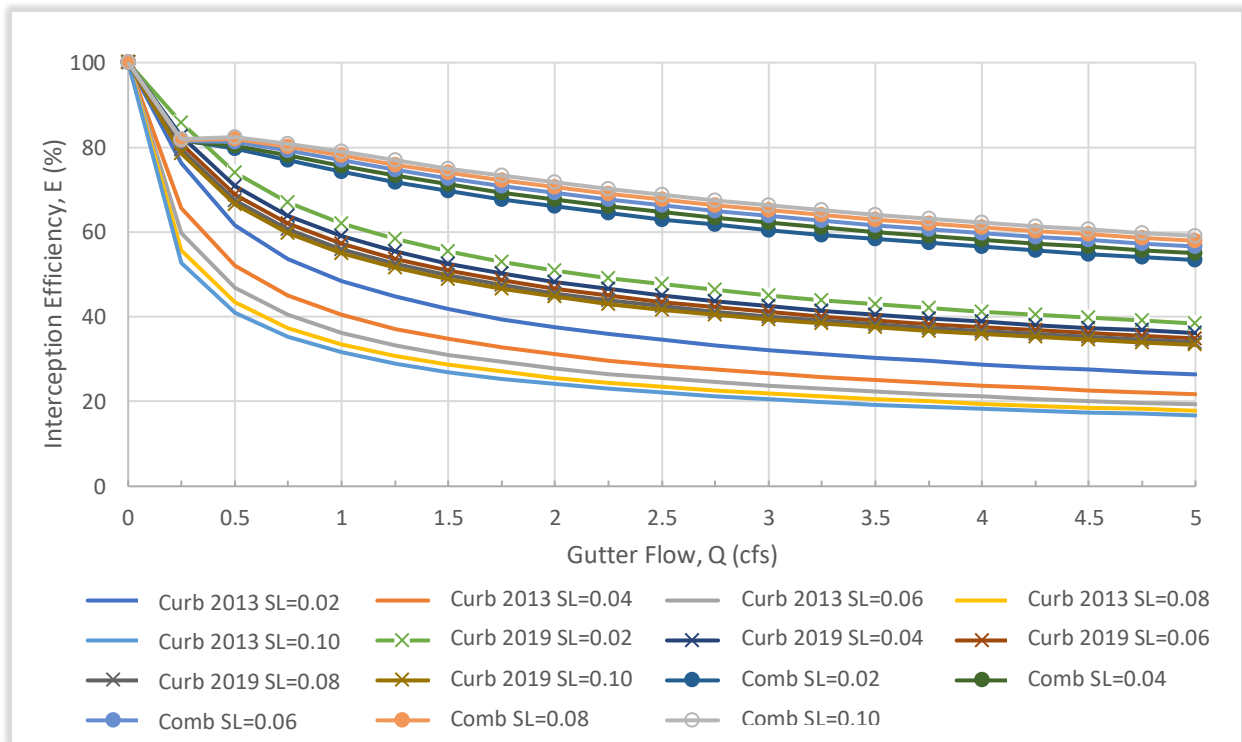


**Chart B2.5** – Triangular Section 6ft Curb-Opening with Cross Slope ( $S_x$ ) = 0.030.

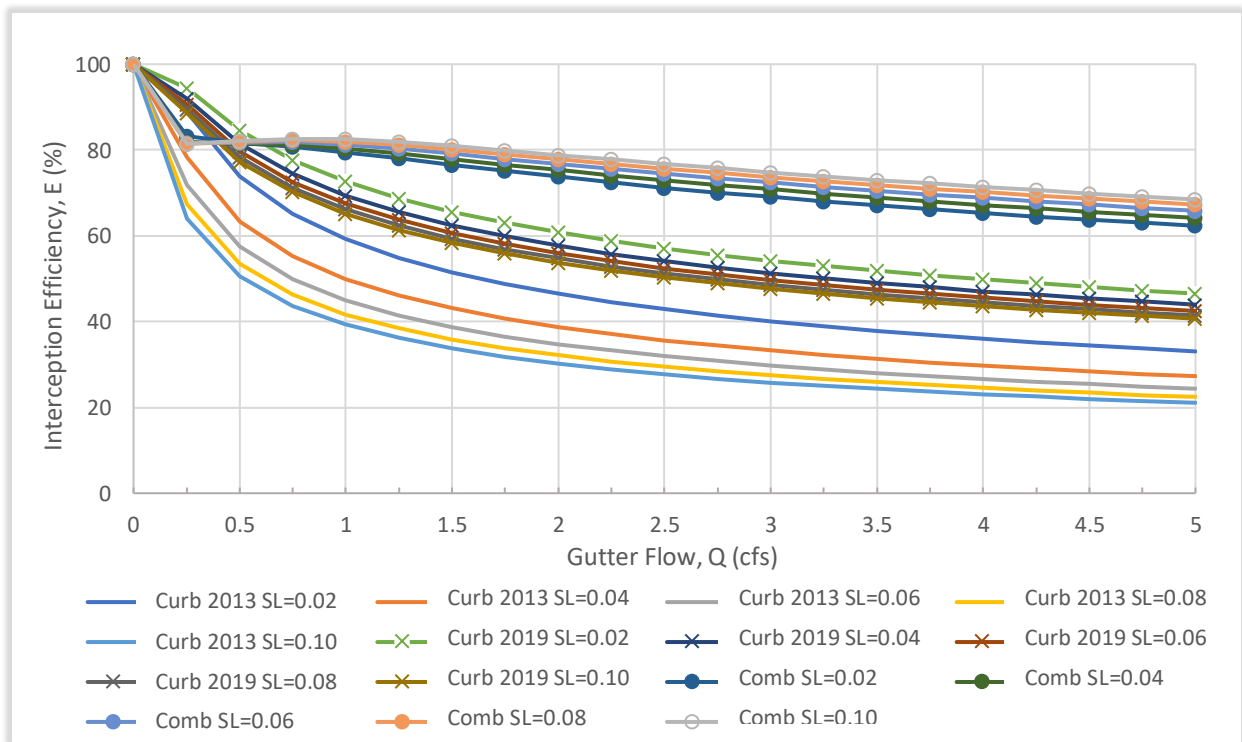


**Chart B2.6** – Triangular Section 6ft Curb-Opening with Cross Slope ( $S_x$ ) = 0.045.

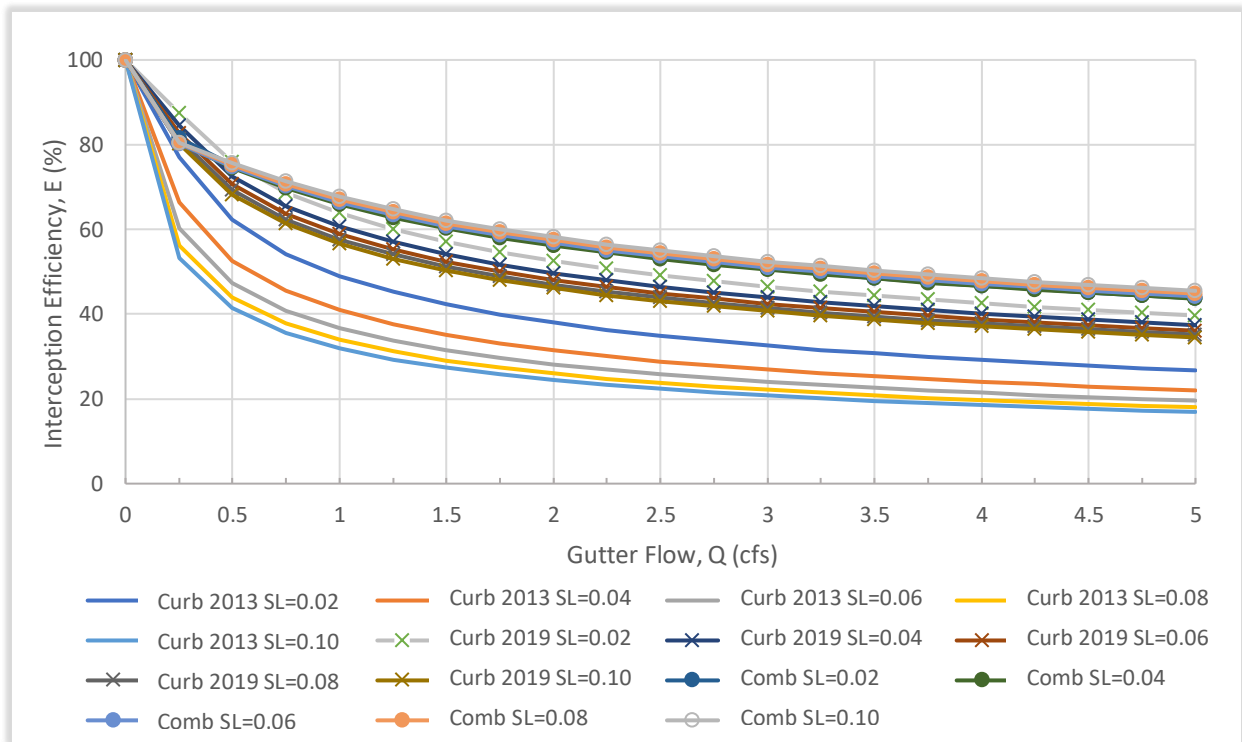


**Chart B2.7** – Triangular Section 9ft Curb-Opening with Cross Slope ( $S_x$ ) = 0.015.

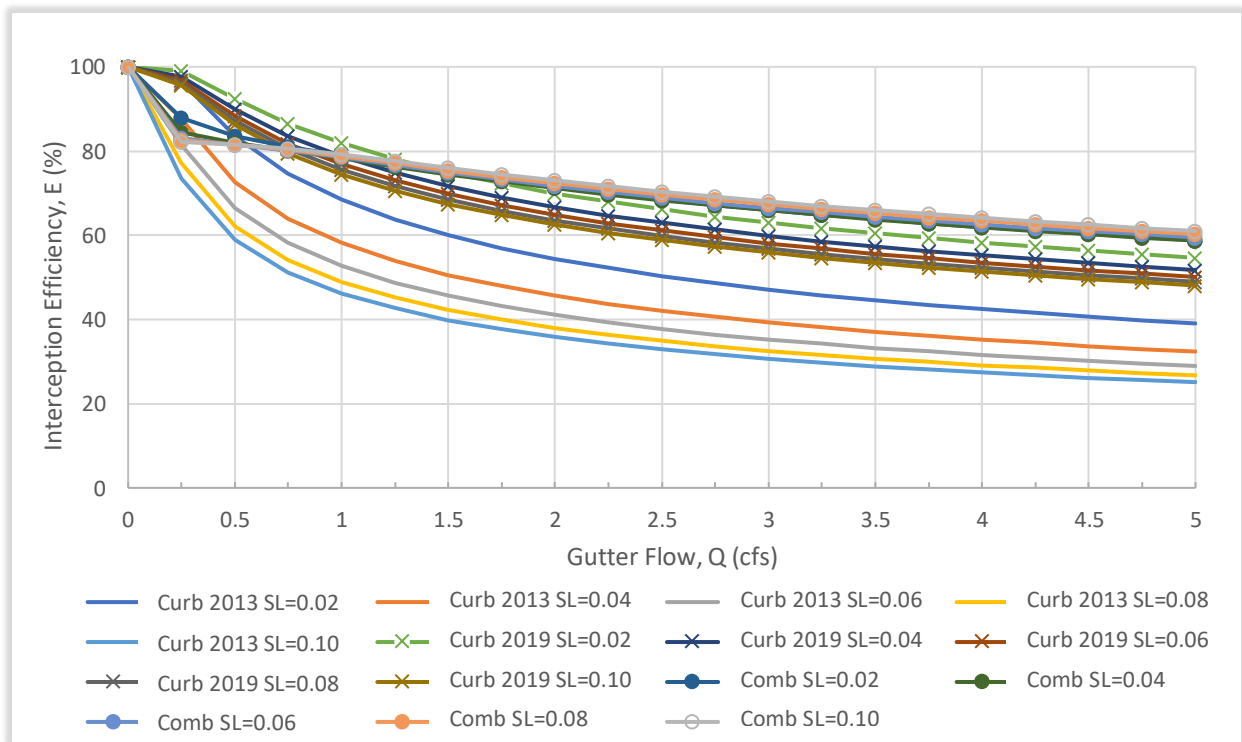


**Chart B2.8** – Triangular Section 9ft Curb-Opening with Cross Slope ( $S_x$ ) = 0.030.

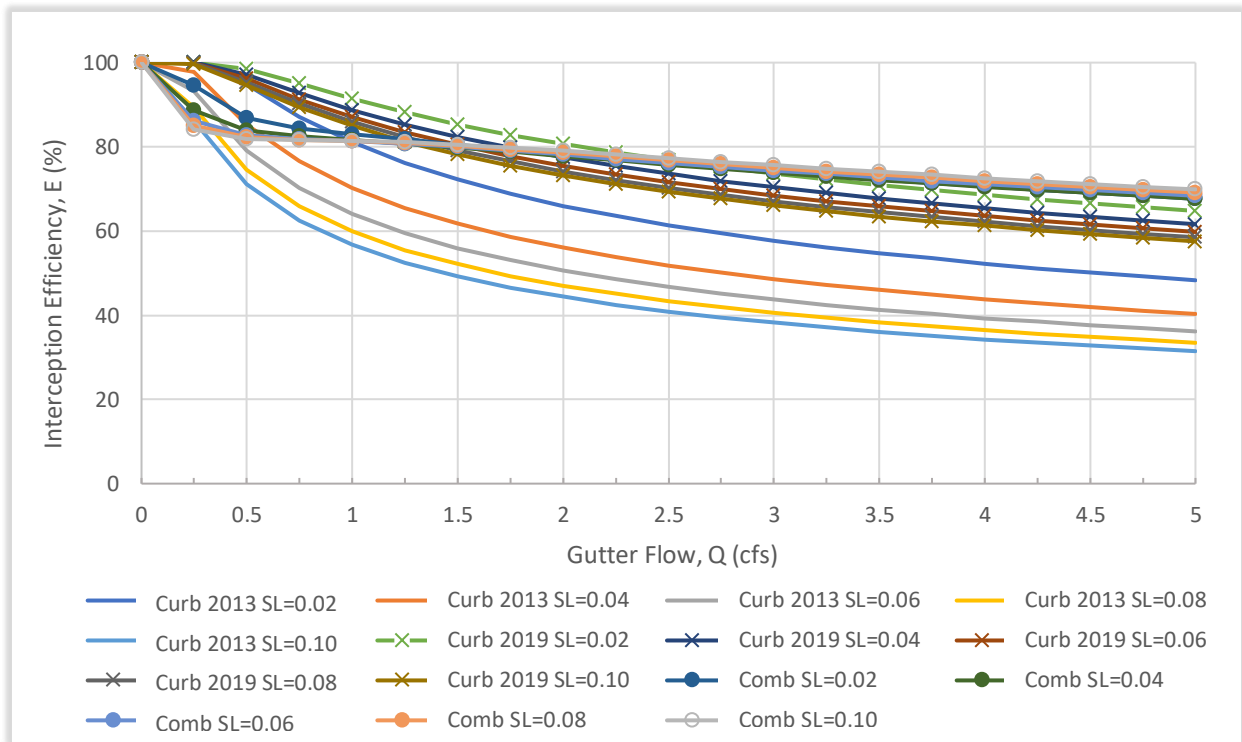


**Chart B2.9** – Triangular Section 9ft Curb-Opening with Cross Slope ( $S_x$ ) = 0.045.

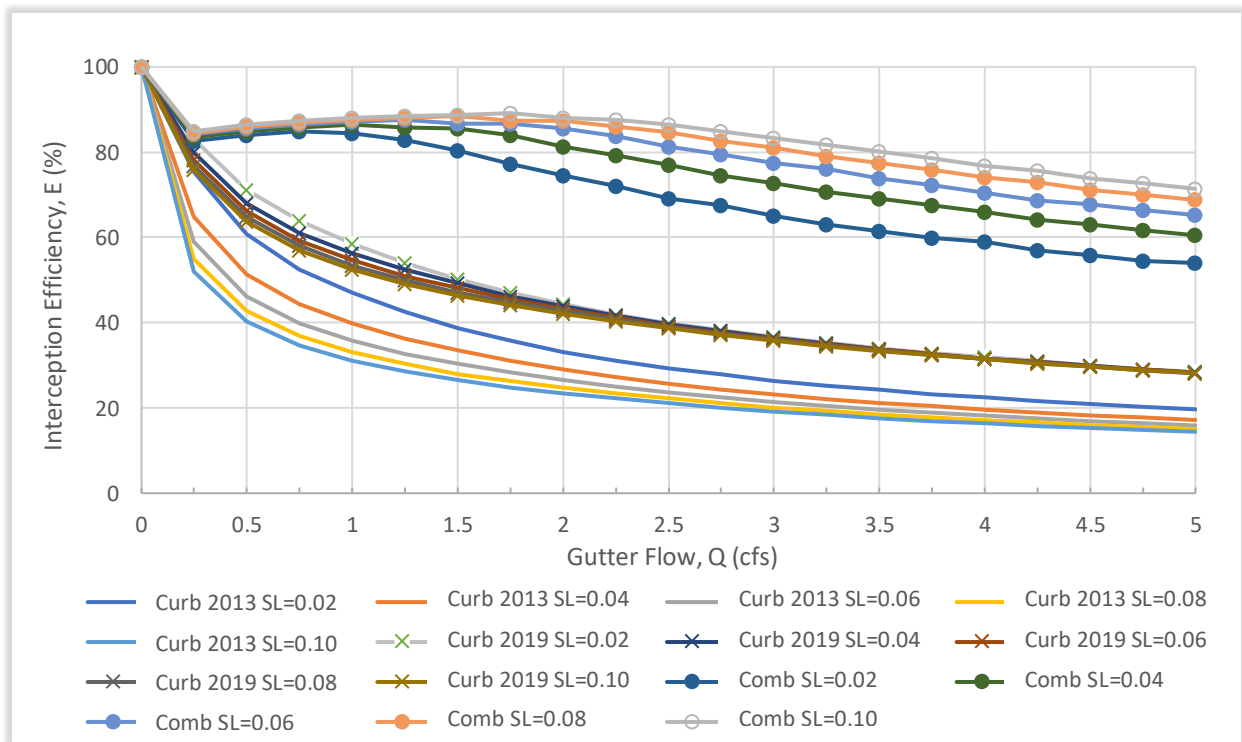


**Chart B2.10** – Composite Section 3ft Curb-Opening with Cross Slope ( $S_x$ ) = 0.015.

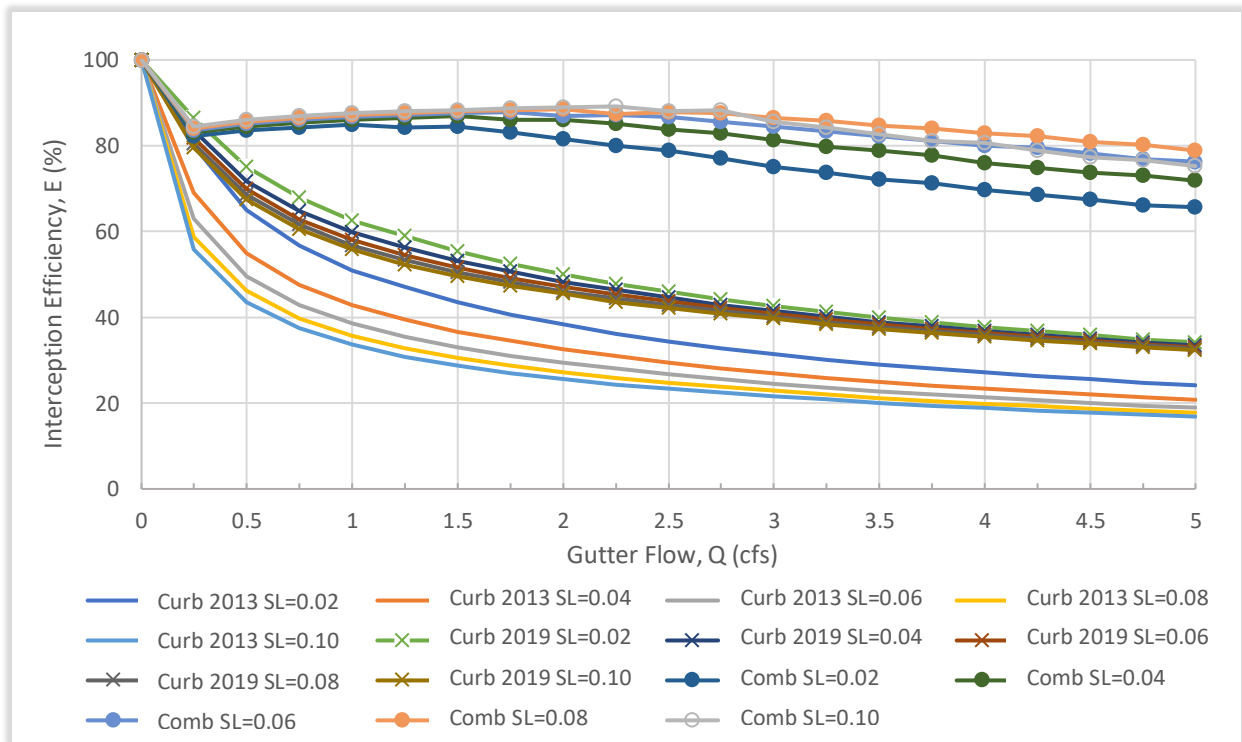


**Chart B2.11** – Composite Section 3ft Curb-Opening with Cross Slope ( $S_x$ ) = 0.030.

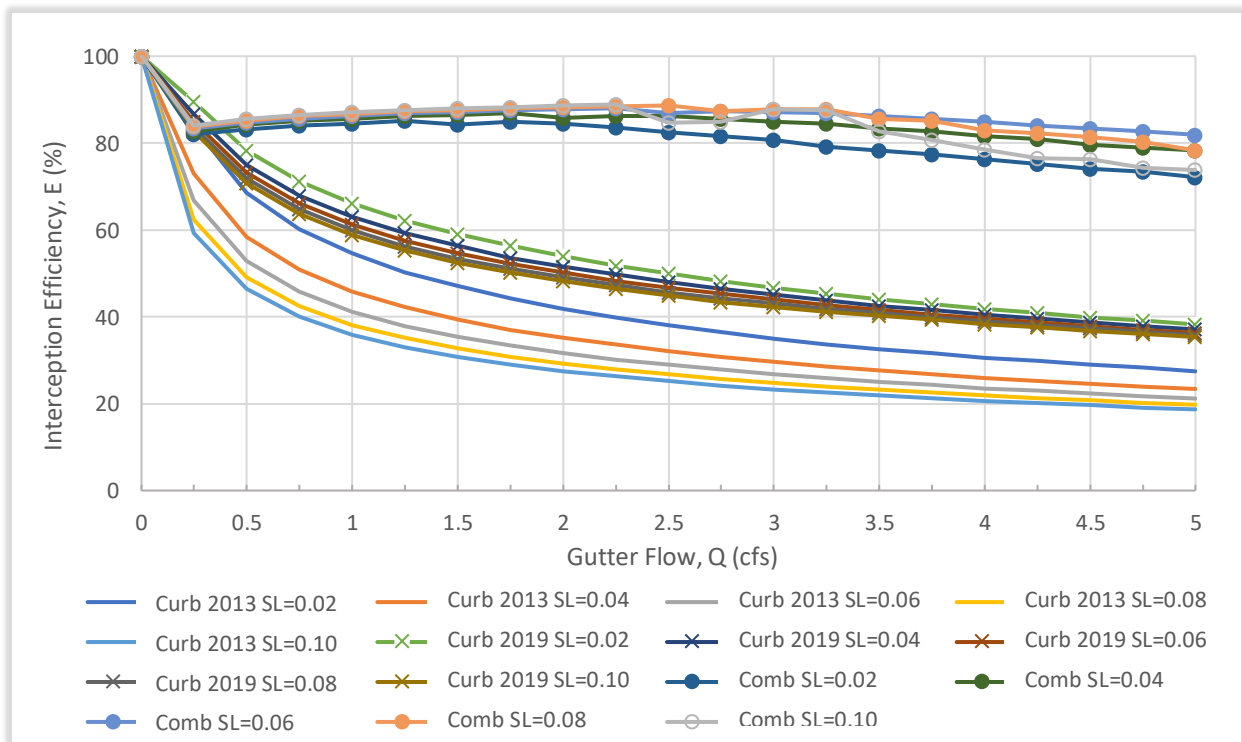


**Chart B2.12** – Composite Section 3ft Curb-Opening with Cross Slope ( $S_x$ ) = 0.045.

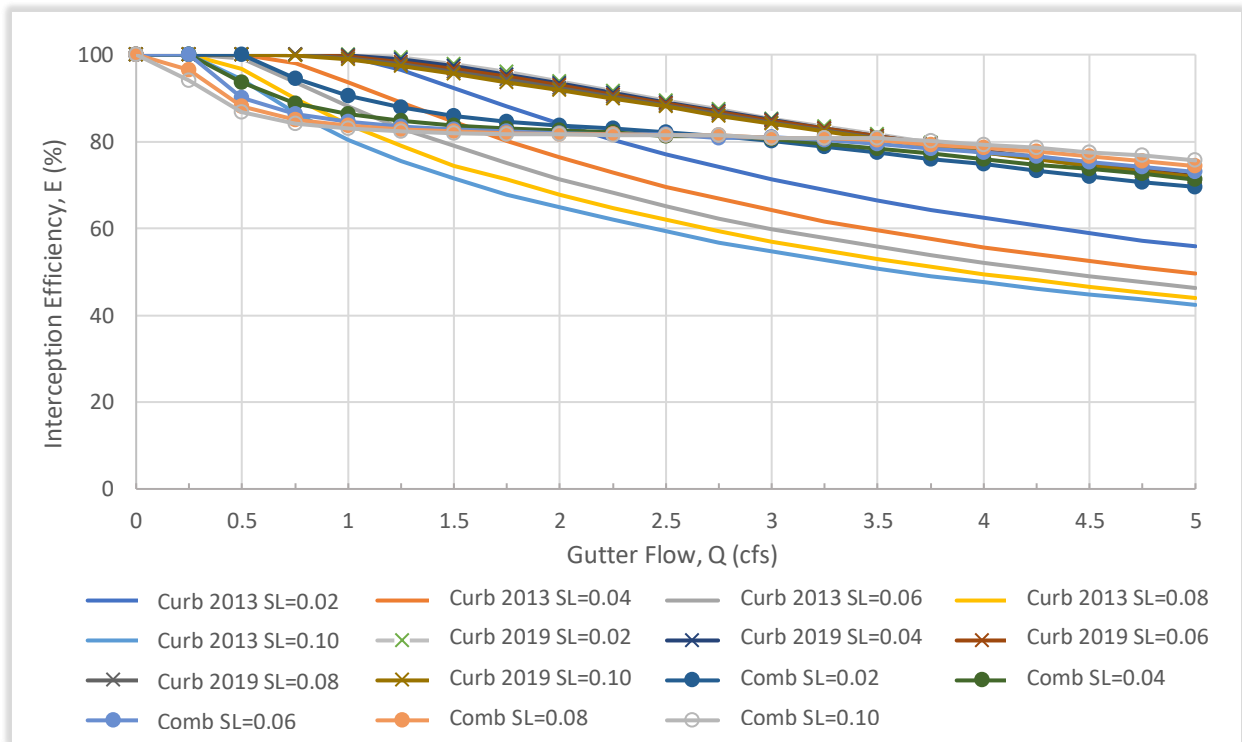


**Chart B2.13** – Composite Section 9ft Curb-Opening with Cross Slope ( $S_x$ ) = 0.015.

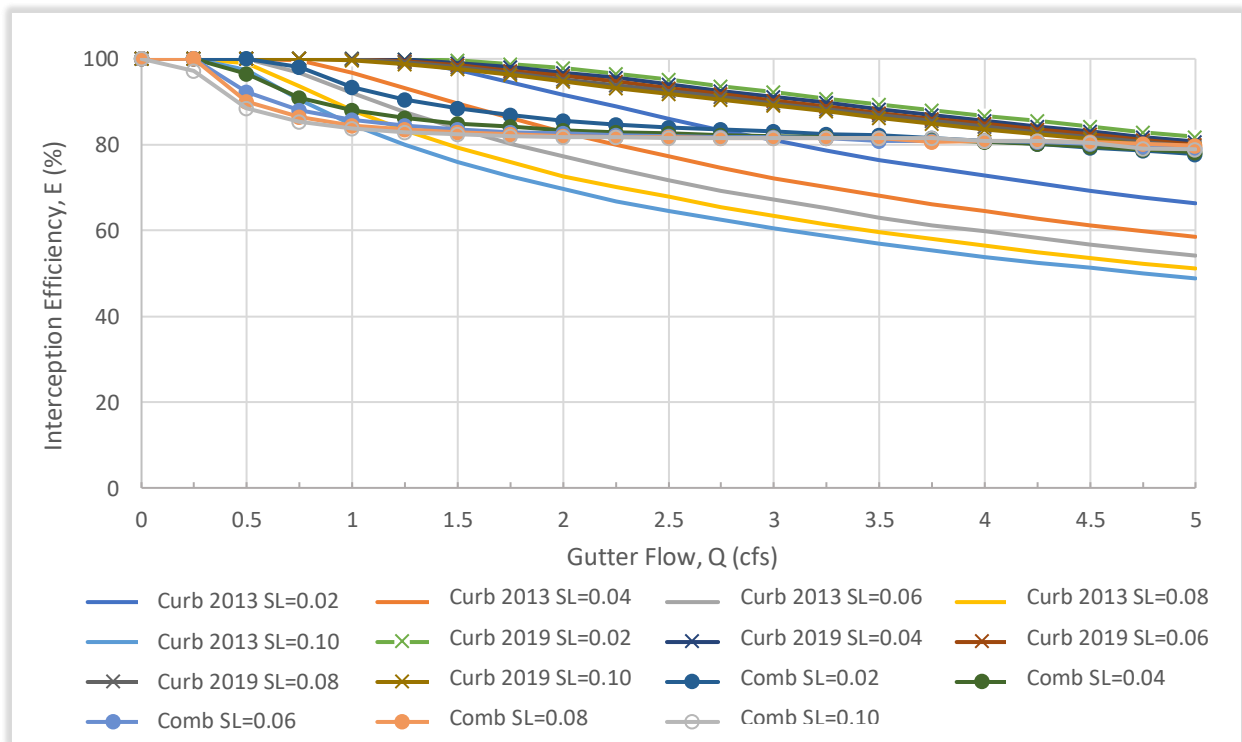


**Chart B2.14** – Composite Section 9ft Curb-Opening with Cross Slope ( $S_x$ ) = 0.030.

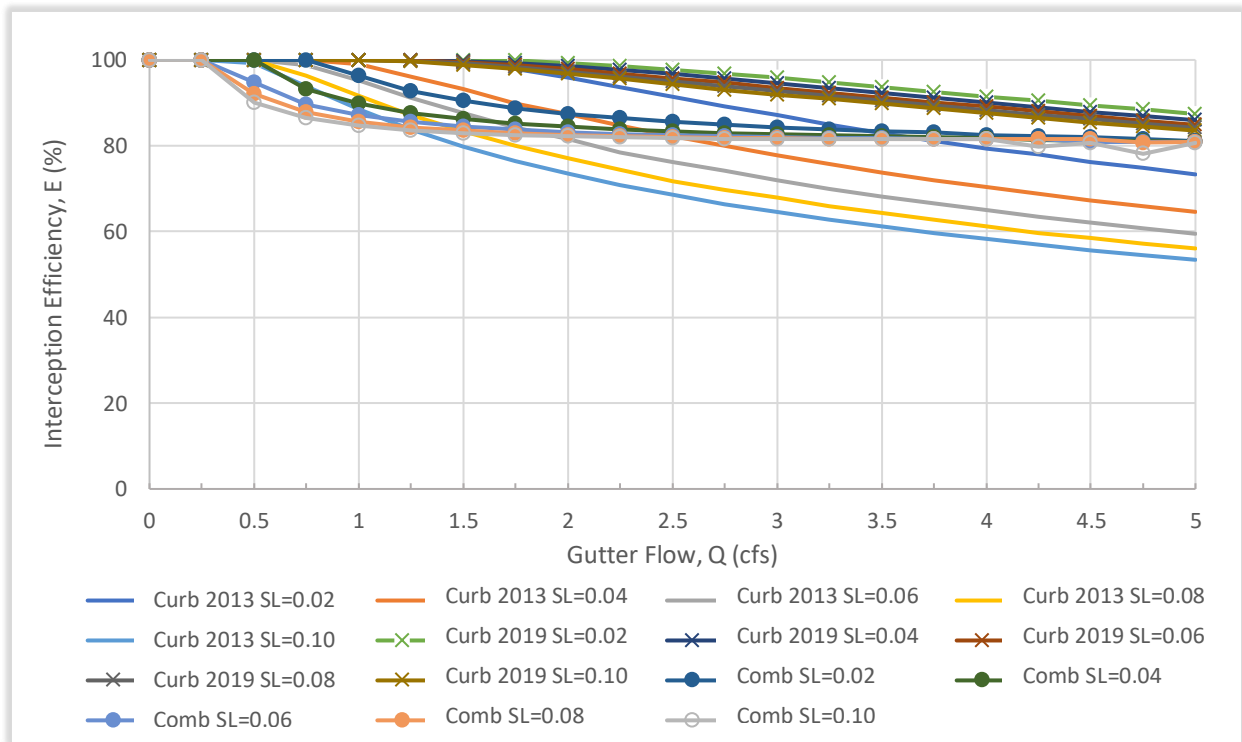


**Chart B2.15** – Composite Section 9ft Curb-Opening with Cross Slope ( $S_x$ ) = 0.045.



### APPENDIX B-3

#### Grate Inlet Efficiency Design Curves (1 Grate: $L = 2\text{ft}$ x $W_g = 2\text{ft}$ )

##### LEGEND:

- Grate SL = 0.02 (line): Interception efficiency (E) of grate inlets with longitudinal slope of 0.02 = 2% when using the HEC-22 (2013) equation (2.19).
- Grate SL = 0.02 (line): Interception efficiency (E) of grate inlets with longitudinal slope of 0.04 = 4% when using the HEC-22 (2013) equation (2.19).
- Grate SL = 0.02 (line): Interception efficiency (E) of grate inlets with longitudinal slope of 0.06 = 6% when using the HEC-22 (2013) equation (2.19).
- Grate SL = 0.02 (line): Interception efficiency (E) of grate inlets with longitudinal slope of 0.08 = 8% when using the HEC-22 (2013) equation (2.19).
- Grate SL = 0.10 (line): Interception efficiency (E) of grate inlets with longitudinal slope of 0.10 = 10% when using the HEC-22 (2013) equation (2.19).

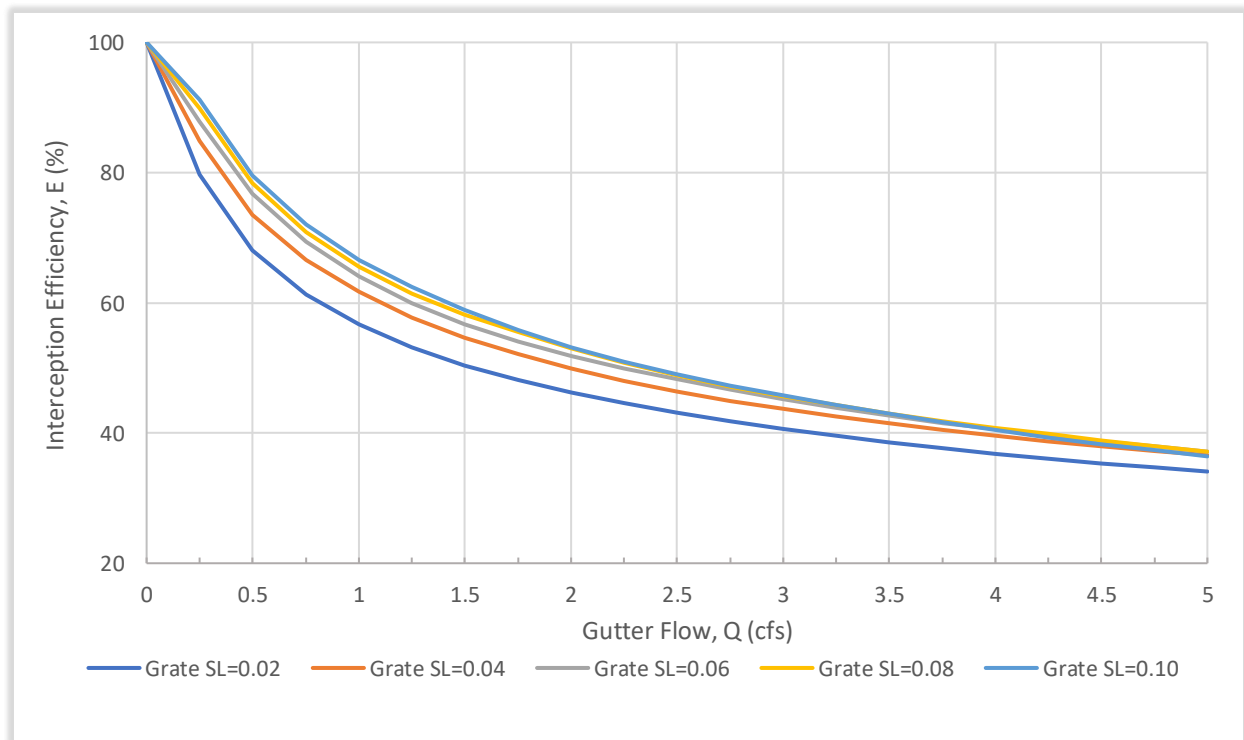


**Chart B3.1** – Triangular Section 1 Grate with Cross Slope ( $S_x$ ) = 0.015.

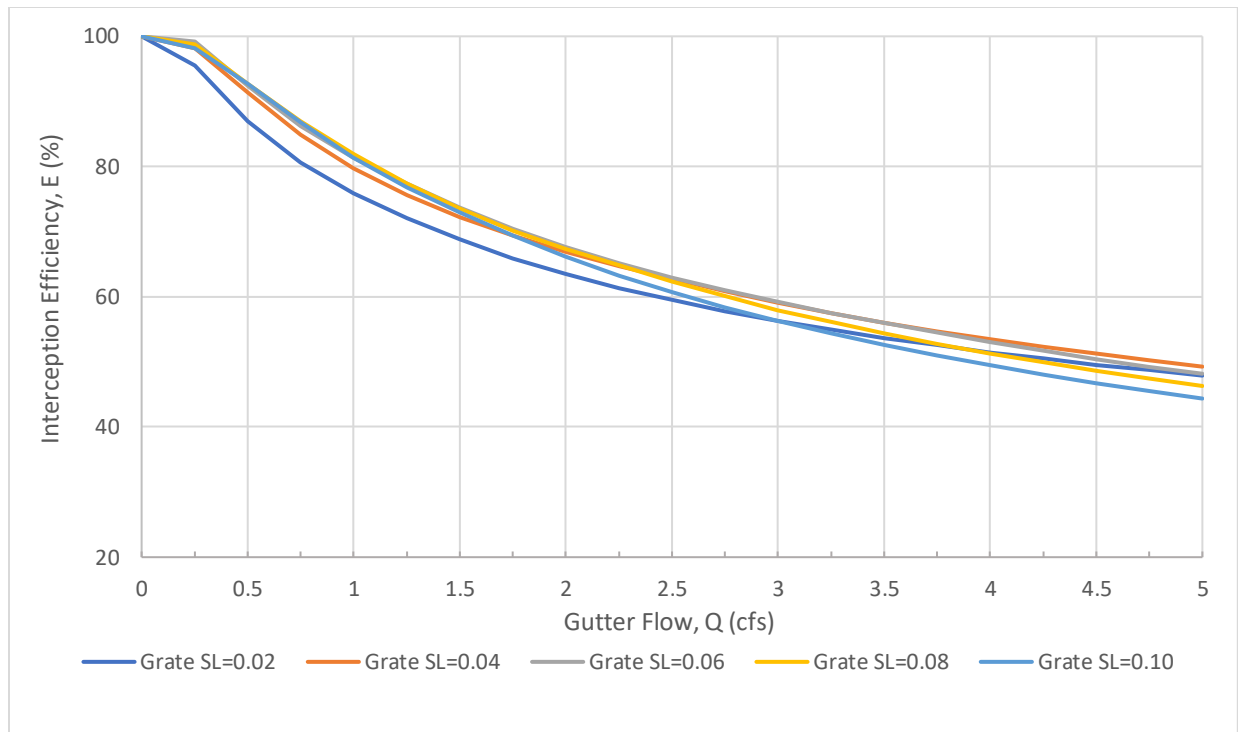


**Chart B3.2** – Triangular Section 1 Grate with Cross Slope ( $S_x$ ) = 0.030.

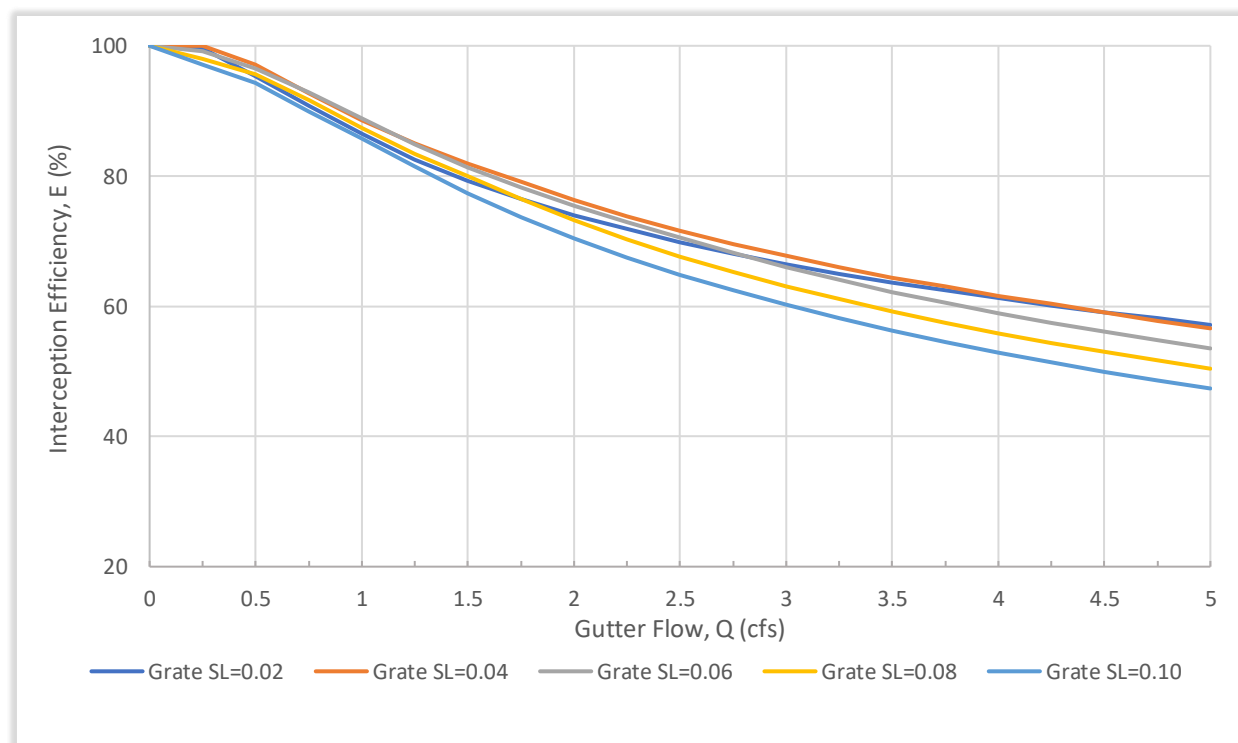


**Chart B3.3** – Triangular Section 1 Grate with Cross Slope ( $S_x$ ) = 0.045.

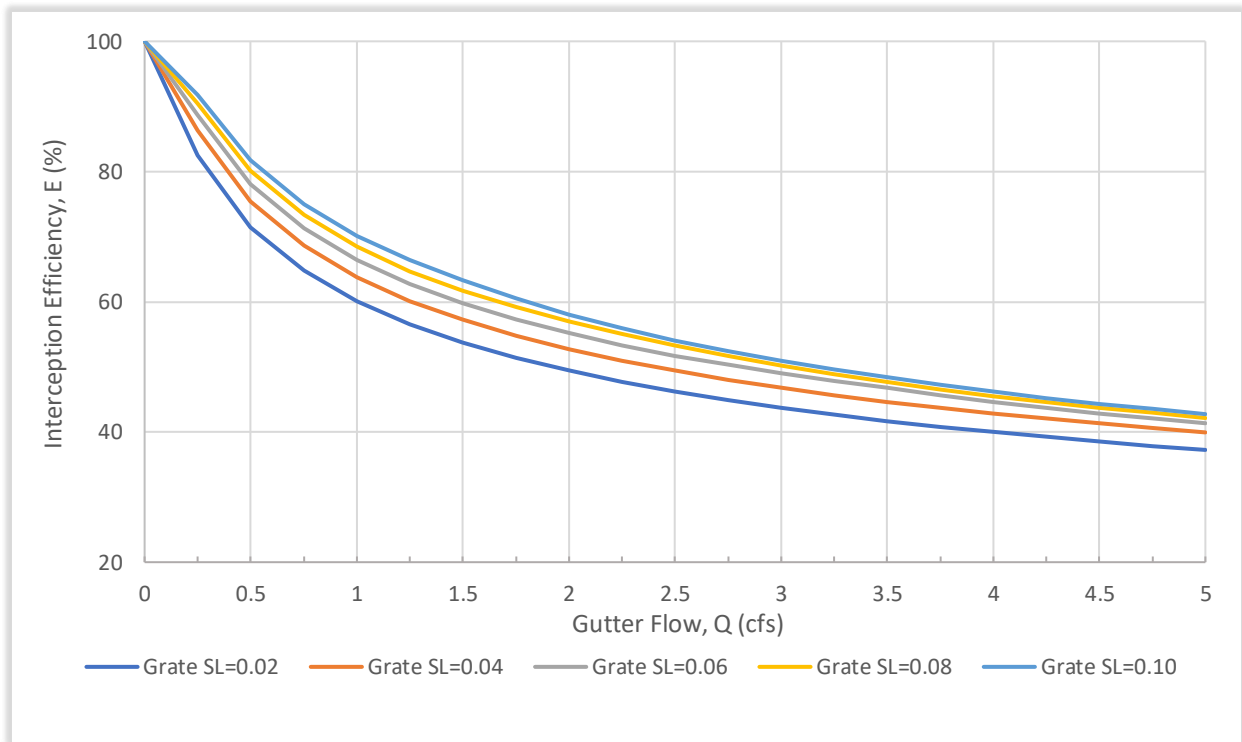


**Chart B3.4** – Triangular Section 2 Grates with Cross Slope ( $S_x$ ) = 0.015.

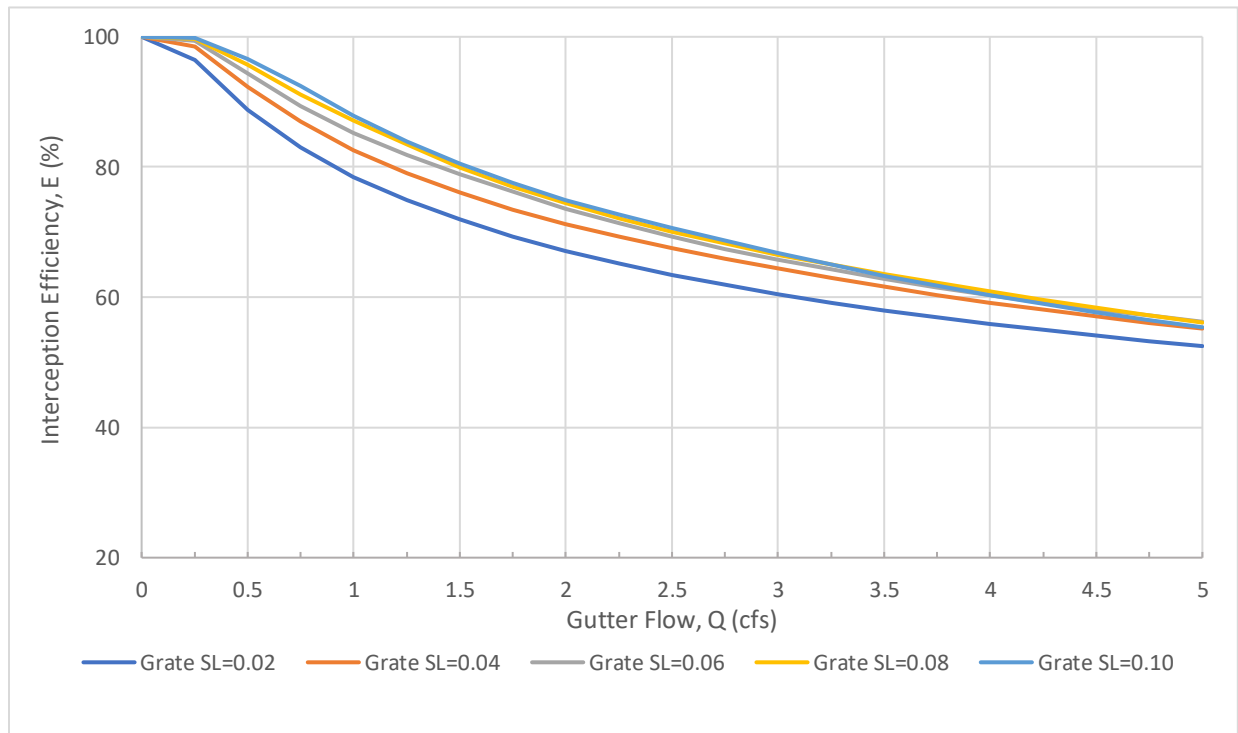


**Chart B3.5** – Triangular Section 2 Grates with Cross Slope ( $S_x$ ) = 0.030.

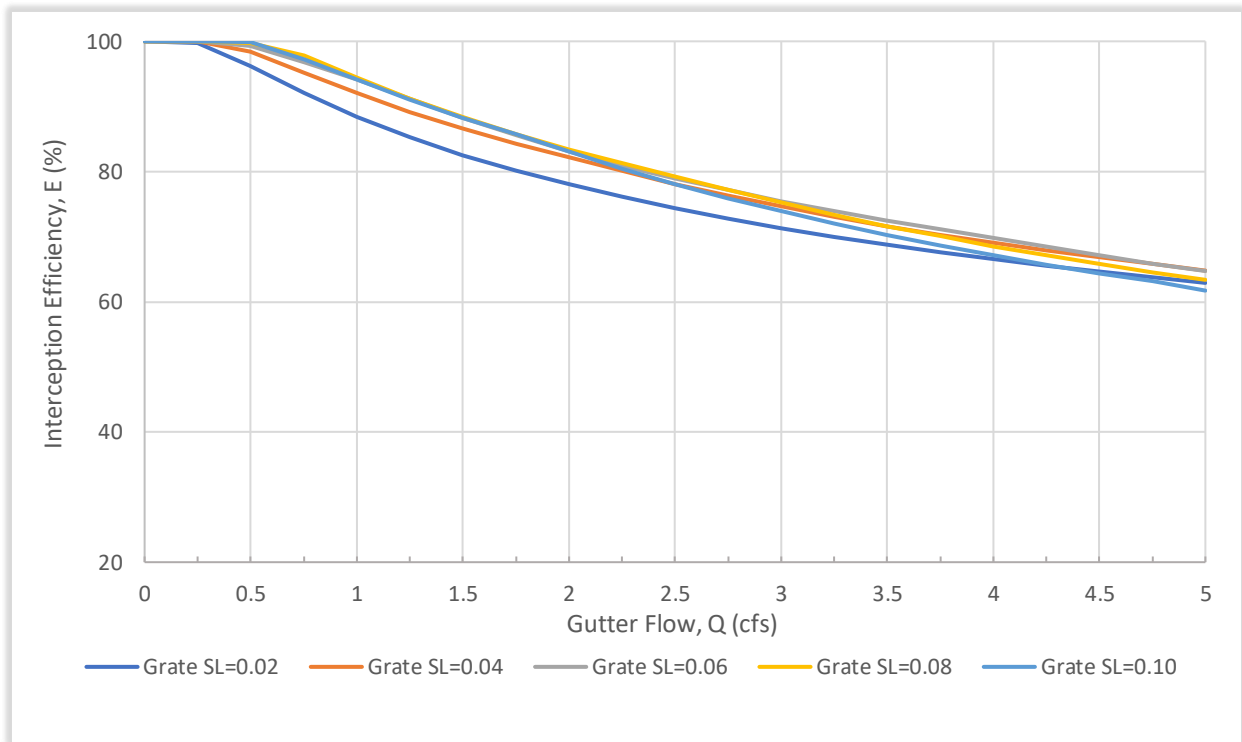


**Chart B3.6** – Triangular Section 2 Grates with Cross Slope ( $S_x$ ) = 0.045.

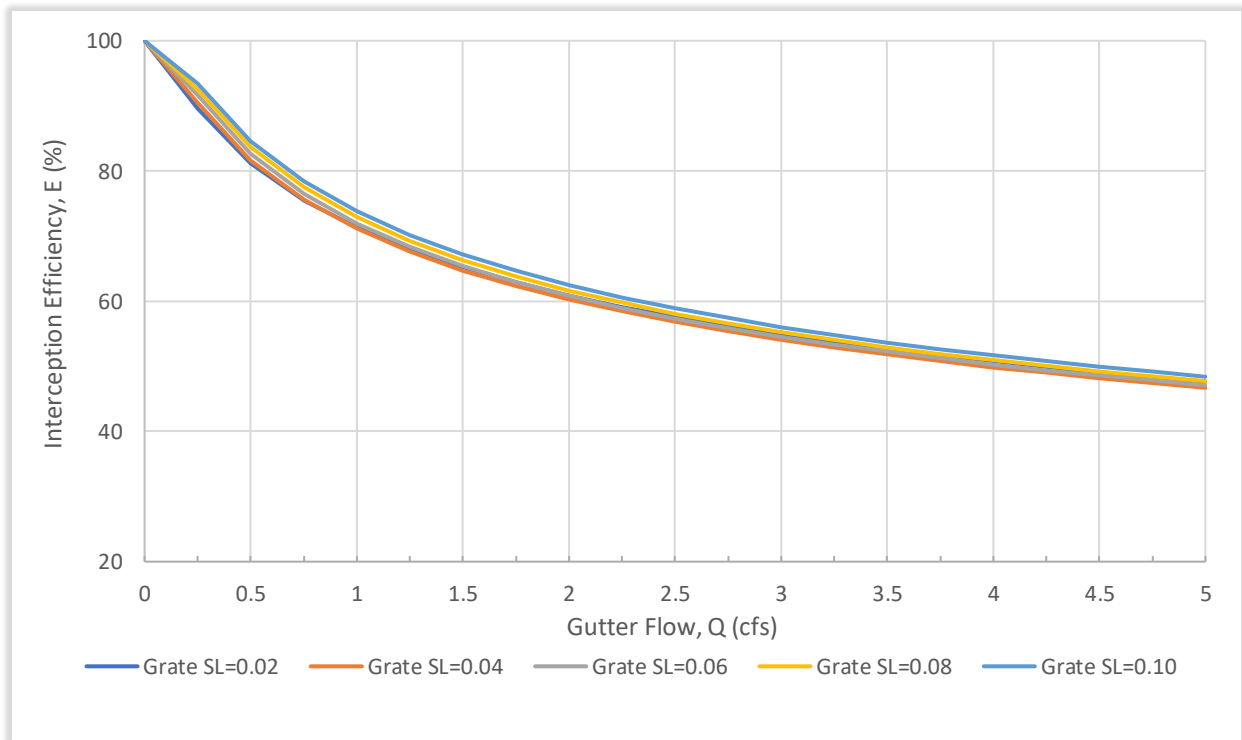


**Chart B3.7** – Triangular Section 3 Grates with Cross Slope ( $S_x$ ) = 0.015.

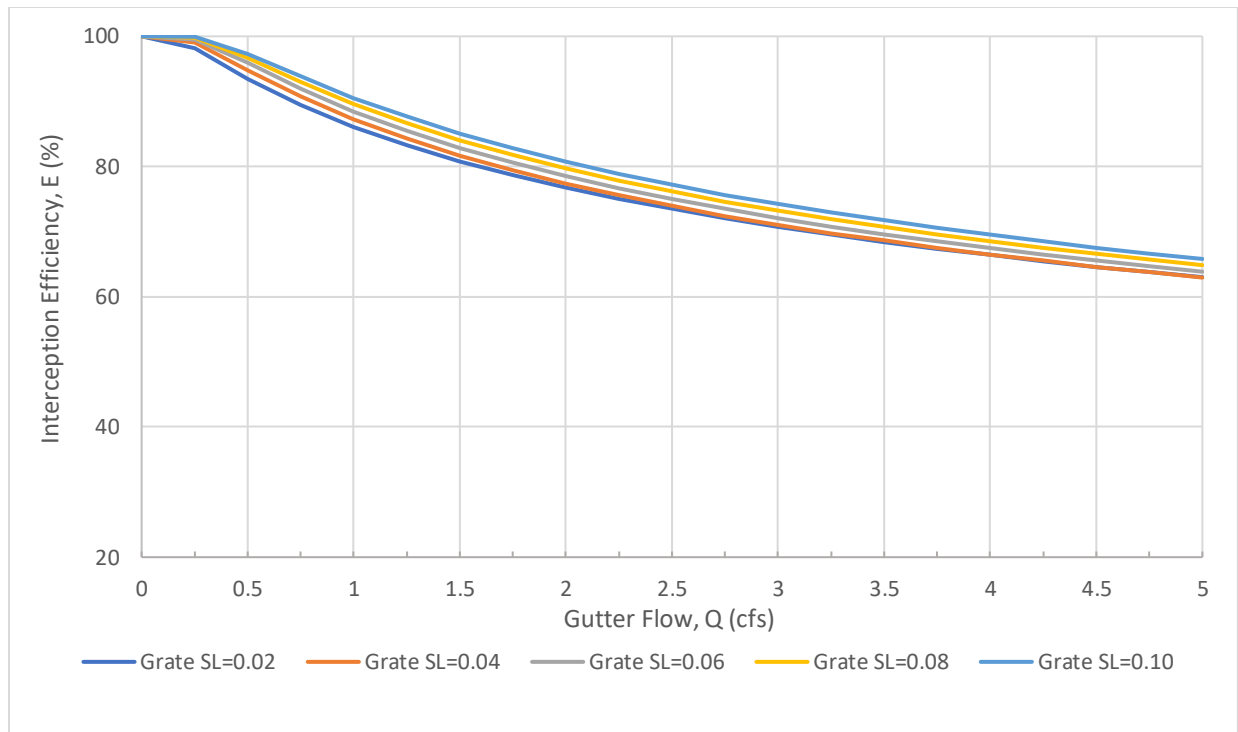


**Chart B3.8** – Triangular Section 3 Grates with Cross Slope ( $S_x$ ) = 0.030.

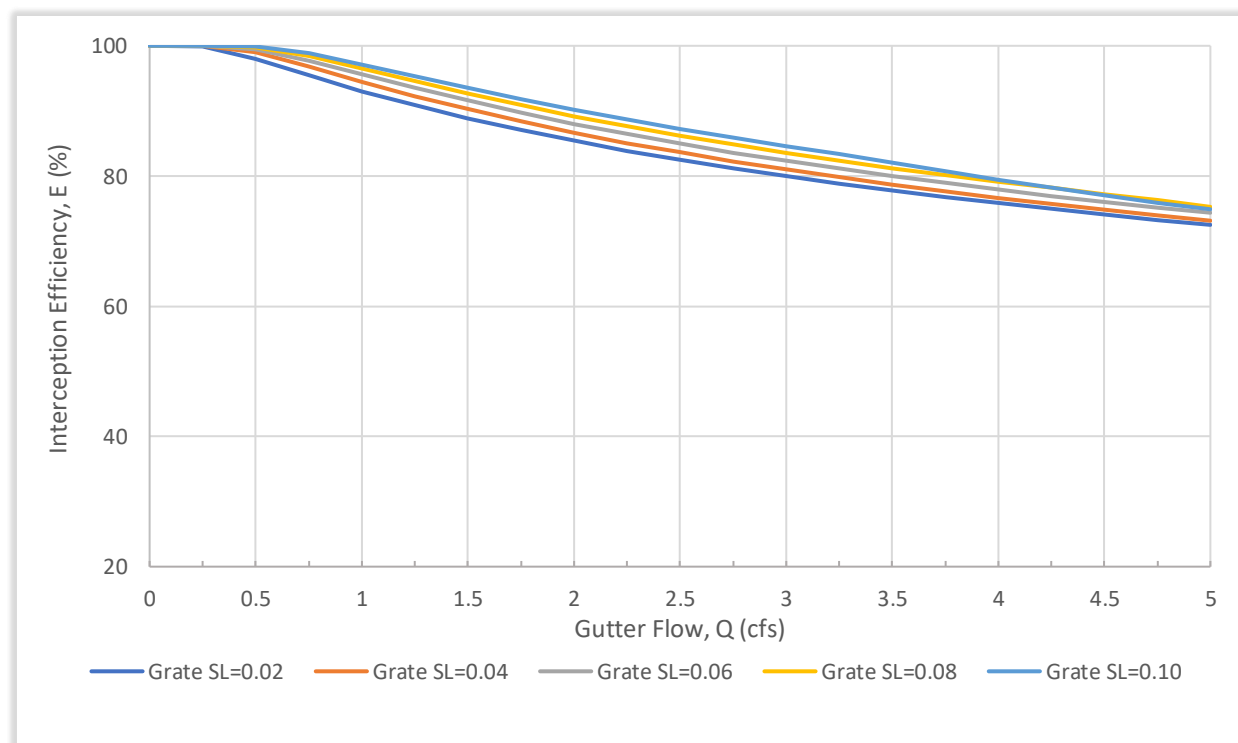


**Chart B3.9** – Triangular Section 3 Grates with Cross Slope ( $S_x$ ) = 0.045.

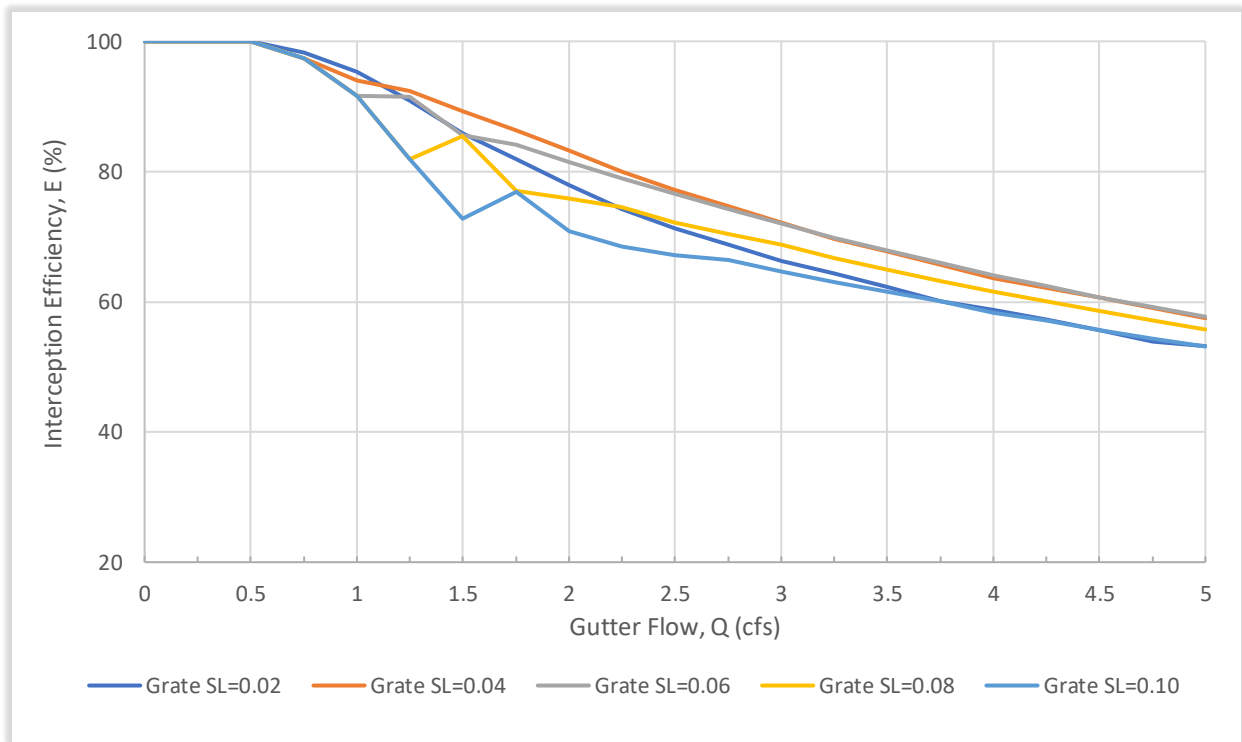


**Chart B3.10** – Composite Section (W = 2ft, a = 2in) 1 Grate with Cross Slope ( $S_x$ ) = 0.015.

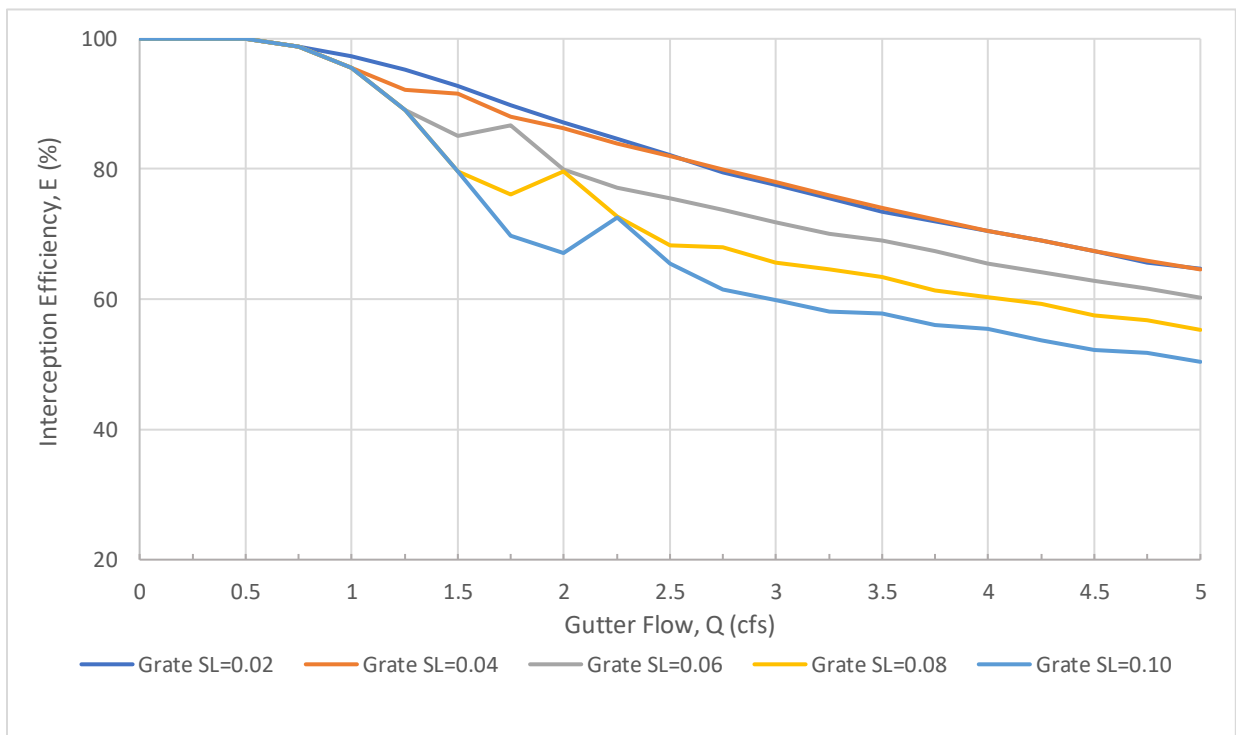


**Chart B3.11** – Composite Section (W = 2ft, a = 2in) 1 Grate with Cross Slope ( $S_x$ ) = 0.030.

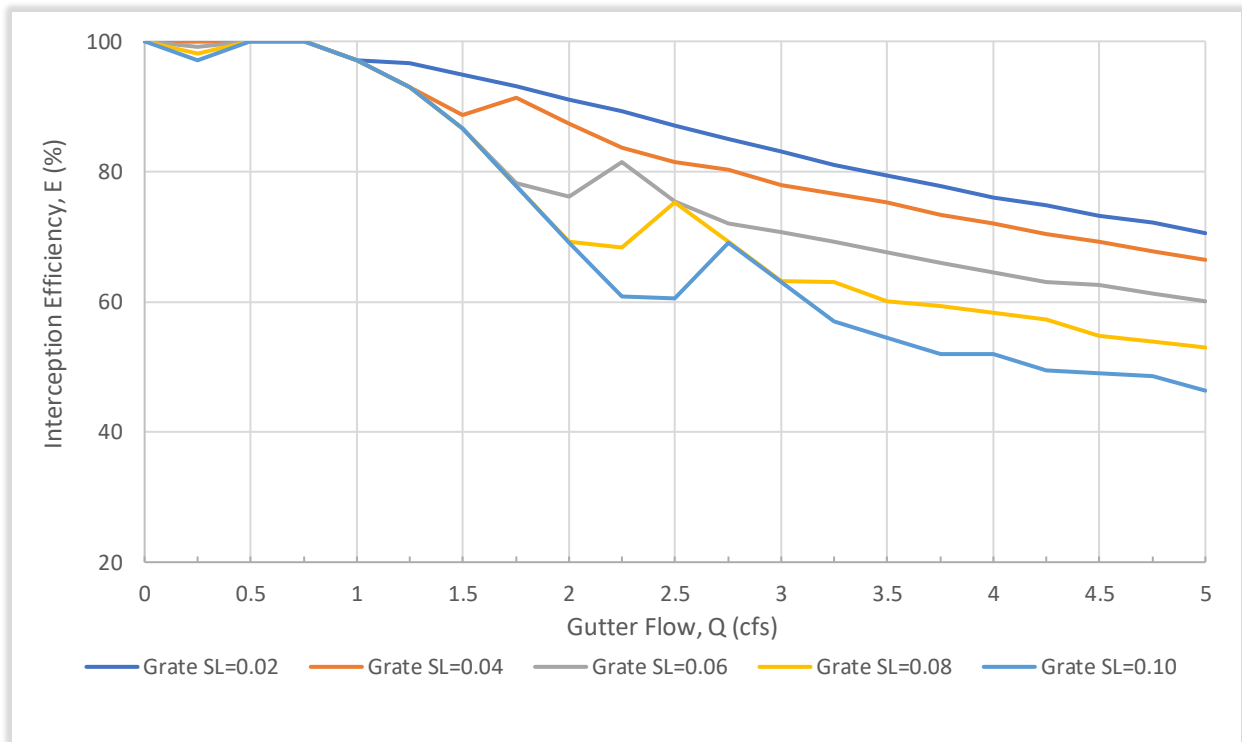


**Chart B3.12** – Composite Section (W = 2ft, a = 2in) 1 Grate with Cross Slope ( $S_x$ ) = 0.045.

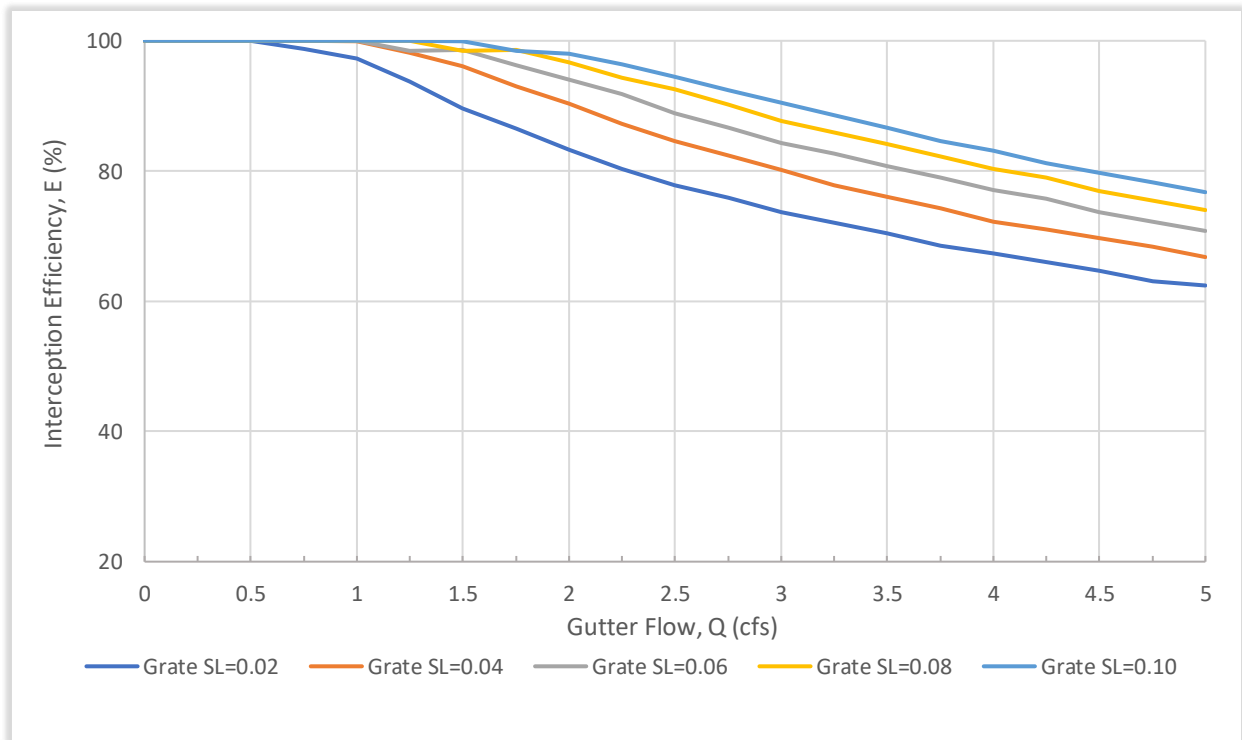


**Chart B3.13** – Composite Section (W = 2ft, a = 2in) 3 Grates with Cross Slope ( $S_x$ ) = 0.015.

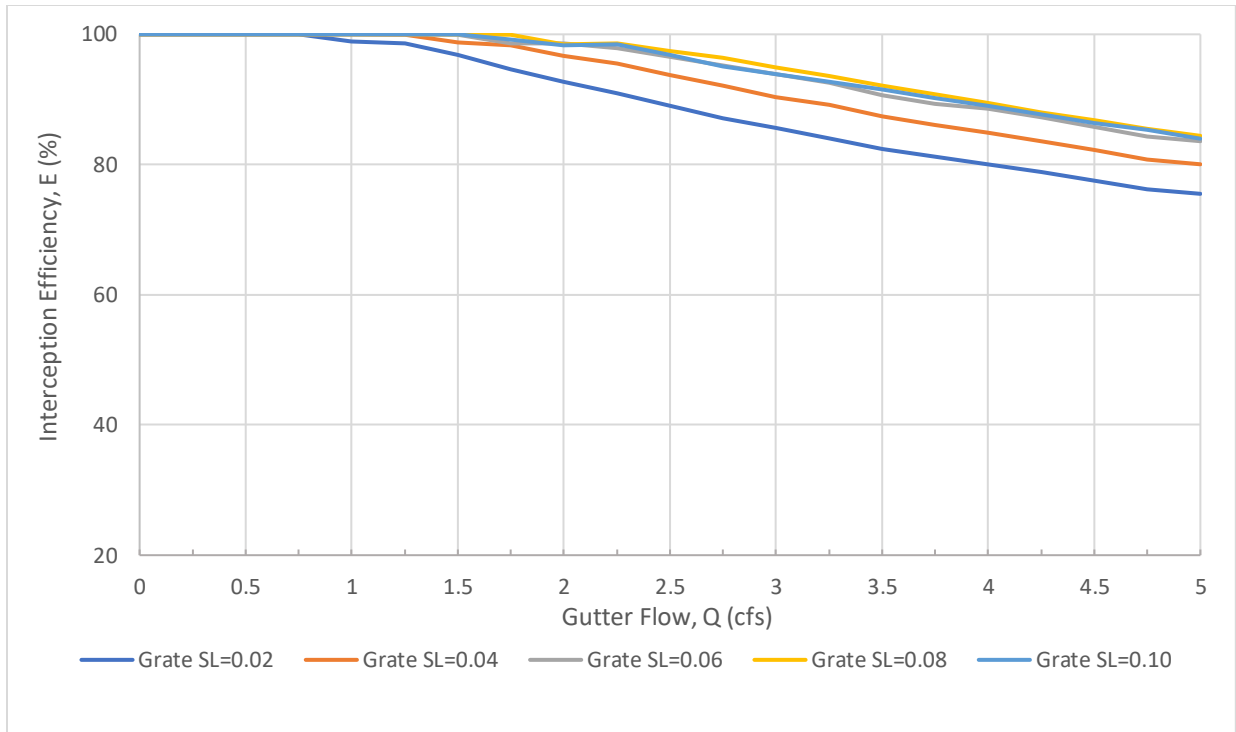


**Chart B3.14** – Composite Section ( $W = 2\text{ft}$ ,  $a = 2\text{in}$ ) 3 Grates with Cross Slope ( $S_x$ ) = 0.030.

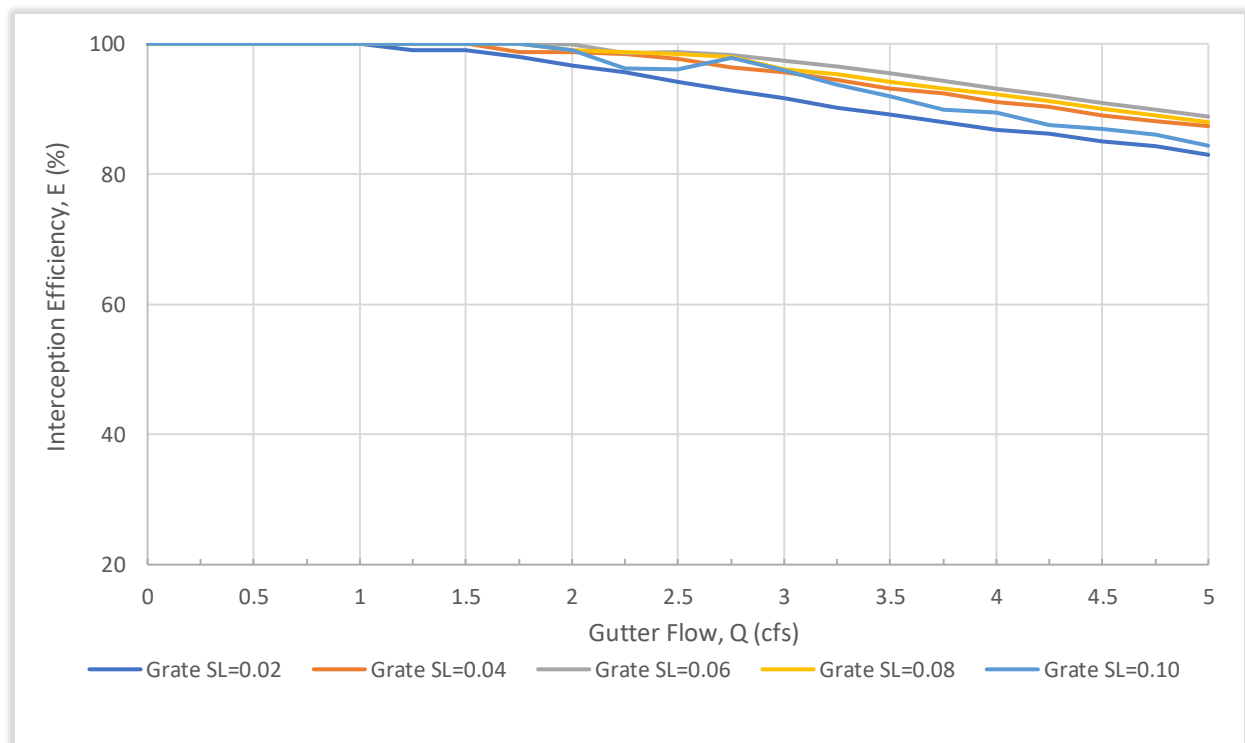


**Chart B3.15** – Composite Section ( $W = 2\text{ft}$ ,  $a = 2\text{in}$ ) 3 Grates with Cross Slope ( $S_x$ ) = 0.045.